Effect of Heat-moisture treatment on quinoa, amaranth, taro, potato, and maize starch

Zhengyu Nan
(418487671)

A thesis submitted in fulfillment of the requirements for the

Master of Science in Food Science

The University of Auckland 2022

Abstract

This research examined at how different starch particle sizes were physically altered by the same hot and humid treatment conditions (120°C, 30% moisture content, 1 hour treatment). The effects and differences of the HMT modification method on the morphological characteristics, pasting properties, thermal properties and gel rheological properties of different particle sizes of starch were also evaluated. In this study, the physicochemical properties of small granular starches extracted from seeds or roots of three plants were analyzed before and after treatment and compared with two New Zealand commercial large granular starches (potato starch and maize starch). Three small granule starches include quinoa starch, amaranth starch and taro starch. After HMT physical modification, the particle size of small starch particles increased significantly. It showed an apparent aggregation phenomenon on the scanning electron microscope photos, while this trend was very low for large starch particles. X-ray diffraction showed that the change of crystal form was not related to particle size. The crystal form of potato starch changed after modification but not that of other starches. At the same time, the relative crystallinity of small grain starch decreased after modification, while that of large grain starch increased. All starch samples showed that HMT physical modification increased the thermal stability of native starch. At the same time, the gel, thermal and gelatinization properties showed that the effect of particle size on the modification of HMT might not be obvious, and it is more affected by amylose. At the same time, for the rheological properties of the gel, it can be observed that particle size will affect the results of oscillation. However, the effect of HMT on the flow properties and particle size is not a decisive factor.

According to the different physical and chemical properties of starch with different particle sizes under the modification of HMT, it has excellent help and application to the food industry. It is helpful for industrial production. When starch with different particle sizes is modified by heat-moisture treatment, it can be adjusted appropriately

according to relevant purposes.

Key words: Heat-moisture treatment, quinoa starch, amaranth starch, taro starch, structural properties, thermal properties, gelatinization properties, rheological properties.

Acknowledgements

I have many people to thank here. In the process of study and research this year, their selfless and fearless efforts have given me the greatest help and guidance so that I can complete my project and thesis.

First, I would like to extend my sincere thanks to my supervisor Dr Fan Zhu. In the beginning, he helped me and led me to the field of starch. In every stage of the subsequent experiment, he guided me to the best of his ability so that I could solve every intractable problem. I want to thank Dr Fan Zhu for teaching me about the direction of experimental research.

Secondly, I would like to express my heartfelt thanks to Dr. Guantian Li. He was very willing to discuss with me whether it was technical problems encountered in the experimental operation or the research direction of starch. He was also very keen to give me helpful suggestions. At the same time, I would like to express my sincere thanks to the other members of my academic group. I want to thank them for providing me with a friendly and warm environment and giving me much help this year—especially the help in life, which allowed me to devote myself to my projects.

I also want to thank Ms. Sreeni Pathirana, who taught me how to operate various instruments and told me the safe operation rules of the laboratory during the year, which was very helpful.

Finally, I would like to express my sincerest love and thanks to my parents for giving me life and supporting me the most spiritually and materially. They always keep me unconditionally, give me the most incredible spiritual comfort, and encourage me not to give up when I meet difficulties. And I want to say "thank you" to everyone because of the problems and challenges brought by COVID.

Table of Contents

List of Figures

List of Tables

Chapter 1 Introduction

As an essential energy source and industrial raw material for human beings, starch plays an irreplaceable role in production and life (Chen et al., 2017). Natural starch often exists in green plants' seeds, roots, stems and leaves and is mainly composed of amylose and amylopectin (Ai & Jane, 2015). Under normal circumstances, the natural starch particle size ranges from 0 to 100μm, and according to the size range, starch can be divided into large and small granule starch (Lindeboom et al., 2004). Different particle sizes tend to show different properties of starch. At the same time, different sources and types of starch have great differences, and the influencing factors of starch characterization are often determined by starch particle size, amylose and amylopectin content, starch internal structure and other trace elements (Li & Zhu, 2018a).

As natural starch often has certain defects in industrial production, such as poor thermal stability and poor tolerance to processing, more and more research directions and industrial production began to develop towards modified starch (Schafranski et al., 2021). Among the many modification methods (physical, chemical and enzymatic), physical modification of starch has attracted increasing attention due to its low cost, safety and non-toxicity (Rafiq et al., 2016; Wang et al., 2016). Among them, starch particles are exposed to a specific temperature (90-120°C), the moisture content is controlled (around 10-30%), and the treatment time is between 15 minutes and 16 hours. This method is called Heat-moisture treatment (Adawiyah et al., 2017). As a standard physical modification method, moist-heat treatment has a history of several decades, during which a large number of starches of different kinds and sources have been studied and reported to study the application of HMT on starch (Schafranski et al., 2021). However, there are few reports on comparing starch with different particle sizes after HMT treatment, especially on small particle starch. Some studies have found that natural small granule starch has unique physical and chemical properties to

a certain extent, and there are particular challenges in industrial production (Li & Zhu, 2018a; Lindeboom et al., 2004).

This study mainly explores three kinds of natural small granule starch and two kinds of commercial large granule starch under the same conditions of HMT. Each starch's physical and chemical properties before and after treatment were analyzed. The analysis of physicochemical properties includes comparing starch particle morphology, swelling power, gelatinization properties, gel properties and rheological properties before and after treatment.

This research is divided into five chapters. The first chapter introduces the purpose and background of this research. The second chapter briefly summarizes the knowledge background of starch and the research results of HMT physical modification over the years. The third chapter describes the methods used in the research and the data processing methods. The fourth chapter introduces the experimental results in detail, and the fifth chapter makes a summary and prospects.

Among them, the small grain starch extracted from three kinds of small granule starch seeds or roots purchased locally in New Zealand was compared with the commercial large grain starch to study the HMT results. Many previous studies were mainly conducted to compare starch of a single type or different genotypes or to explore the effects of different HMT processing parameters on starch. This study supplemented the possible effects of particle size on Heat-moisture treatment.

Chapter 2. Literature review

2.1 Starch

Starch, an essential human diet source, provides most of the calories for humans. At the same time, starch is ubiquitous in cereal crops and is an excellent energy source for human beings. Also, starch and modified starch would provide a broad industrial role due to their unique chemical and physical properties (Zhou et al., 2017). In general, starch is often used as a food thickening agent (Gałkowska et al., 2013; šarka & Dvořaček, 2017), stabilizer (Dickinson, 2017; B. Zhang, Tao, et al., 2017) and gelling agent (B. Zhang, Pan, et al., 2017).

Normally starch, as the most abundant polysaccharide in nature, is a polymer made of D-glucose bonded by α-1, 4 glycosylic bonds and α-1, 6 glycosylic bonds (Ai & Jane, 2015). There would be two types of starch, amylose and amylopectin. Amylose (AM) is a linear D-glucose-molecule linked by an α-1, 4 glycosidic bonds (Figure 1). Amylose is a kind of starch molecule that tend to be linearly polymerised and composed of α-1, 4 glycosidic bonds; meanwhile, amylose is generally located in the amorphous region of starch granules (Ai & Jane, 2015; Chen et al., 2017).

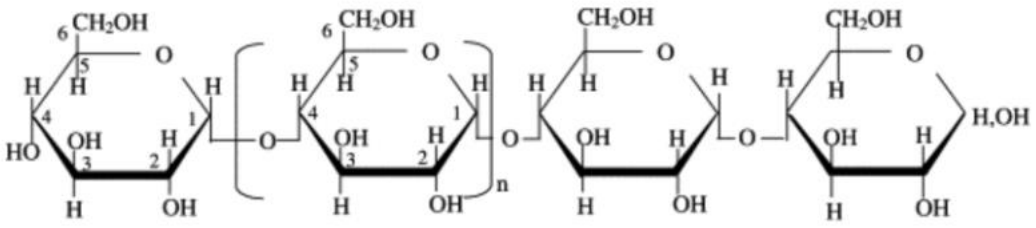

Figure 2.1. Amylose structure (Tester et al., 2004)

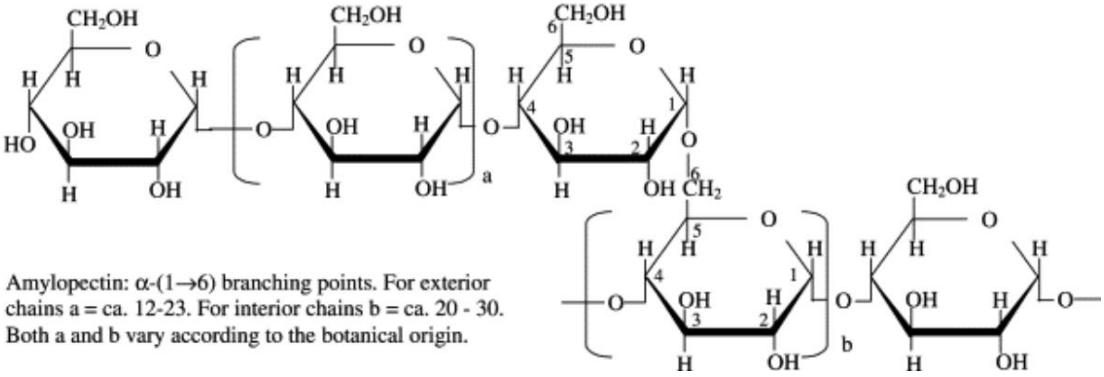

Figure 2.2. Amylopectin structure (Adapted from Tester et al., 2004)

Amylopectin is a macromolecule of D-glucose linked by α-1, 4 and α-1, 6 glycosidic bonds (figure 2), and each branched molecule contains a main chain and several side chains (Tester et al., 2004). Among them, α-1, 6 glycosidic bonds account for 5% of the total, and amylopectin is highly branched (Ai & Jane, 2015). In general, the main chain is called the C-chains and the side chains are called the A and B-chains. As the outer chain, A-chains are connected with B-chains by α-1, 6 glycosidic bonds; The same B- chains are linked to the C-chains by an α-1, 6 glycosidic bonds (Hizukuri, 1986; Kobayashi et al., 1986, as cited in Hoover, 2001). The C-type chain also has a reducing group at the end, and the overall chain length determines the crystal structure of the corresponding starch (Pérez & Bertoft, 2010).

The ratio of amylose and amylopectin is different in starch from different sources. Normally, most starch contains 20-25 amylose; but wax starch's composition is all amylopectin, and high amylose contains more than 50% amylose (Schafranski et al., 2021). According to Table 2.1, it would be found that the amylose content of natural amaranth starch varies greatly. Influenced by species and genotypes, there were waxy amaranth starch and deficient amylose content species (Zhu, 2017). Amylose tends to form complexes with hydrophobic guests, and amylopectin's branched chains form a double helix (Ai & Jane, 2015; Chen et al., 2017). Amylopectin and amylose have significant effects on starch structure and properties (Pérez & Bertoft, 2010).

Table 2.1. Amylose content of three small granule starches.

Sample name	Amylose content (%)	Reference
Native Quinoa	3-20 %	(Li & Zhu, 2018a)
Native Amaranth	0-34%	(Zhu, 2017)
Native Taro	10.4-14.7%	(Aboubakar et al., 2008; Simsek & El, 2012)

The starch grain structure contains crystalline regions and amylopectin branches, which are amorphous in alternating layers (Schafranski et al., 2021). Starch grains contain crystalline regions and amorphous regions. X-ray diffractometry is a method to analyse the crystal structure and characteristics of starch grains (Zobel, 1988a; Hizukuri et al., 1983, as cited in Hoover, 2001), and the results show that amylopectin branches in clusters as helical structures, and they pile up together to form many small crystalline forms; generally, there are three crystalline forms: A-, B- and C- type, and C-type can be seen as a superposition of A- and B- type (Imberty et al., 1991; Hoover, 2001). Furthermore, according to the similarity between A-type and B-type, C-type can be further divided into Ca-type, Cb-type and Cc-type (Hizukuri, 1960). Most of the tuber and root starch is B-type (Zobel, 1988), and cereal starches generally show A-type, while B-type shows the true crystalline form of starch (Buléon et al., 1998). The other chains that do not participate in forming the microcrystal strand constitute an amorphous region. The crystalline region formed a compact layer, and the amorphous region formed a sparse layer arranged alternately to form a complete starch grain.

When starch particles are examined under a polarising microscope, polarised crosses or Maltese crosses are found, dividing starch particles into four white regions or quadrants, a phenomenon known as birefringence (Tester et al., 2004). It means there is crystal structure in starch granules, and the starch molecules are arranged radially and orderly. Also, one idea is to call its four regional centres the umbilicus, or growth centres, from which branching molecules radiate outwards (Tester et al., 2004). At the same time, microscopic observations of starch grains also reveal ring layer fine lines similar to tree rings, also known as ringlets, with different densities. These "growth rings" are pronounced in potato starch granules, which are formed by layers of concentric shells with different diameters stacked outwards from the umbilicus (Tester et al., 2004). From Figure 4, Donald found the growth rings structure of starch, and the "tree rings" structure shows the accumulation day and night and the cyclical property (Tester et al., 2004). Also, from the research, each growth ring is 120-400nm thick, and the radial growth of amylopectin in the structure has 16 clusters per growth ring (Tester et al., 2004). This model would contain different crystalline polymorphs compounds, which includes A-type and B-type.

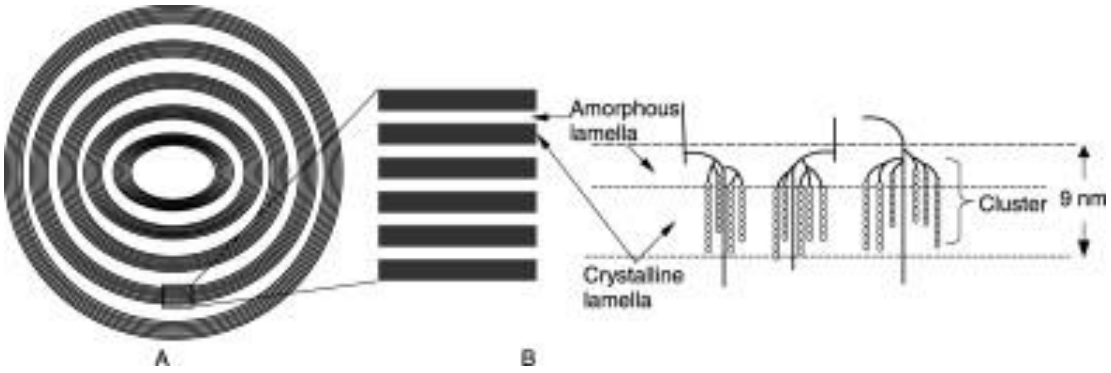

Figure 2.3. Diagrammatic representation of the lamellar structure of a starch granule. (A) Microchip layers separated by amorphous growth rings. (B) Enlarged view of amorphous and crystalline regions (Adapted from Tseter et al., 2004).

In short, starch, as a water-insoluble particulate matter, is composed of amylose and amylopectin through intermolecular hydrogen bonds and hydrophobic bonds (Singla et al., 2020). Many studies have shown that the ratio of amylose to amylopectin in starch largely determines the properties of different kinds of starch (Ambigaipalan et al., 2014; Bian & Chung, 2016b; Li & Zhu, 2018a; Singla et al., 2020; Sui et al., 2015).

2.2 Small granule starch

Different kinds of starch have different molecular sizes, and the size of starch particles is an important factor affecting starch's physical and chemical properties but also affects the process of starch industry refinement (Lindeboom, Chang & Tyler, 2004). However, the structure of starch granules is highly complex, mainly natural starch, which mostly comes from plants. In addition to amylose and amylopectin, their contribution to crystallisation is different, and the environment will affect the shape and size of starch granules in the process of plant growth (Buléon et al., 1998). According to this, different kinds of starch particles are not the same. Some starch particles' shape is not regular, so generally take the average diameter of starch particles to determine the size of starch particles index.

Generally, the average diameter of starch grains is usually between 1-200μm and comes from different plants (J.-L. Jane et al., 1994). When starch granules larger than 25μm is called large granules, 10-25μm are medium granules, 5-10μm is small granules and less than 5μm are very small granules (Lindeboom, Chang & Tyler, 2004). The common small granule starch is mainly rice, wheat and oats, while there are some potential small starch particles, such as quinoa, amaranth, taro, dropwort, grain tef, dasheen, pigweed, cow cockle, canary grass and cattail

(Lindeboom, Chang & Tyler, 2004). In this experiment, quinoa, amaranth and taro starch were selected as experimental sources of small grain starch, and their particle size range is shown in Table 2.2.1.

Table 2.2.1. Granule size of selected small granule starch.

Source	Diameter [μm]	Reference
Native Quinoa Starch	0.4-2.0	(Li & Zhu, 2018)
Native Amaranth Starch	0.5-2.0	(Zhu, 2017)
Native Taro Starch	2.0-3.0	(Lindeboom et al., 2004)

Starch particle size would directly affect the physicochemical properties of starch. Lindeboom, Chang and Tyler (2004) found the relationship between the granule size and the gelatinisation temperature: some studies show that the gelatinisation temperature of small starch particles would be usually lower than that of large starch particles; however, there are some special cases: taro starch has a much higher gelatinisation temperature than other small starch particles, while the gelatinisation temperature of small starch particles with single mode mimicry is higher than that of large starch particles. So, in this study, there would be three normal types of small granule starch (quinoa, amaranth and taro) which would be treated by heat-moisture treatment. Moreover, the difference between small and ordinary starch would be compared by analysing physicochemical properties. These days, small starch is becoming more and more popular with research

development. Due to their small particle size and narrow distribution, small particles began to be used in fine printing manufacturing, as a binder in oral active substances and as a carrier for cosmetics (Lindeboom, Chang & Tyler, 2004).

Therefore, three kinds of typical small-grain starch were selected in this experiment. After HMT modification, the changes in their physical and chemical properties were explored, such as particle size, crystal structure, particle morphology, rheological properties, gelatinisation properties and swelling ability. Then compared with two kinds of common large granule starch, it is very helpful to explore the influence of particle size and HMT on starch in the future. As studied by Chen et al. (2018), starch plays an irreplaceable role in the food and drug industries, and it is highly dependent on the physicochemical properties of starch while being a thickener, stabiliser and gelling agent.

2.3 Heat-moisture treatment of starch

Heat-moisture treatment (HMT) is a kind of hydrothermal method. As a common treatment method under the combined action of water and heating, starch often experiences a transition from dense ordered structure to lose disordered structure (Chen et al., 2018). In this process, the structure and properties of starch are often changed, and the amplitude of change is affected by the water content, temperature and time in the treatment process (Wang et al., 2017). But other studies suggest that HMT is a milder method. It can also show that the starch structure would not change, but its physicochemical properties were affected (Sarka & Dvoracek, 2017). As a method of physical modification, HMT would usually control the water content of starch at a low state (generally below 35%) and then heat it for some time at a

temperature of 80-140°C (Li et al., 2020). Due to the wide range of treatment temperature, water content, and treatment time, a large number of studies on these three treatment parameters have been conducted on a large number of different starch model systems, such as Jackfruit seed (Kittipongpatana & Kittipongpatana, 2015), Red Adzuki bean (Gong et al., 2017), brown rice (Bian & Chung, 2016a), Cassava (Chatpapamon et al., 2019) and mango seeds (Bharti et al., 2019). In this experiment, the results of previous studies were referenced, and a common HMT method used by Chung, Liu & Hoover (2008) was referenced, which controls the moisture content of starch up to 30% in an airtight container and heat it at 120°C for 1 hour after being thoroughly mixed with water. The experiment time is shorter and easier to control, and the higher water content can change the parameter. Many experiments have shown that the amount of wet base will directly affect the experimental results. Studies on the modification of HMT controlling the water gradient show that, with the increase of the water content in the treatment process, the corresponding gelatinisation parameters, swelling force and solubility index all increase. Rafiq et al. (2016) found that when starch was modified by HMT, with the continuous increase of water content, the changes of various parameters were more obvious than those of natural starch, which indicated that water was susceptible during HMT modification. Often during the HMT process, excess water and the heating process result in gelatinisation of the starch, and the distance between the starch chains would be increased (Biliaderis, 2009). Because HMT is conducted under sealed conditions, it can not only prevent evaporation of water during heating but also monitor water concentration; At the same time, the pressure generated during the heating process increases the heat energy, which is then converted into kinetic energy by the water molecules, so the method can also control the movement of molecules at high temperatures (Schafranski et al., 2021). Wang, Li and Zheng (2020) found that HMT can change the surface characteristics and size of starch particles by adjusting the parameters and starch source; Starch crystals, helix structures and molecular structures can also be altered. Furthermore, they found that during this process, a large-scale truncation movement occurs, which transforms the

amorphous starch domain from a glassy state to a more flexible state; Moreover, the additional reordering of starch chains can be promoted by prolonging the heating time or cycle time and increasing the treatment temperature, thus increasing the influence of HMT on the physicochemical properties and structure of starch (Wang, Li and Zheng, 2020; Wang, Li and Zheng, 2021). This result indicates that the corresponding physicochemical property parameters will change significantly with the increased HMT treatment time. For example, Deka & Sit (2016) conducted HMT on natural taro starch with a large span of various treatment times and found that with increasing treatment time, the treated starch showed higher gelatinisation parameters. Therefore, it is vital to select appropriate treatment parameters. It is also necessary to understand the changes in internal starch structure during HMT treatment to reasonably explain the parameter changes.

From Figure 2.3.1, it is clear to see the effect of HMT on starch by observing the lamellar structure of starch. When comparing the native starch's crystalline growth ring and the Heat-Moisture Treatment starch's crystalline growth ring, it is found the change from the Highly ordered chains to partially ordered chains, which means HMT would increase the interaction between starch chains, and double helix structure would separate; also the broken crystalline region would be rebuilt be rearranged (Schafranski et al., 2021).

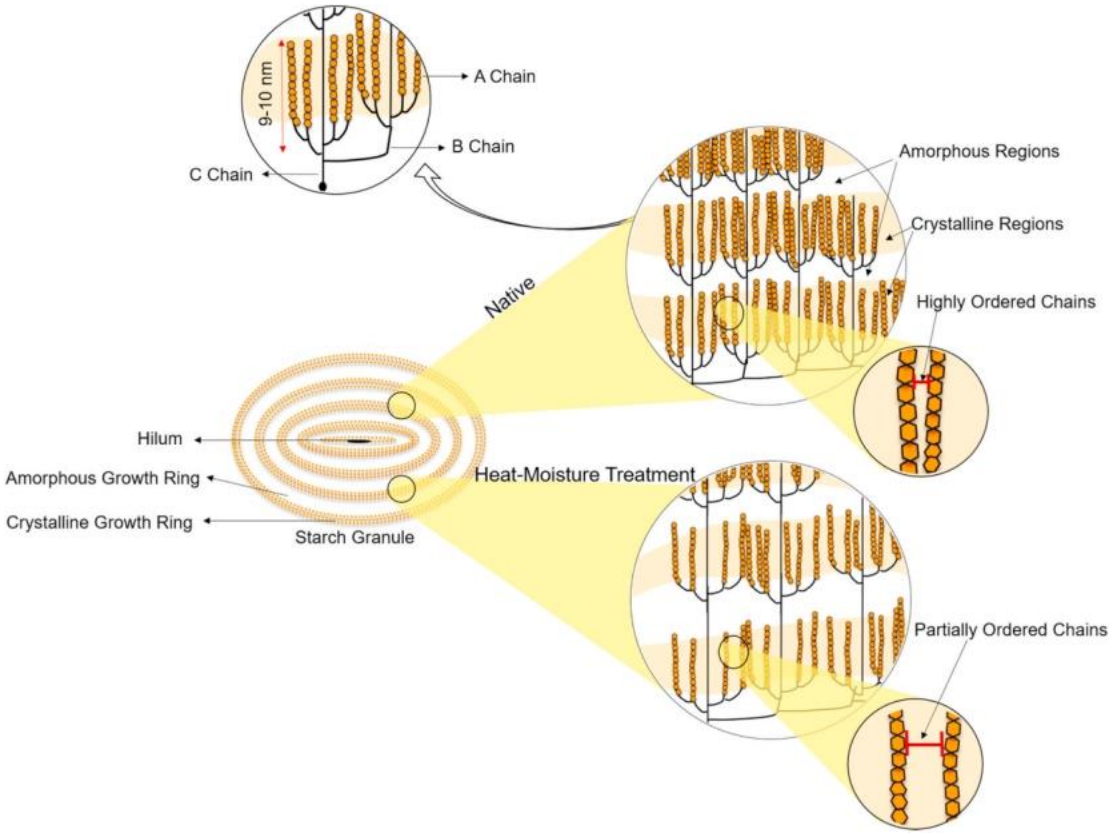

Figure 2.3.1. Structure of native starch granules and after HMT-modified (Schafranski et al., 2021)

Therefore, according to the characteristics of HMT, this method tends to destroy the surface of starch particles, which makes the interior of starch particles more vulnerable to the action of α-amylase (Gunaratne & Hoover, 2002) and does not change the particle morphology (Wang, Li & Zheng, 2021). At the same time, due to many defects of natural starch, in addition to being almost insoluble in cold water, easy to revive, especially its inert structure, so starch modification becomes particularly important. The structure of starch modified by HMT changes, and its physical properties, such as swelling power and solubility are affected, so the modified starch can be used in broad industrial applications. In addition, compared with chemical modification, physical modification is more environmentally friendly and safe; In addition, when the HMT method modifies starch, bacterial toxins existing in

grain will be inactivated, and bioactive phenolic substances will be released (Wang, Li & Zheng, 2021). Also, as well as being a widely applicable and low-cost treatment method, HMT also effectively avoids any biochemical issues related to genes or chemical additives (Bet et al., 2018). According to this, HMT has broad prospects of many advantages.

2.4 Gelatinisation

Gelatinisation and rheological properties of starch are two of the most important properties determining the direction and scope of starch application. Gelatinisation of starch is usually defined structurally as a process from ordered semicrystalline particles to an amorphous state, during which the Maltese cross is often lost (Ai & Jane, 2015). This Maltese cross pattern observed under polarised light indicates a high degree of ordering within starch granules (Greenwood, 1979). The gelatinisation process of starch is usually realised under the joint action of water and temperature. At the same time, it has been reported that partial plasticisers or alkaline solutions can also dissociate the double helix structure of the starch chain, resulting in gelatinisation (Ai & Jane, 2015; Nashed et al., 2003; Ragheb et al., 1995). However, most gelatinisation reactions are achieved by water and heating, and this study mainly focuses on gelatinisation reactions caused by water and heating. In short, gelatinisation, which involves hydration and expansion reactions of starch particles, is not only a phase transition of starch particles from an ordered state to a disordered state but is also affected by whether excess water is involved in the phase transition and whether the temperature reaches the gelatinisation range (Oyeyinka & Oyeyinka, 2018). When starch is heated in water, along with the physicochemical interaction between AM and AP, the grain structure of starch tends to undergo glass transition, gelatinisation and melting of the amylose-lipid complex (Schirmer et al., 2015). As shown in the figure, the state change of starch occurs during heating.

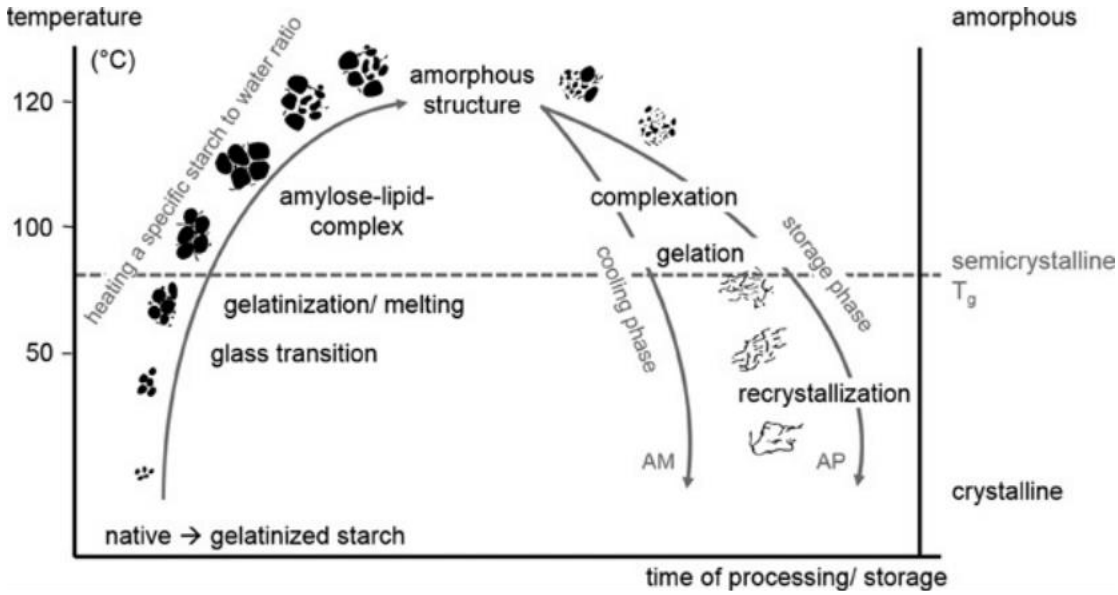

Figure 2.4. The state change of starch particles with temperature during heating (Schirmer et al., 2015)

It can be seen that the gelatinisation reaction of starch usually occurs after the initiation of glass transition temperature (Schirmer et al., 2015). The interval of Tg (gelatinisation temperature) is similar to that of semicrystalline. The degree of gelatinisation results is affected by different proportions of water and starch, and different starch has different gelatinisation temperature ranges (Belitz & Grosch, 2013). At the same time, many factors affect gelatinization. It has been reported that sugars, salts and lipids affect gelatinisation (Ai & Jane, 2015). Among them, Beleia et al. (1996); Kohyama & Nishinari (1991) found that the presence of monosaccharides significantly increased the gelatinisation temperature and gelatinisation enthalpy of starch. Therefore, starch from different sources showed different gelatinising properties after HMT modification. In this experiment analysed and studied the influence of such physical modification on gelatinisation performance by exploring HMT under specific parameters applied to starch from different sources.

Because the gelatinisation process is affected by many factors and the reaction in the heating process is very complex, it is very important to select a reasonable measurement and analysis of gelatinisation characteristics. For the determination of the gelatinisation temperature of different starch sources, differential scanning calorimetry (DSC), polarised light microscopy equipped with a hot table, thermomechanical analysis and nuclear magnetic resonance spectroscopy are usually used to determine the gelatinisation temperature of starch (Ai & Jane, 2015). There is also evidence that specific enzymes (glucoamylase) can measure starch gelatinisation and have certain advantages, such as specificity (Ratnayake & Jackson, 2008). However, the measurement of gelatinisation by digestion of starch by glucoamylase has been shown to have a large error, which is attributed to contamination by other enzymes (Ratnayake & Jackson, 2008). Therefore, most of the gelatinisation degree is measured physically. Among them, DSC, as a method to determine the parameters related to gelatinisation and rejuvenation, is widely used because it is fast and consumes fewer experimental samples (Ratnayake et al., 2009). DSC can not only measure gelatinisation information qualitatively and quantitatively but also draw the temperature function with the parameters such as initial temperature (To), endothermic peak (Tp), end temperature (Tc) and gelatinisation enthalpy (ΔH) obtained (Schafranski et al., 2021; Yu & Christie, 2001). Generally, the gelatinisation temperature range of common starch is about 60°C to 80°C, and the gelatinisation temperature of type A starch is higher than that of type B starch (Zhu & Xie, 2018). Gelatinisation temperatures of different types of starch (type A, type B) as shown in Table 2.4.1. The gelatinisation properties of some common starches with different crystalline types are listed as determined by differential scanning calorimetry (J. Jane et al., 1999). In addition to common type A and B starch, type C starch was also displayed. Type A and B starches are primarily found in grains or some tubers, while type C is more commonly found in fruits, beans and tubers (Espinosa-Solis et al., 2011; He & Wei, 2017; Schafranski et al., 2021; Stevenson et al., 2006). There is also evidence that C-type starch may exist in traditional Chinese medicine (Xia et al., 2013).

Table 2.4.1. Differential scanning calorimetry was used to determine the gelatinization characteristics of common starch with different crystal types (Ai & Jane, 2015).

Type	To (°C)	Tp (°C)	Tc (°C)	Range (°C)	ΔH (J/g)
A-type starch					
Normal maize	64.1 ± 0.2	69.4 ± 0.1	74.9 ± 0.6	10.8	12.3 ± 0.0
Waxy maize	64.2 ± 0.2	69.2 ± 0.0	74.6 ± 0.4	10.4	15.4 ± 0.0
du Waxy maize	66.1 ± 0.5	74.2 ± 0.4	80.5 ± 0.2	14.4	15.6 ± 0.2
Normal rice	70.3 ± 0.2	76.2 ± 0.0	80.2 ± 0.0	9.9	13.2 ± 0.6
Waxy rice	56.9 ± 0.3	63.2 ± 0.3	70.3 ± 0.7	13.4	15.4 ± 0.2
Sweet rice	58.6 ± 0.2	64.7 ± 0.0	71.4 ± 0.5	12.8	13.4 ± 0.6
Wheat	57.1 ± 0.3	61.6 ± 0.2	66.2 ± 0.3	9.1	10.7 ± 0.2
Barley	56.3 ± 0.0	59.5 ± 0.0	62.9 ± 0.1	6.6	10.0 ± 0.3
Waxy amaranth	66.7 ± 0.2	70.2 ± 0.2	75.2 ± 0.4	8.5	16.3 ± 0.2
Cattail millet	67.1 ± 0.0	71.7 ± 0.0	75.6 ± 0.0	8.5	14.4 ± 0.3
Mung bean	60.0 ± 0.4	65.3 ± 0.4	71.5 ± 0.4	11.5	11.4 ± 0.5
Chinese taro	67.3 ± 0.1	72.9 ± 0.1	79.8 ± 0.2	12.5	15.0 ± 0.5
Tapioca	64.3 ± 0.1	68.3 ± 0.2	74.4 ± 0.1	10.1	14.7 ± 0.7
B-type starch					
ae Waxy maize	71.5 ± 0.2	81.0 ± 1.7	97.2 ± 0.8	25.7	22.0 ± 0.3
Amylomaize V	71.0 ± 0.4	81.3 ± 0.4	112.6 ± 1.2	41.6	19.5 ± 1.5
Amylomaize VII	70.6 ± 0.3	N.D.	129.4 ± 2.0	58.8	16.2 ± 0.8
Potato	58.2 ± 0.1	62.6 ± 0.1	67.7 ± 0.1	9.5	15.8 ± 1.2
Green leaf canna	59.3 ± 0.3	65.4 ± 0.4	80.3 ± 0.3	21	15.5 ± 0.4
C-type starch					
Lotus root	60.6 ± 0.0	66.2 ± 0.0	71.1 ± 0.2	10.5	13.5 ± 0.1
Green banana	68.6 ± 0.2	72.0 ± 0.2	76.1 ± 0.4	7.5	17.2 ± 0.1
Water chestnut	58.7 ± 0.5	70.1 ± 0.1	82.8 ± 0.2	24.1	13.6 ± 0.5

* To, onset temperature; Tp peck temperature; Tc, conclusion temperature; ΔT (Tc-To), gelatinization temperature range; ΔH, gelatinization enthalpy.

As can be seen from the table, in addition to the high amylose content of B-type starch, the rest of the B-type starch pasting temperature is generally lower than that of type-A starch, and type-C range of gelatinisation temperature and pasting in the gap between them is not great. Moreover, it would show the same result that most natural starch gelatinisation temperature ranges from about 60°C to 70°C.

2.5. Starch morphology

Nowadays, various techniques are used to observe starch particles morphologically, such as light microscopy, scanning electron microscopy, transmission electron microscopy, Coulter counter and laser diffraction (Li & Zhu, 2018a). However, due to the low resolution of light microscopy, the details of starch particles cannot be observed (Lindeboom et al., 2004). In addition, the Coulter counter cannot accurately measure samples with a diameter less than 3mm, and laser diffraction has a significant error in determining non-spherical samples (Raeker et al., 1998). Therefore, the SEM method, which can be used for rapid determination and more detailed characterisation of particle surface and morphology, is more suitable for determining starch particle morphology (Chmelik et al., 2001).

Starch from different sources has different morphology, and most tuber and rhizome starches exhibit oval shapes (Lindeboom et al., 2004). However, there are also circular, polygonal, spherical and even polygonal irregular particles, especially small starch particles, which have the characteristics of a very irregular polygon (Das & Sit, 2021; J.-L. Jane et al., 1994). Among them, quinoa starch, an ordinary small grain starch, has a low difference in shape and size between individual grains (Li & Zhu,

2017). Individual quinoa starches tend to be polygonal, angular and irregular in shape (Li & Zhu, 2018a). Most of the individual amaranth starch grains showed a polygonal shape, and only a small amount of amaranth starch showed an oval or round shape (Wankhede et al., 1989; Zhu, 2017). At the same time, individual taro starch also shows a polygonal shape (Singla et al., 2020). This phenomenon indicates that the small starch particles selected in this experiment exhibit similar starch morphology in their natural state. In addition, Lindeboom et al. (2004) found that pea granule starch presented a disk shape with cuts, while some nut starch was hemispherical. However, the morphology of starch often expresses some different starch properties, and there is also starch particle size to express starch appearance characteristics. Most natural starches have particle sizes in the range of 0.1-10μm mentioned above, and small grains tend to be in the range of 0.1μm. However, starch particle size distribution is often determined by particle aggregation and the actual size of individual starch particles (Lindeboom et al., 2004). At the same time, natural small grain starch often has the property of particle aggregation, such as quinoa and amaranth starch (Lorenz, 1990). However, the modified starch often expressed different particle size distributions. A large amount of evidence shows that the size characterisation of small grain starch after HMT treatment is often much larger than that of the corresponding natural small grain starch (Chin et al., 2011; Namazi et al., 2011). Among them, a large number of starch granule aggregations was observed in the SEM results of small granule starch after heat-moisture treatment, which also indicated that the aggregation characteristics of small granule starch after HMT treatment tended to increase.

At the same time, a large amount of evidence shows that the size of starch in the natural state is not uniform, its surface is smooth, and there is no obvious crack (Gani et al., 2016; J.-L. Jane et al., 1994; Yang et al., 2019). However, HMT modification under certain parameters may significantly change particle surface. Many studies confirmed this: Fadimu et al. (2018) explored the effect of heat-moisture treatment on sweet potato starch; The HMT potato starch studied by Bartz et al. (2017) and the

legumes experiment conducted by Xiong et al. (2019) all obtained SEM results of various starches after HMT modification, which showed that starch was destroyed. As for the cause of starch destruction, F. Zhang et al. (2019) believed it was particle rupture and melting caused by high temperature. There is also evidence that the amount of water added during the treatment affects the results. Experiments showed that the higher the moisture content, the greater the starch damage after treatment (H. Liu et al., 2015; Marta et al., 2019). At the same time, as a critical factor affecting the effect of HMT modification on starch morphology, when the moisture content is low, this physical modification method may not affect the starch particle morphology. Tan et al. (2017) found that starch morphology did not change significantly when the moisture content was lower than 25%. However, some related studies showed that although the moisture content of HMT treatment was high, the starch particles after HMT treatment did not show the result of destruction: As jackfruit starch, barley starch, sweet potato starch (Schafranski et al., 2021); and oat starch (Ziegler et al., 2018). Therefore, the effect of HMT modification on starch morphology is also related to the selected starch type. As studied by Wang et al. (2021), the change in particle morphology of HMT is influenced by a variety of factors, including the selection of water, time, and temperature parameters in the treatment, as well as the plant source of starch.

2.6 X-ray diffraction analysis

X-ray diffraction analysis (XRD) is a common method to distinguish starches with different crystalline structures based on the X-ray scattering of 1-10 nm nanoparticles. All natural starches exhibit one of four XRD patterns, including type A, B, C and V (Tan et al., 2017). Oyeyinka & Oyeyinka (2018) found that the structural difference between type A and type B crystals is the difference in the double helix packing and hydration degree of amylopectin between them. The A-type double helix packs more

tightly and is less hydrated, while the B-type has more hydrated and double-helical cores. Type C is usually a mixture of A+B types (Perez et al., 2011). At the same time, the difference between different crystal types is usually based on the diffraction peak of the main 2θ in the diffraction pattern. Among them, the A-type diffraction pattern often shows peaks at 15.3°, 17.1°, 18.2° and 23.5°, and this type of starch is usually cereal or tuber starch (Schafranski et al., 2021). The diffraction Angle of the type B X-ray pattern at 2θ shows the maximum value at 5.6°, 14.4°, 17.2°, 22.2° and 24° (Nwokocha & Williams, 2011). The peak values of type C were 5.6°, 15.3°, 17.3° and 23.5°, and the peak values of type V were 12.6°, 13.2°, 19.4° and 20.6° when amylose and lipids were crystallised (Schafranski et al., 2021). Numerous studies show that the HMT X-ray diffraction diagram of the modified starch could change: type B crystallised natural, delicious potatoes after HMT model of the crystal into the pattern of A + B (Lee & Moon, 2015); After HMT treatment, the crystal type of Red Azuki bean changed from Ca type to A type (Gong et al., 2017). Furthermore, the crystal of natural grass pea starch changed from type C to type A after HMT modification (Piecyk et al., 2018). At the same time, there is also evidence that the diffraction pattern of starch modified by HMT does not change, but it will increase the diffraction intensity. The crystal pattern of coconut starch did not change after treatment, but the diffraction intensity increased (Lawal, 2005). Moreover, Kaur & Singh (2019) found that the peak value of HMT starch would be enhanced at a specific 2θ diffraction Angle.

2.7 Swelling power

Under a certain water content, starch particles absorb water and expand during heating, while starch components leach and dissolve (Zhu & Wang, 2014). At the same time, the swelling capacity of starch is one of the important properties of observing the rheology of starch particles, which represents the content

characteristics of amylopectin in starch particles, and amylose, as an inhibitor and diluent, affects the swelling capacity to a certain extent (N. Singh et al., 2003). For the characterisation of swelling capacity, swelling power (SP) and water solubility index (WSI) are usually used to represent the water retention of starch (Zhu & Xie, 2018). At the same time, the swelling capacity of starch is affected by a variety of factors. In addition to the aforementioned characteristics of amylose and amylopectin in starch particles, Zhu et al. (2011) found that SP and WSI are affected by the source and type of starch, and the swelling capacity of different types of starch varies greatly. At the same time, the starch of different genotypes also showed significant differences (Zhu & Wang, 2014). In addition, the swelling capacity also affects the swelling and dissolution mode of starch with temperature, starch particle difference and phosphorus content (Abegunde et al., 2013).

A large number of studies have shown that the HMT modified tend to reduce the swelling power and solubility of starch, rice starch (Hormdok & Noomhorm, 2007; Kong et al., 2015); Corn starch (Chung et al., 2009; Tester & Morrison, 1990); And barley starch (Waduge et al., 2006). The reduction of swelling power and solubility of natural starch caused by HMT can be attributed to the increase in crystallinity, the decrease of hydration, the leaching of amylose, the increase of interaction between amylose and amylopectin, and the formation of amylopectin lipid complex (Zavareze & Dias, 2011). Although Eerlingen et al. (1997) pointed out that the solubility of starch after HMT modification would increase by a small amount, it was found through research that the surface of starch particles was crevice caused by HMT modification, which resulted in the dissolution of weak structures.

2.8 Pasting property

A physical analysis is usually used to explore the changes in starch gelatinisation-related parameters during heating, and a rapid visco analyser (RVA) can characterise viscosity changes during gelatinisation. This change is due to the viscosity change caused by the expansion and macromolecular leaching of starch particles in excess water content and temperature change (Schirmer et al., 2015). As a rotational viscometer, RVA can not only measure shear resistance during temperature changes but also simulate starch heating and cooling systems (Schafranski et al., 2021). The drawn RVA curve (Figure 2.8) can characterise starch gelatinisation parameters and relative sample gelatinisation characteristics (Schirmer et al., 2015).

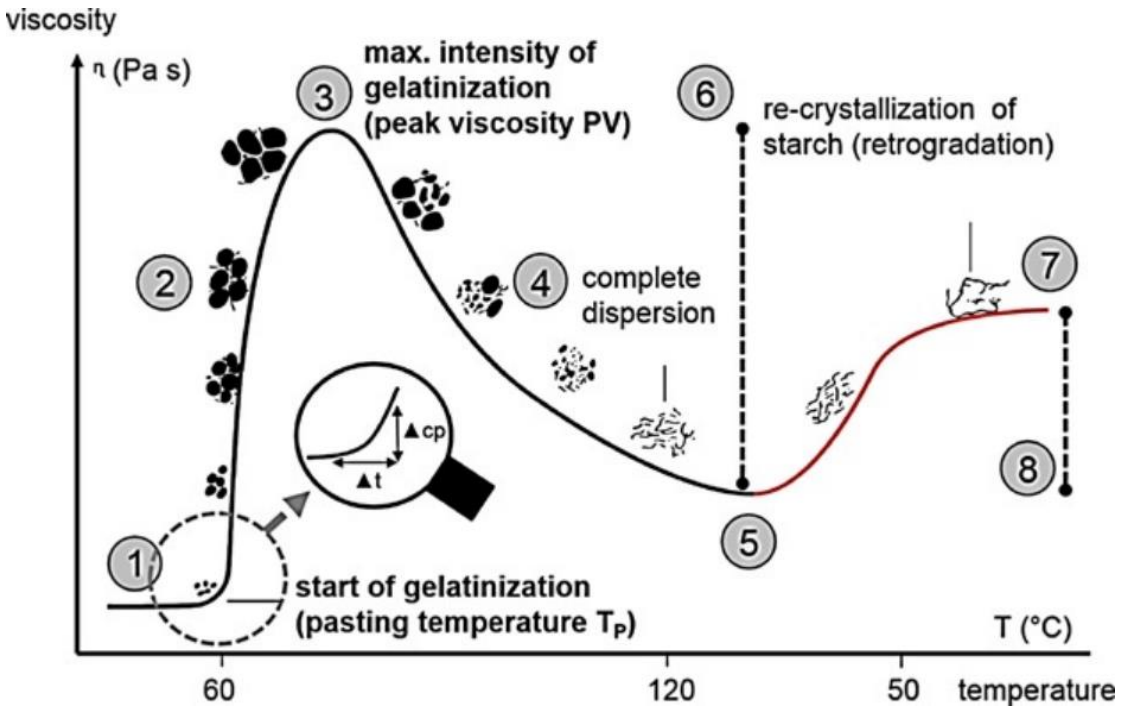

Figure 2.8. RVA viscosity diagram of natural starch. (1) TP, pasting temperature, (2) hydration of starch granules, (3) PV, peak viscosity, (4) enzymatic and shear destruction of starch granules, (5) HPV, hot paste viscosity, (6) BD, breakdown, (7) final viscosity (FV), and (8) SB, set back (Schirmer et al., 2015)

From the figure, the RVA curve shows the five stages of the experiment, including adding water, heating, maintaining the highest temperature, cooling process and the final maintenance stage. The pasting temperature (PT) for judging gelatinization characteristics and the maximum viscosity (PV) during the process were also shown (Balet et al., 2019). Heating stage in the process of starch granules swell and viscosity increases, the amylose from particles precipitate; In the final stage, the phenomenon of retrogradation occurs because of the rearrangement of starch (Schafranski et al., 2021). Also, the HPV means minimum viscosity of the gel during colling stage, the BD means the viscosity loss and the difference between the final viscosity and HPV would be named by total set back (Li et al., 2016). At the same time Schirmer et al. (2015) believe that the parameters obtained by RVA can be widely used in the food industry. For example, Tp indicates the beginning of the gelatinisation stage and is applied to the production of malt pulp. As an expression of gelatinization strength, PV can be applied to the production of sauces.

The image of RVA after HMT modification is quite different from that before treatment. The gelatinisation temperature of HMT-modified starch was higher than that of natural starch, and the peak viscosity and setback viscosity were lower than the nature starch. This not only indicates the optimisation of long- and short-range structure during HMT modification but also enhances crystallinity and particle agglomeration and produces more molecular cross-linking and in-chain association (Schafranski et al., 2021). In short, HMT modification mostly enhanced the thermal stability of natural starch (Cherakkathodi et al., 2020). At the same time, the improvement of natural starch gelatinisation parameters by HMT is often influenced by the treatment temperature and water content during the modification. Rafiq et al. (2016); Sun et al. (2014) found that gelatinisation temperature and water content increase, and the peak viscosity is inversely proportional to water content. Some studies have also shown that the correlation between crystallinity and amorphous regional chains after the HMT process leads to a decrease in starch's peak viscosity and setback value (K. Liu et al.,

2019). Moreover, the type of starch often affects the RVA curve. For example, the RVA curve of waxy corn starch after HMT modification has no significant change compared to natural waxy corn starch; this result is due to the low content of amylose in waxy corn starch (Sui et al., 2015).

2.9 Differential Scanning Calorimetry (DSC)

As a method that can simulate the starch gelatinization process, DSC can measure the relevant parameters quantitatively and qualitatively. As endothermic reactions often occur during gelatinisation, differential scanning calorimetry can be used to monitor the gelatinisation of starch (Zhu, 2019). Natural starches often show different DSC results, which are not only affected by the starch source but also by the structure of the starch (Ai & Jane, 2015). Plenty of evidence suggests that the HMT modification makes natural starch pasting parameters (as the To, Tc, Tp, delta T as and ΔH) change. Some research results showed that the treated HMT starch exhibited higher To, Tc, Tp and ΔH (Huang et al., 2016; Pinto et al., 2015; Van Hung et al., 2017). However, as for the value of gelatinisation enthalpy, the gelatinisation enthalpy decreases in most cases. Xie et al. (2019); Chung et al. (2009); Zeng et al. (2015) found that the gelatinisation enthalpy of HMT starch decreased significantly compared with that of natural starch and speculated that this phenomenon was caused by the destruction of the double helix structure of starch in the process of HMT treatment. However, the interwinding of amylose and amylopectin increased during the modification of most HMT, which promoted the diffusion of starch molecules. This often makes starch need more energy and temperature to swell. However, the higher swelling temperature may exert pressure on the crystallisation region of starch, thus destroying the crystallisation region and increasing the transition temperature (Schafranski et al., 2021; Sui et al., 2015).

2.9 Gel texture

When water and starch contact, it will penetrate the starch and will not cause disturbance of micelles. However, the hydrogen bond structure will break when water and heat act together. As a result, water will infiltrate into the micelles, and the particles will irreversibly expand, a phenomenon known as gelation (Schafranski et al., 2021). The starch gel is a solid-liquid system with a continuous network structure; starch particles are part of the solid continuous network, and amylose in the continuous phase can form a strong gel after cooling (Collado & Corke, 1999). In addition, Collado & Corke (1999) also found that hydrogen bonds would be formed between free amylose and amylopectin in the gel system. Therefore, amylopectin can form a continuous phase in some starch with less amylose content. Therefore, the change in starch gel properties caused by HMT may be related to the types of continuous phases in the gel (Collado & Corke, 1999). At the same time, Bao et al. (2004) found that the texture of gels was significantly correlated with the content of characterised amylose, whether in free state, absolute state or compound amylose with lipids. Therefore, the change degree of starch gel characteristics on HMT is affected by amylose content. For starch gel characterisation, gel strength can usually be determined using a texture analyser with "single point" measurements (Ai & Jane, 2015). Starch modified by HMT often exhibits stronger hardness (Adawiyah et al., 2017). The change of gel adhesion and cohesion on HMT is often affected by starch source and internal structure, and gel texture also affects characteristics to a certain extent (Kong et al., 2009).

2.10 Flow property

The shear stress of starch pastes formed from natural starch does not increase linearly with the increase in shear rate, which indicates that most natural starch pastes are non-Newtonian fluids (Ai & Jane, 2015). At the same time, the flow characteristics

are often characterised by exploring the relationship between shear rate and viscosity; the power-law and Herschel-Bulkley (H-B) model are often used to express starch flow (Kong et al., 2010; Li & Zhu, 2018b). The results of H-B model fitting show the consistency coefficient, flow behaviour index and yield stress of starch samples (Li & Zhu, 2018b). These fluid parameters not only express the fluid properties of starch, but also show the gelatinization properties of starch. The HMT-modified starch paste showed different rheological properties from the natural starch: shear thinning phenomenon increased (Li & Zhu, 2017).

2.11 Oscillation property

As a common machine for characterising starch gel, a dynamic rheometer can continuously measure and analyse its dynamic modulus at various temperatures and shear rates (Ai & Jane, 2015). The obtained values of the energy storage modulus, loss modulus and loss Angle tangent (Tan δ = G"/G') of starch gels will be recorded, and each parameter expresses different properties of starch gels (Biliaderis, 2009). Where G' represents the elastic behaviour of starch gel, and G'' represents the viscous behaviour of gel. Moreover, the value of tan δ expresses the state of the gel. The larger the value, the more liquid the starch gel is, and the harder the gel is otherwise (Li & Zhu, 2018b). The gel viscosity expressed by different natural starch varies greatly, which is not only affected by the starch source but also by the grain structure, particle size, amylose content and amylopectin structure of the same kind of starch (Li & Zhu, 2018B; J. Singh et al., 2002; N. Singh et al., 2003; Zhu et al., 2016). In general, the energy storage modulus of HTM-modified starch will increase, the loss modulus will decrease, and different starches will be affected by HMT treatment in different ways (X. Liu et al., 2016; S. Singh et al., 2005).

Chapter 3: Materials and methods

3.1 Materials

The quinoa seeds were purchased from Countdown (Auckland, New Zealand). The amaranth seeds were collected from the online shop Goodfor (Auckland, New Zealand). The fresh taros were collected from green grocery located in Auckland South, and the suppliers were from Fiji. Potato and maise starch were purchased from the online shop Goodfor (New Zealand). The quinoa and amaranth seeds were ground into grain flour by a high-speed blender. The Megazyme total starch content kit (Megazyme, Bray, Ireland) was used to analyse the total starch content for each starch sample.

3.2 Chemicals

All the chemicals used in the experiments are shown in Table 3.2.1. And all the experiments equipment is shown in Table 3.2.2.

Table 3.2.1. Chemicals.

Chemical	Supplier
Calcium chloride (CaCl2)	Sigma-Aldrich, USA
Ethanol C2H5OH	Ecp-Laboratory Reagent
Hydrogen chloride (HCl)	ECP, Ltd, New Zealand
Milli-Q water (H2O)	Millipore Corporation, USA
Rice bran oil	Countdown, New Zealand
Sodium acetate (C2H3NaO2)	Sigma-Aldrich, USA
Sodium acetate (C2H3NaO2)	Sigma-Aldrich, USA
Sodium Dodecyl Sulfate	Sigma-Aldrich, USA
Sodium hydroxide (NaOH)	Sigma-Aldrich, USA
Sodium metabisulfite (Na2S2O5)	Sigma-Aldrich, USA
Total Starch Assay Kit (AA/AMG)	Megazyme International, Ireland

Table 3.2.2. Equipment.

Equipment	Model	Manufacturer
Aluminum pan	-	Two dollars shop, New Zealand
Balance	Mettler Toledo XS 205	Mettler-Toledo Ltd., Australia
Centrifuge	Thermofisher Scientific Sorvall Lynx 4000 Centrifuge	Thermo Fisher Scientific, USA
Centrifuge	ThermoFisher, HeraeusTM LabofugeTM 400 Centrifuge	Thermo Fisher Scientific, USA
Differential scanning calorimeter	Q1000 Series	TA Instruments, USA
Freezer	Model 8425	Sonics & Materials, Inc, USA
Gel Texture Analyzer	TA–XT plus	Stable Micro Systems Ltd., UK
Hot plate	RCT B S104 IKA	Germany
Oven	Model MOV-112P Program Oven	Sanyo Electric Co, Ltd., California
pH meter	Schott Instrument pH Metre, Lab 850	Xylem Inc, Germany
Pipette	Eppendorf 200 µL /1000 µL volume pipette	Eppendorf, Germany
Refrigerator	Model SRS 535NW	Samsung, Korea
Rheometer	Physica MCR 301 Stressed Controlled Rheometer	Anton-Paar, Austria
Rheometer	Physica MCR 302 Stressed Controlled Rheometer	Anton-Paar, Austria
Scanning electron microscope	HITACHI SU-70	Tokyo, Japan
Shaking water bath	W28, Grant	Barrington, England
Stirring hot plate	MR 3001 Magnetic Stirring Hotplate	Heidolph Instruments Gmbh & Co., Germany
UV spectrophotometer	Spectronic 200	Thermo Fisher Scientific, USA
Vortex mixer	Vortex Mixer VF2	IKA Laboratory, Germany

3.3 Starch extraction

3.3.1 Quinoa starch extraction

Quinoa starch was extracted by the method according to Li et al. (2016), and partial optimisation was carried out. First, the quinoa seeds were frozen by liquid nitrogen for 2 minutes and then used the coffee bean grinder pulverise the seeds into flour for 1 min. Each 100g quinoa powder mixed with 1 L sodium borate buffer (12.5mM, pH 10, including 0.5% sodium dodecyl sulfate (SDS) [w/v] and 0.5% $Na_2S_2O_5$ [w/v]) for 30 min to remove the lipids and proteins. Then centrifuge the mixed solution containing solid seeds under 6000 x g for 10 min and remove the supernatant completely. The solid was washed with 1 L of deionised water and repeated the centrifuge step to wash the buffer. Because of quinoa starch's characteristics, the residue was suspended in 1 L of distilled water and stirred overnight to fully release protein from starch granules. Afterwards, the mixed solution passed through four layers of cheesecloth and 140 μm nylon mesh. The rest of the suspension was centrifuged six times under 6000 x g for 10 min. For each centrifuge, brown proteins would appear at the top with distinct layers of starch; there were obvious particulate matter impurities at the bottom of the centrifuge bottle, which has a distinct stratification with starch as well. After each centrifugation, the upper protein and lower impurities are scraped or removed to ensure starch purity. And each centrifugation, 100 g residue was washed with 1 L deionised water to make sure to remove the SDS. The remaining starch, after six centrifuges, is put into the air-forced oven at 35°C for 48 h. The starch was then ground and sieved (250μm nylon mesh) to obtain starch for experimental use. The starch was stored in a desiccator.

3.3.2 Amaranth starch extraction

The extraction method of amaranth starch is roughly the same as that of quinoa starch. The method referred from Zhu (2017) was selected, and some modifications were made. Because amaranth starch is very small grain starch, the centrifuge parameter was changed to 10000 x g for 10 min.

3.3.3 Taro starch extraction

Taro starch was extracted using the process of Jane et al. (1992); Wang and Wang (2004) and with some improvement. Fresh taros were cut into evenly sized pieces about 2 to 3 centimetres wide after peeling. Beat the sliced taro with ice for 2 minutes in a blender. After that, each 100 g taro (including ice) was stirred with 1 L NaOH solution (0.05%) and stirred in the mixture for another two minutes. Afterwards, the taro starch slurry was through four layers of cheesecloth, and the ice was added to the residue to repeat the mixing and sieving step. The last remaining residue was mixed into the remaining buffer with a magnetic stirrer (500 RPM) for 1 hour and through cheesecloth again. The residue was recovered by centrifugation at 3000 x rpm for 20 min. There would be a brownish red protein layer appears in the upper layer, which is clearly separated from the lower starch and completely scraped off the upper protein after centrifugation. This step was repeated four times to remove the protein utterly. The starch fraction was dried in an air-forced oven at 45°C for 48 h. Then starch was ground to powder and sieved into the nylon mesh (250μm). Finally, the starch obtained was sealed and stored in a desiccator.

3.4 Heat-moisture treatment

Heat-moisture treatment is a common thermal treatment method, and the range of temperature and moisture content is wide, so the specific parameters of the experiment refer to many methods (Andrade et al., 2014; Bharti et al., 2019; Bian & Chung, 2016; Pinto et al., 2015; Singh et al., 2005; Tan et al., 2017) and make corresponding changes to them. The starch sample (80 g, dry basis) was weighed into a glass container. The weight of the added water (Q) was calculated by equation (1), and water was gradually added to the container, making sure that the water and starch were thoroughly mixed in the process so that the final starch sample with 30% moisture content was obtained. The starch samples were sealed and placed in a refrigerator at 4°C for 24 hours. The oven should be preheated to a constant temperature of 120°C. Put the prepared starch sample into the oven quickly and keep it for 1 hour. Then, after the processed starch sample cooled, the lid was opened and dried in an oven at 40°C for 48 hours. Finally, the obtained starch samples were ground, sieved (250 μm nylon mesh), and stored in a desiccator.

$$Q = \frac{(Mf - Mo)}{(100 - Mf)} \times w$$

Equation (1)

Q = Water added, ml

Mf = Final moisture content, %

Mo = Initial moisture content, %

W = Sample weight, g

3.5 Moisture content (MC)

An air oven (Heratherm OMS180, Thermo Scientific CO LTD, Germany) was preheated to 120°C before testing, and the aluminium pans were placed in the oven

to dry for at least 15 minutes to make sure the constant weight could be gained.

Then the pan was weighted (W). 200mg (W0) starch powder was weighed into aluminium plates and put in the oven for 24 hours. The weight (W1) of starch and pan after drying should be recorded.

$$MC = \frac{W1 - W}{W0} \times 100\%$$

Equation (2)

3.6 Total starch

The method of testing the total starch was followed by the AOAC method 996.11 & AACC method 76-13.01, as cited in Megazyme (2020). Starch samples were taken through a 0.5mm mesh, and 100mg samples were weighed and divided into experimental and control groups. For both groups of starch, 10ml of sodium acetate buffer swirl for 5s to ensure uniform mixing. In the experimental group, 0.1ml kit of one reagent was added, and in the control group, 0.1ml sodium acetate buffer and calcium chloride solution were added to vortex 3s. The experimental group and the control group were simultaneously transferred to a boiling water bath and heated at a constant water temperature of 50 degrees for 15min. Swirl 5 seconds every 5 minutes during heating. In the experimental group, 0.1 AMG (bottle 2) was added, and in the control group, 0.1ml sodium acetate solution was added, and they were heated in a 50°C water bath for 30min. After heating and taking out at room temperature for 10min, 2mL suspension was centrifuged for 5min, 1.0ml supernatant was taken out, and 4mL sodium acetate was added. In the experimental group, 0.1ml of GOPOD Agent was taken from the control group. 3 ml GOPOD Agent was added to the control group and heated in a 50°C water bath for 20min, and the absorbance was measured at 510nm. At the same time, add 3mL GOPOD into 0.1ml glucose solution, a total of four copies; In the blank group, 0.1ml sodium acetate buffer and calcium chloride

were added, as well as 3ml GOPOD agent, two copies in total.

3.7 Protein content

The extracted starch was determined for protein content to ensure the accuracy of the experiment. This experiment selected the Kjeldahl method (AOAC, 2000, as cited in Sáez-Plaza et al., 2013). Around 0.3g (wet basis) starch was weighted and in duplicate. The weighed samples were transferred to the digestion tube, and an empty tube was kept as a blank group. After that, about 10g of potassium sulfate was added to each experimental sample, and 0.1g of a mixture of titanium dioxide and copper sulfate (1:1) was mixed. This process ensures that the two powders are well-mixed. After evenly mixing with the sample, 20ml of concentrated sulfuric acid was weighed and poured into each digestion tube. The digestion process was performed using a speed digester numbered Buchi B-426. The digestion tube with concentrated sulfuric acid was successively fixed on the instrument and heated. After heating the sample to light green and ensuring that the green colour does not disappear for 10 minutes, the instrument is turned off, and the sample is cooled.

In the next stage, a boric acid solution is prepared for titration. Type-1 water is selected to prepare 2% boric acid solutions and to reach 60ml equivalents in each conical flask. Then ten drops of methyl red indicator were added to the boric acid solution to give each conical solution an orange pink colour. Next, the cooled mixed sample solution was subjected to Kjeldahl distillation using a distillation apparatus (K-350). During this process, NaOH solution was added to the reaction sample, and the lower end of the instrument was connected to a preconfigured boric acid solution. This process continues until the sample turns blue or brown, and the resulting distilled sample is titrated when NaOH solution is added without jolting. A 0.1M solution of HCl was used to titrate the blue solution after Kjeldahl distillation, and the volume of HCl used to restore the blue to the pink solution was recorded. Finally, the starch samples

selected protein content calculated by the following formula:

$$\text{protein content } \% = \frac{\text{F}\times 14\times(\text{ml of HCl})}{\text{sample weight}} \times \frac{0.1\text{M HCl}}{1000\text{ ml}} \times 100 \qquad \textbf{Equation (3)}$$

Where ml of HCl=sample reading - blank reading.

Where F is the conversion factor used.

3.8 Pasting analysis

The method of pasting was referenced by Li et al. (2016), and the equipment was selected the MCR 301 Rheometer (Anton Paar, GmbH, Ostfildern, Australia). This equipment was equipped with a starch cell and ST24-2D probe.

2.0 g starch was mixed with 20 mL deionised water. There were four stages during the test. First, the beginning temperature was 50°C, and the sample was kept for 5 min. Then the samples were heated to 95°C for 7.5 min and kept at 95°C for 5 min. The next step was cooling to 50°C for 7.5 min. Finally, the starch sample was kept at 50°C for 2 min. The pasting temperature (PT), peak viscosity (PV), peak temperature (PKT), hot paste viscosity (HPV) and cool paste viscosity (CPV) were recorded. The remaining parameters breakdown (BD=PV - HPV), setback (SB=CPV - HPV), stability ratio (SR=100 x HPV/PV), and setback ratio (BR=CPV/HPV) were calculated. The viscosity was shown in Rapid Visco Unit (RVU).

3.9 Gel texture analysis

The gel texture analysis was selected by the method from Li and Zhu (2017, as cited

in Zhu & Li, 2019). The gels were selected by a 5 mL glass canister after the pasting and centrifuged under 1000 x g for 5 min to ensure the top layer of the gel was flat. Then the canisters were stored at 4°C for 24 h. The gel texture property of starches was measured by a TA-XT plus Texture Analyser (Stable Micro Systems Ltd., Surrey, UK) with a 15 mm diameter cylinder probe under Texture Profile Analysis (TPA) mode. Each test was compressed to 15 mm depth and set the speed under 0.5 mm/s with a 0.03 N trigger force. Moreover, hardness (HD), adhesiveness (AD) and cohesiveness (CH) were measured. The gumminess (GUM) was equal to HD×CH. The maximum force of the probe in the first compression is hardness, the negative area under the curve in the first rebound process is adhesiveness, and the final cohesiveness force is the ratio of the positive force area in the first compression (Zhu, 2017).

3.10 Flow properties of starch

The method of starch flow analysis was selected by Zhu et al. (2016) and modified. Around 0.402 g of starch flour (db) was weighed and mixed with distilled water, reaching a wet weight of 6 g in total. On the other hand, ensure that the gel concentration after the experiment was 6.7% (w/w). The samples were then continuously shaken in a 90°C-water bath for 15-30 minutes to ensure uniform heating and then heated in a 90°C constant temperature water bath until 1 hour in total. Finally, the MCR 301 Rheometer was selected, and the PP-50 probe was used. The heated starch samples gel was transferred to the plate of the machine with a dropper to ensure that the gel was even and flat on the surface. Then a few drops of rice oil were added to seal the gap between the plate and probe. The flow analysis experiment parameter was selected, shearing from $0.1s^{-1}$ to $1000s^{-1}$ in the first stage and changing from $1000s^{-1}$ to $0.1s^{-1}$ at 25°C. The consistency coefficient (K), flow behaviour index (n), coefficient of determination (R^2), and yield stress (δ0) were recorded during the test. Then the data was calculated by the following equations:

$$\delta = K.\gamma^n$$

Equation (4)

$$\delta = \delta_0 + K.\gamma^n$$

Equation (5)

3.11 Oscillation analysis

The starch oscillatory properties were analysed by a method described by Zhu, Bertoft, & Li (2016), using a rheometer (Physica MCR 301 Stressed Controlled) with the PP-25 probe. Briefly, around 0.22 g to 0.23 g (wb) of starch samples were accurately weighted to ensure the starch flour weight could be above 0.2 (db) and put into the EP tube. The amount of Milli-Q water (around 750 ml) added was four times the dry weight of the powder and mixed well in a vortex. 0.515ml starch suspension was transferred to the rheometer instrument plate with a pipette, and a few drops of rice oil were removed with a dropper to seal the gap between the probe and the plate. Then the experiment parameter amplitude gamma was set to 2%, and the frequency was selected at 1 Hz. At the beginning of the test, the sample was equilibrated under 40°C for 2min and heated up to 95°C at the rate of 2°C/min. Then cooled from 95°C to 20°C with the same speed rate. At the end of testing, the frequency sweep was increased from 0.1 to 40Hz at 25°C and was maintained at 25°C for 5min. The storage module (G') and loss module (G") would be recorded. Also, the damping factor (tan δ = G"/G') would be obtained. At the same time, the gel obtained after the end of the temperature change part of the oscillation experiment was measured by frequency sweep. The samples were kept at 25°C for five minutes and then scanned at frequencies ranging from 0.1 to 40Hz, with rates ranging from 0.628 to 249.944 radians/SEC (Li & Zhu, 2018). G 'and G' at 0.1Hz and 40 Hz were recorded.

3.12 Thermal analysis

The thermal property of starch was measured due to Li et al. (2016). Briefly, samples were tested by a Q1000 Tzero Differential Scanning Calorimeter (DSC) machine (TA Instrument, New Castle, USA). Starch flour (3.5mg, db) was weighted into an aluminium pan (Φ 5.4 x 2.0 mm) and mixed with 3x w/v Milli-Q water. The water was injected by a micropipette and stirred with the tip of a needle to ensure a complete mix. Before each sample was tested, the sealed sample should be placed at room temperature for 1 h to ensure that the water balance of the tested sample was complete. An empty pan which contains air was used as a reference. The range of thermal scan was selected from 10°C to 90°C for native starch, and HMT samples were chosen over a range of 10°C to 105°C. All the samples were under a heating rate of 10°C/min in a nitrogen atmosphere. The starch tested was stored in a 4°C refrigerator attached to a crucible tray for four weeks to do the retrogradation analysis at the same instrument parameters. The onset temperature (To), peak temperature (Tp) and conclusion temperature (Tc) were recorded during thermal transitions of each starch sample. The enthalpy of gelatinisation (ΔH) was measured by Universal Analysis 2000 software (version 4. 1D, TA Instruments, New Castle, USA) due to the area of the endothermic peak. And the range of gelatinisation temperature (ΔT) was calculated by Tc and To (ΔT=Tc-To).

3.13 Swelling power (SP) and water solubility index (WSI)

The SP and WSI of the starch sample were using the method according to Li et al. (2016) with modification. Starch flour (0.15 g, db) was accurately weighed and added into a 15ml centrifuge tube. The tubes were weighed and recorded before adding samples. Then each starch sample was mixed with 10 ml Milli-Q water and shaken rapidly. After mixing thoroughly, the sample was quickly put in an 85°C water bath for

1h. During the first 15 to 20 minutes of the heating process, all the samples were swirled to ensure uniform heating until the bottom of the sample gelatinises. After thermal treatment, all the tubes were cooled in ice water for 5 minutes and centrifuged under 3000 x g for 30 minutes. The sample from the tube was poured into the aluminium plate after centrifugation, and the remaining solid was weighted (Ws). The aluminium pans were dried in 120°C air-oven for 15 min before the supernatant was dropped into them. Moreover, the supernatant in aluminium was put into a 120°C air oven for 48h to ensure to dry a constant weight (W1). Finally, the water solubility and swelling power were calculated by the following equations:

$$WSI = (\frac{W1}{W0}) \times 100\%$$

Equation (6)

$$SP\ (g/g) = \frac{Ws}{W0 \times (1 - WSI)}$$

Equation (7)

3.14 X-ray diffraction analysis of starch (XRD)

The method of starch crystallinity analysis was followed by an XRD-based method from Zhang et al. (2017). A desiccator containing 44 % potassium carbonate (K_2CO_3) was used to balance starch samples. Around 1g to 1.5g (wb) starch sample was weighted into a small plastic pan and stored on the top K_2CO_3 solution for one month. The crystallinity of starch was determined using XRD (PANalytical Empyrean X-Ray Diffractometer Almelo, The Netherlands). The determination method was according to Wang et al. (2016), and some were modified. Using CuK as the radiation source, the operating parameters are 40mA and 40KV, and the wavelength parameter is 0.1540nm. The diffraction angles range from 4° to 40°.

Then the X-ray diffractometer was used to test the starch crystallinity, and the results were calculated by the following equation:

$$\text{Degree of crystallinity}(\%) = \text{Ac} \times 100/(Ac + Aa)$$

Equation (8)

Ac: total area of crystalline peak.

Aa: amorphous of the diffractogram.

3.15 Scanning electron microscopy (SEM)

Treated and untreated starch samples are pasted with black double-sided tape and fixed to a metal substrate. The treatment was then performed under vacuum conditions using Hitachi E-1045 ion sputtering machine (Tokyo, Japan). Finally, the morphology of all starches was observed by Hitachi SU-70 scanning electron microscope (SEM) (Tokyo, Japan) at an accelerated potential of 10kV.

3.16 Particle size analysis

The particle size analysis method was done according to Li and Zhu (2018), using the Mastersizer 2000 particle size analyser (Malvern Instruments, Malvern, UK). Each starch sample was taken and mixed with Milli-Q water to prepare a starch suspension of a concentration of 10g/kg before the test. Due to small grains of natural starch tend to aggregate (Lindeboom et al., 2004), the prepared suspension was placed in an ice water bath for ultrasonic treatment for 1 hour. During this time, ice cubes should be added to ensure the temperature is not too high to prevent the starch from gelatinising. The reason for ultrasonic treatment is to break up the starch before and after treatment, especially the small starch so that the particle size of individual starch can be accurately measured.Then the suspension was drawn by a dropper and added to the dispersion unit of the instrument. This process should be done slowly to ensure the proper obscuration factor is between 5% and 10%. Finally, the volume-weighted

mean diameter (D [4, 3]), surface-weighted mean diameter (D [3, 2]), and median diameter (d (0.5)) will be obtained.

3.17 Statistical analysis

All the experimental data for statistical analysis were performed using Origin software (version 8.6, MA, USA: Originlab corp) and SPSS statistical software (IBM SPSS Statistics for Window, Version 22.0. Armonk, NY: IBM Corp). The analysis method chose the One-way analysis of variance (ANOVA) method. The Tukey method was selected for the ANOVA, and the significance level was defined as $p<0.05$. The image was drawn using Origin software. Furthermore, the Highscore Plus (version 4.5. Almelo, Netherlands; PANalytical corp) software was selected for the XRD data analysis.

Chapter 4: Result and discussion

4.1 Isolation starch

Table 4.1 Moisture content of native starches and HMT starches.

Sample	Moisture Content (%)
NQ	11.87 ± 0.55 d
NA	12.23 ± 0.44 d
NT	14.10 ± 0.27 b
NP	18.47 ± 0.30 a
NM	13.26 ± 0.41 c
HQ	10.58 ± 0.42 ba
HA	9.42 ± 0.33 ba
HT	8.16 ± 0.20 b
HP	10.51 ± 0.05 a
HM	10.48 ± 0.09 a

* Results from moisture content distribution NQ, Native Quinoa; NA, Native Amaranth; NT, Native Taro; NP, Native Potato; NM, Native Maize; HQ, HMT Quinoa; HA, HMT Amaranth; HT, HMT Taro; HP, HMT Potato; HM, HMT Maize. Values in the same column with the different letters differ significantly ($p < 0.05$).

The proximal components of three kinds of natural starches were as follows:
Moisture content: quinoa 11.87 ± 0.55%, amaranth 12.23 ± 0.44%, taro 14.10 ± 0.27%;
The rest of the component content: Quinoa starch has 90.04 ± 1.11% starch and 1.31± 0.02 % protein. Amaranth starch has 93.47 ± 0.40% starch and0.37 ± 0.00% protein. Taro has 88.30 ± 0.54% starch and 0.37 ± 0.00% protein.

Despite these three kinds of small granular starch extraction methods, there is a difference. However, compared to the other amaranth isolation data from Roa et al. (2014), there would be some differences. Roa et al. (2014) found that the amaranth starch extracted by water showed 87.7 ± 0.4% carbohydrate, 5.0% ± 0.1 protein and 1.5 ± 0.1 % of lipid. In addition, because nowadays, the phenomenon of organic products has become popular, Bet et al. (2018) used pure water to wash chemicals to extract method of starch and collected 83.18 ± 0.19% carbohydrates; 2.01 ± 0.03% protein for amaranth starch. These results may prove that the water extracting starch method is feasible.

By comparing the proximal fractions of the extracted starch, it can be found that the results shown by the water extraction method and the method of washing with SDS solution and water are slightly different. Due to this, using SDS to isolate protein and centrifugal with water washing many times can effectively improve the purity of starch. The protein content would affect the accuracy of subsequent experiments. Lim et al. (1999) found through research that protein molecules in starch can often combine strongly with amylose in starch, and the binding mode is mostly through a disulfide bond or hydrophobic bond. Therefore, when extracting natural starch, it is necessary to ensure that the content of other substances in starch is low to reduce the influence on the experimental results. Liu et al. (2015) determined the judgment standard of starch low protein content (0.50-1.09%). The natural starch extracted in this experiment was within the acceptable range. As Zhu (2017) found, since fibre and protein precipitate into a brown layer with starch, it is difficult to extract amaranth starch from amaranth seeds and flour, and sodium hydroxide solution is generally used by the alkali wet-milling method.

4.2 Particle size of starch granules

Table 4.2 Particle size distribution of native starches and HMT starches.

Sample	D (4, 3) (µm)	D [3, 2] (µm)	D (0.5) (µm)
NQ	2.91 ± 0.02 e	1.72 ± 0.00 d	1.75 ± 0.00 e
NA	1.83 ± 0.00 d	1.73 ± 0.00 d	1.79 ± 0.00 d
NT	3.60 ± 0.00 c	2.73 ± 0.00 c	3.39 ± 0.00 c
NP	42.49 ± 0.05 a	35.67 ± 0.05 a	39.47 ± 0.05 a
NM	15.14 ± 0.01 b	13.53 ± 0.01 b	14.42 ± 0.00 b
HQ	84.60 ± 2.55 b	6.27 ± 17.39 c	39.37 ± 0.94 b
HA	55.99 ± 1.27 c	4.14 ± 0.03 e	15.92 ± 0.65 d
HT	11.63 ± 0.11 e	5.95 ± 0.02 d	6.75 ± 0.04 e
HP	87.50 ± 0.75 a	45.57 ± 0.21 a	71.87 ± 0.48 a
HM	30.38 ± 0.56 d	18.74 ± 0.03 b	21.67 ± 0.04 c

* Result from particle size distribution NQ: Native Quinoa; NA: Native Amaranth; NT: Native Taro; NP: Native Potato; NM: Native Maize; HQ: HMT Quinoa; HA: HMT Amaranth; HT: HMT Taro; HP: HMT Potato; HM: HMT Maize.

*D (4,3), mass moment mean; D (3,2), surface area moment mean; D (0.5), volume median diameter; Values in the same column with the different letters differ significantly ($p < 0.05$).

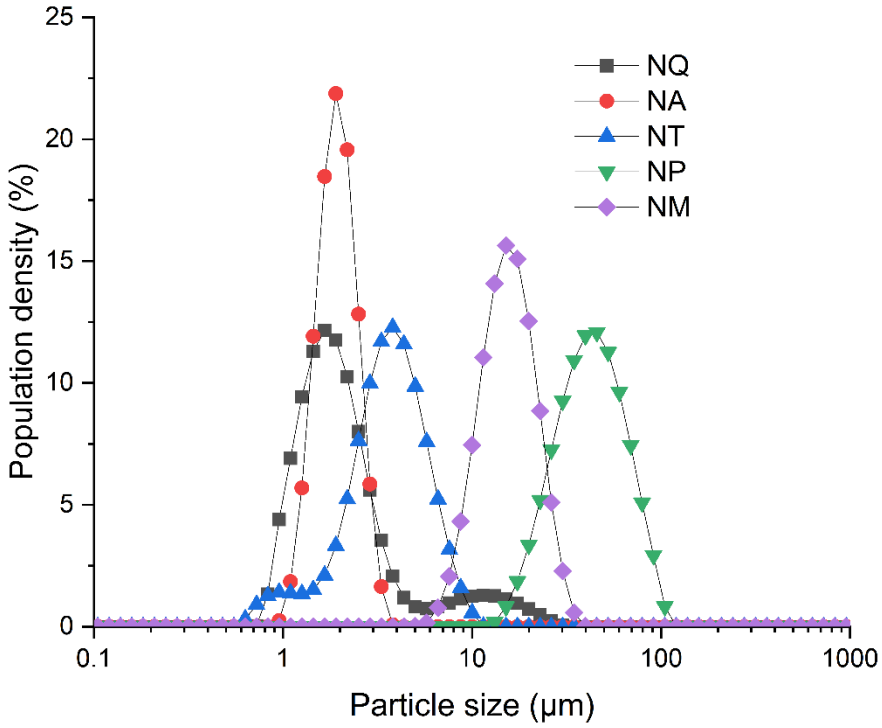

Figure 4.2.1. The size distribution of different natural starches.

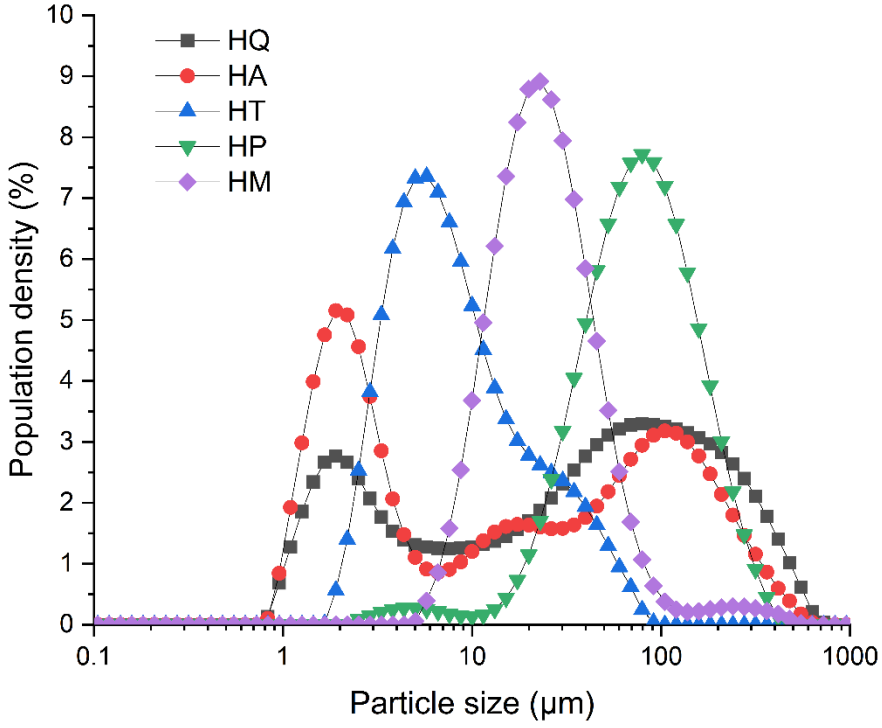

Figure 4.2.2. The size distribution of different HMT starches.

The particle size of starch granules results is shown in Table 4.2. It can be seen from table 4.2 that the five natural starches selected had significant differences ($p>0.05$) before and after treatment. For natural quinoa, amaranth and taro starches are typical small starch grains, and their particle sizes are less than 5 μm. Especially the native amaranth showed the lowest D (4,3) value which was1.83 μm. Lindeboom et al. (2004) had the same research results: amaranth granule size tends to be 1 to 2 μm. At the same time, potato starch and maize starch, known as large starch, especially potato starch, achieved the highest size level, around 42.49 μm for the D (4,3) mass moment mean. By comparing D (3,2), another expression parameter of starch particle diameter, potato starch still had the largest starch particle diameter, and corn starch's grain size was much larger than the three very small starch particles. This phenomenon is consistent with the research results of Bet et al. (2018), Schafranski et al. (2021), and Shi et al. (2018). Moreover, D (0,5), volume median diameter, represents the median size of starch particles, largely reflecting the proportion of starch particles in the total particles. This parameter is of great help for the analysis of starch particle size after treatment.

To some extent, the difference in starch particle size will affect the treatment results of HMT. It can be seen from Table 4.2 that all the small starch grains in the treated starch have obvious multiple increases, while the growth degree of potato starch and maize starch with large starch grains is much smaller than that of small starch grains. After treatment, the value of D (4,3) of very small starch quinoa was increased to 84.60 ± 2.55 μm, which is as large as HMT potato starch (87.50 ± 0.75 μm). Also, amaranth had a similar increase, from 1.83 to 55.99 μm of the D (4,3) value. Comparing the D (4,3) value of starch before and after treatment, very small granule starch quinoa and amaranth increased significantly, quinoa increased 28 times, and amaranth increased around 29 times. Taro, another small granule starch, was around four times larger after treatment. This phenomenon suggested that HMT had similar effects on quinoa and amaranth starches. Pinto et al. (2015) found that the average particle diameter of amaranth starch increased by 320% after HMT treatment with 25% moisture and

120°C, 95.2 ± 0.19μm. At the same time, further investigation of SEM results showed that starch had apparent aggregation after treatment, so it could be concluded that such a large increase of amaranth starch was due to particle aggregation caused by HMT (Pinto et al., 2015). In the subsequent SEM results, a similar aggregation phenomenon also existed. As shown in the figure, part of starch has accumulated to gelatinize, and its structure accumulated from small agglomeration. At the same time, there is not only a mutual aggregation of starch particles but also damage to the external structure of starch. This phenomenon can be seen in the results of SEM later. The Figure 4.2.1 & 4.2.2 show the distribution of starch particle size before and after treatment. It also confirmed that the natural starch particle size is different. For the starch modified by HMT, quinoa and amaranth starch showed two prominent peaks, while taro starch showed no obvious second peak. However, large grain starch did not show this phenomenon. The second peak of the expression of small starch particles was in a higher particle size range, indicating that the small starch particles aggregated after HMT modification, thus making the particle size result much larger.

Finally, according to the experimental results, the particle size of HMT-modified starch increased significantly compared with that of natural starch. At the same time, when comparing the growth range of large particle size and small particle size, it can be found that the growing range of large particle starch under hot and humid treatment is far less than that of small particle size. In other words, the particle size of small starch particles was more obviously modified by HMT.

4.3 Scanning electron microscopy (SEM)

The morphological properties of both native starches and HMT starches were used through scanning electron microscopy, and the results are illustrated in Figure 4.3. And by using different magnifications, the morphology of a single starch granule and the arrangement structure of starch granule in space were observed in detail. As Lindeboom et al. (2004) found that there are two types of particle size distribution: The first is the aggregation of starch particles, as in typical quinoa starch and amaranth starch, the small starch particles are clustered together to minimize the surface area; another manifestation is the actual distribution of individual starch granules. The SEM result (Figure 4.3) can show the particle size distribution of the selected starches from these two aspects.

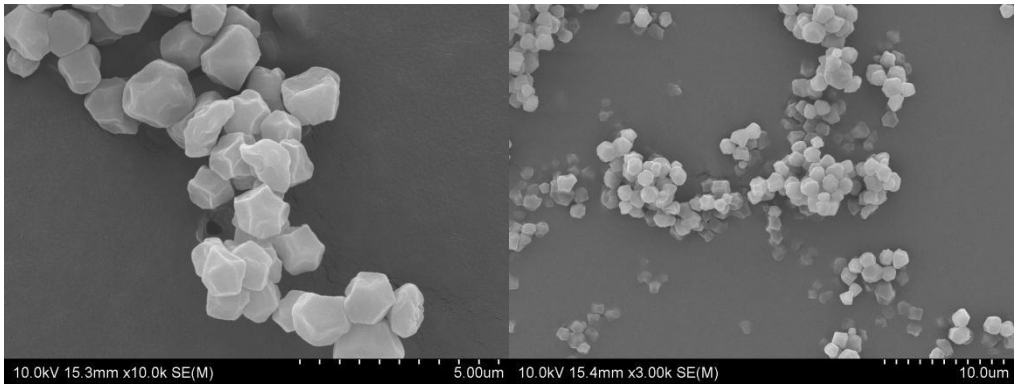

(a-1) **(a-2)**

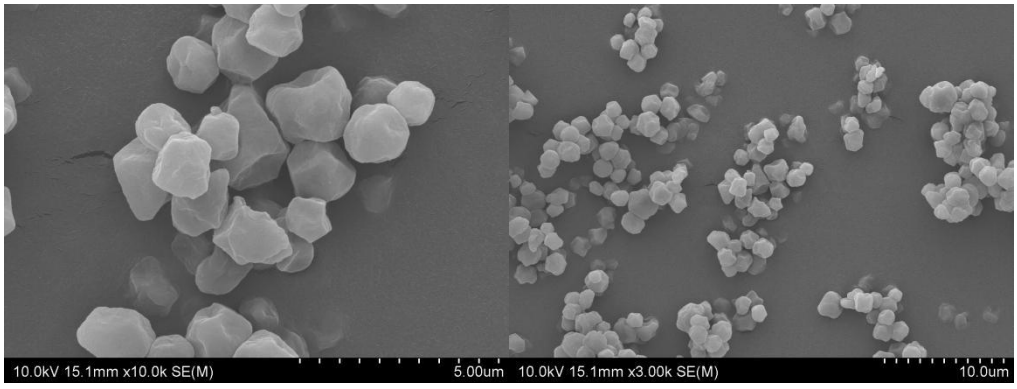

(b-1) **(b-2)**

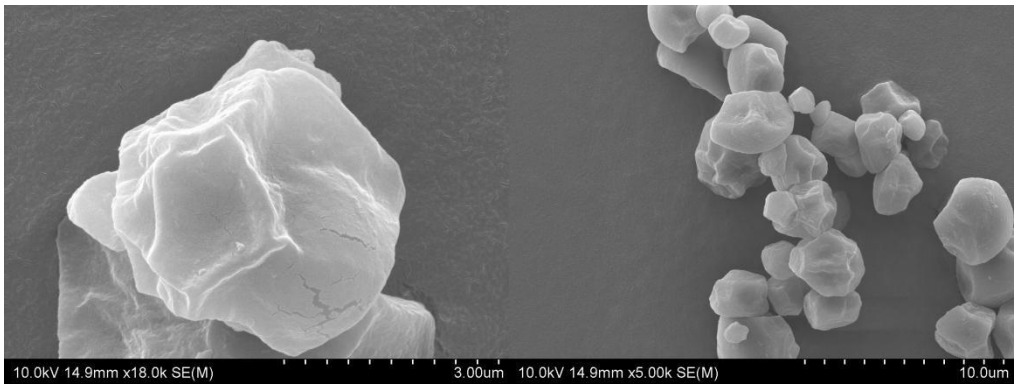

(c-1) **(c-2)**

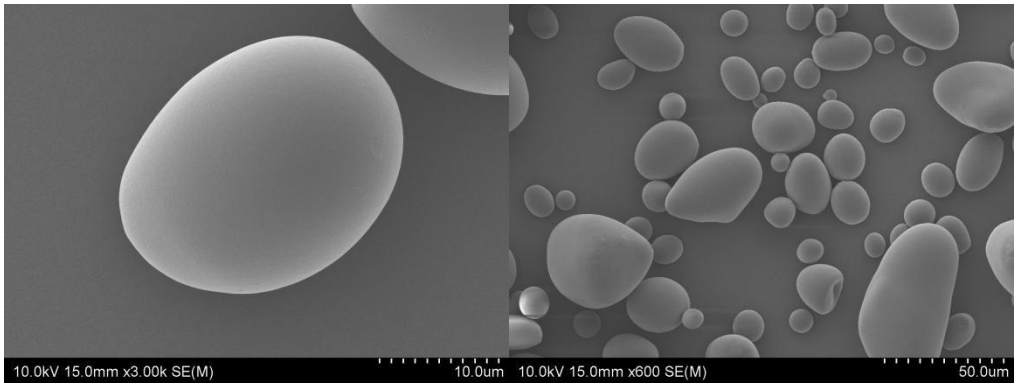

(d-1) **(d-2)**

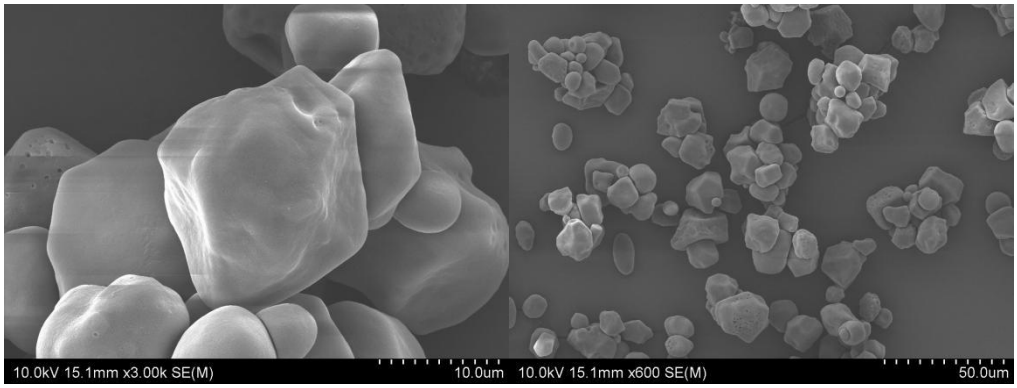

(e-1) **(e-2)**

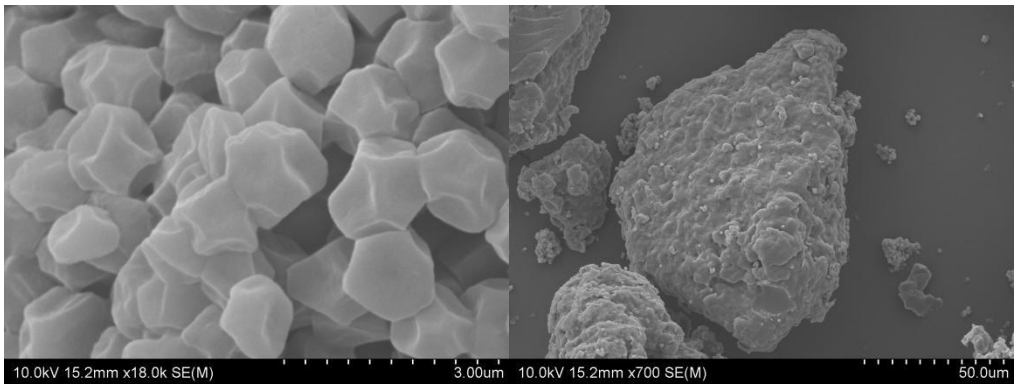

(f-1) **(f-2)**

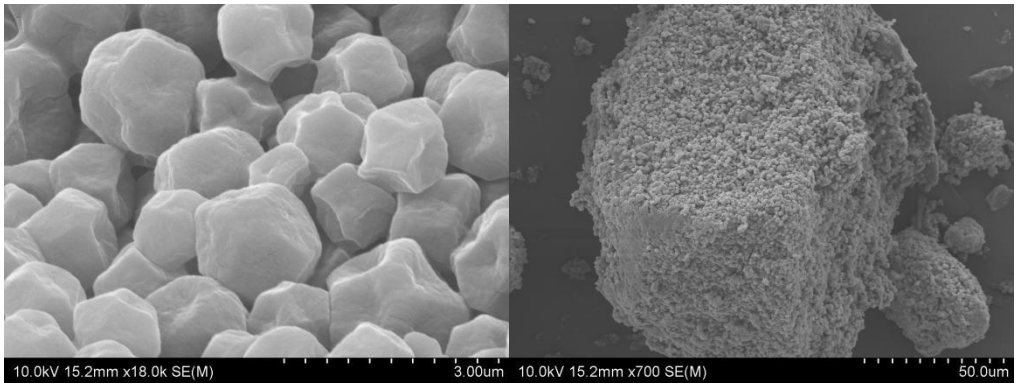

(g-1) **(g-2)**

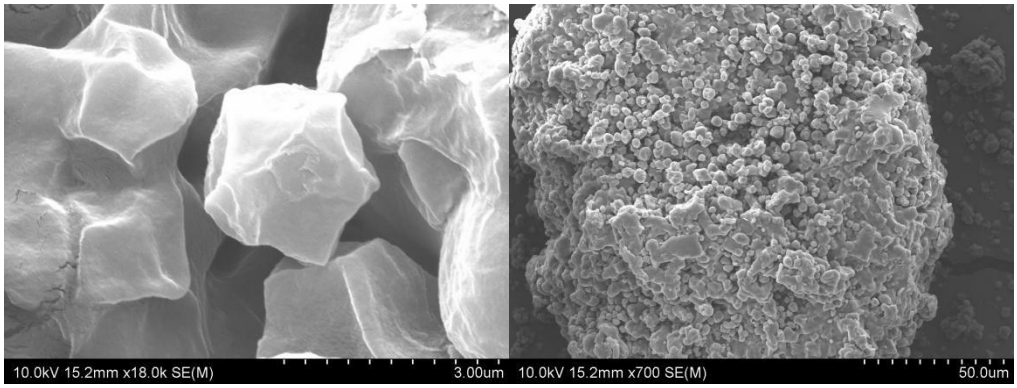

(h-1) **(h-2)**

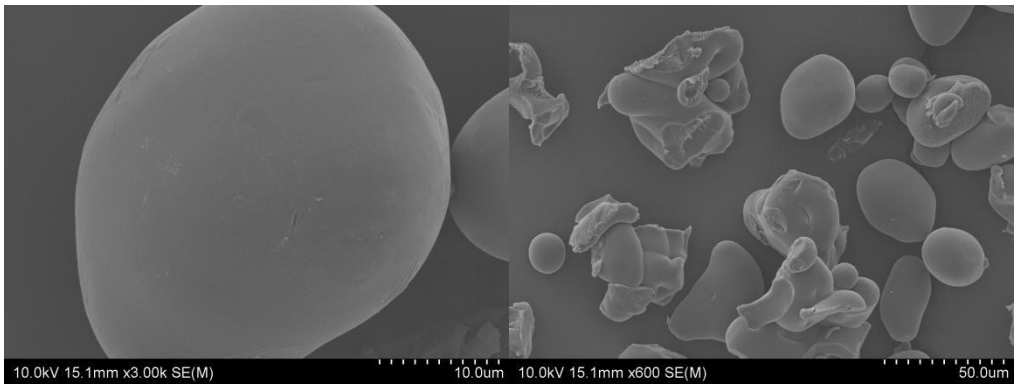

(i-1) **(i-2)**

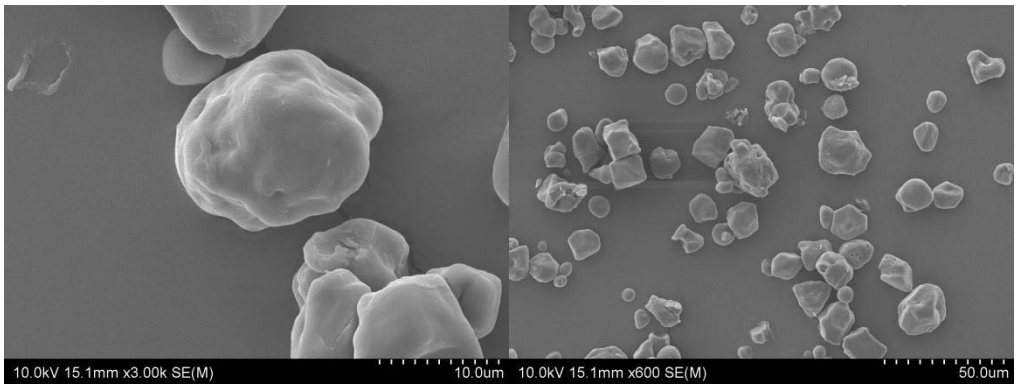

(j-1) **(j-2)**

Figure 4.3 SEM of native starches and HMT starches: (a-1&2), Native Quinoa; (b-1&2), Native Amaranth; (c-1&2), Native Taro; (d-1&2), Native Potato; (e-1&2), Native Maize; (f-1&2), HMT Quinoa; (g-1&2), HMT Amaranth; (h-1&2), HMT Taro; (i-1&2), HMT Potato; (j-1&2), HMT Maize.

By comparing the SEM images of various starch before and after modification, Figure 4.3 showed that the small particle starch appeared to have apparent aggregation after HMT modification. In contrast, the large particle starch aggregation degree was much smaller. This phenomenon would also explain that the particle size of small granule starch increased in a large range, while the large granule starch seems to increase in a small range. Also, the SEM results showed significant differences in the morphology and size of the five natural starches before and after treatment. First, it can be seen

from Figure 4.3 that quinoa, amaranth and taro as small grain starch. Their particle sizes are not more than 5μm; potato starch was still the largest of the five starches, followed by maize starch, so these results were consistent with previous particle size results. Although SEM may not accurately reflect the detailed values of the starch particles to some extent since most starch particles tend to be irregular, it would generally reflect conclusions and values similar to particle size. At the same time, further observation of starch particles after HMT treatment, especially small starch particles, showed that they have the phenomenon of agglomeration obviously, and many large granules are formed in space, which also explains the data in Table 2.2. According to the g (1&2) and h (1&2) from Figure 2.2, part of quinoa and amaranth starch has accumulated to gelatinization, and its structure accumulated from a small agglomeration to a large one after HMT treatment. This would be very similar to the result of Das & Sit (2021). Not only do most starch particles gather with each other, but also some external starch structures are destroyed. Bet et al. (2018) found that by comparing the effects of different HMT parameters on amaranth starch, under the condition of high-water content, no matter how long the treatment time is, amaranth starch will aggregate under SEM observation. Comparing (b-2) and (g-2) from Figure 4.3, it can be found that the original natural small grain amaranth starch in the space of a small amount of aggregation, to the treatment of the amaranth starch under the condition of 30% high water content in many agglomerations. It was also well verified that small starch particles would lead to better aggregation under the condition of HMT. On the one hand, this may be related to the small size of the natural starch particles, which tend to accumulate with each other during treatment due to the relatively high moisture content conditions and the similar electrostatic forces between the particles (Mohanraj & Chen, 2006). At the same time, Lindeboom et al. (2004) found that small starch grains such as quinoa and amaranth could get large spherical particles with a diameter of 30-80mm after spray drying. This phenomenon would also be a reasonable explanation for the formation of very large spherical particles under the heat-moisture treatment because spray drying would also be a method that controls the moisture content and temperature. The HMT starch aggregation would be

because the coupling of pressure and heat in natural starch converts loose particles into compact ones (Watcharatewinkul et al., 2009). On the other hand, the approximation of starch during cooling can be affected by the pre-gelatinization caused by HMT treatment, and the complex (protein-lipid-starch) can also affect the approximation (Pinto et al., 2015). It is often difficult to obtain accurate particle size distribution due to the formation of aggregates or the aggregation of small starch particles, which is also one of the reasons why SEM cannot accurately express the size of starch particles.

Second, the five different natural starches presented different shapes before treatment in terms of particle shape and appearance. Most starch granules are irregular polygons, and elliptical circles and irregular starch shapes can also be seen in SEM images, especially starch with different size particles, whose shapes also seem to be different. Further observation of the treated starch particles, it is not difficult to see that no matter the particle size, the surface of all starch particles appeared to have different degrees of change. The potato starch was slightly damaged, while the other four starches were dented. This result was also verified by the experiment from Shi et al. (2018) which showed that only breakage was observed in potato starch, while relatively large depression was observed in corn and pea starch under 25% moisture content and 120°C HMT treatment (Shi et al., 2018). Similarly, Yang et al. (2019) found that natural polished rice starch particles with different amylose contents were angular, polygonal and without cracks; and after HMT modification, starch particles with higher amylose content showed more agglomeration and melting on their surfaces due to the amylose-amylopectin interaction. Even according to Marta et al. (2019), after HMT physical modification (120°C and 1 h) of breadfruit starch with a natural irregular shape and particle size of 3.0-7.9um, it was found that the physical integrity of starch particles was lost, which may be caused by starch gelatinization. This change was conducive to starch expansion and particle fusion. Generally, the surface of starch particles treated with HMT will be destroyed from slight to complete, and the degree of destruction will be

different according to different parameters of HMT and different types of starch selected (Dai et al., 2019; Deka & Sit, 2016; Dudu et al., 2019; Lee & Moon, 2015). At the same time, Liu et al. (2016) found that there were more deep holes and cracks on the surface of corn starch treated with 30% and 35% moisture content than that treated with 20% and 25% moisture content, which indicated that water content was an important factor affecting the morphological characteristics of starch in the process of HMT treatment, and the formation of holes and holes on the surface could be attributed to AM and AP chains recombined due to the tight amorphous regions in the starch particles so that the holes are formed because of the thermally induced. So, the interaction between chains may be the reason why the morphology of most starches would change after HMT treatment. However, many studies have shown that HMT modification did not significantly change the morphology of starch granules recently (Bian & Chung, 2016; Ji et al., 2015; Kittipongpatana & Kittipongpatana, 2015; Ziegler et al., 2018). The natural starch selected in these studies, in addition to the typical common large grain starch, there is also small grain starch. Both starch particles did not change significantly before and after treatment. Therefore, the particle size difference does not seem to affect the effect of HMT on the starch surface.

In conclusion, the SEM results before and after the treatment of the five selected starches showed that the natural starches had different morphology and size but also expressed that the various starches after the treatment were different by HMT modification. The aggregation degree of small granule starch seems much larger than that of large granule starch. To some extent, it indicated that small starch particles were more affected by HMT and more sensitive. However, when comparing the changes in starch particle surface after HMT, it was found that the effect of starch particle surface seemed to be independent of particle size.

4.4 X-ray diffraction（XRD）

The X-ray diffraction patterns of untreated starch and HMT starch are shown in Figures 4.4.1-4. The X-ray diffraction patterns of all the starches after treatment did not change significantly compared with those before treatment, and the crystal forms of the selected starches did not change.

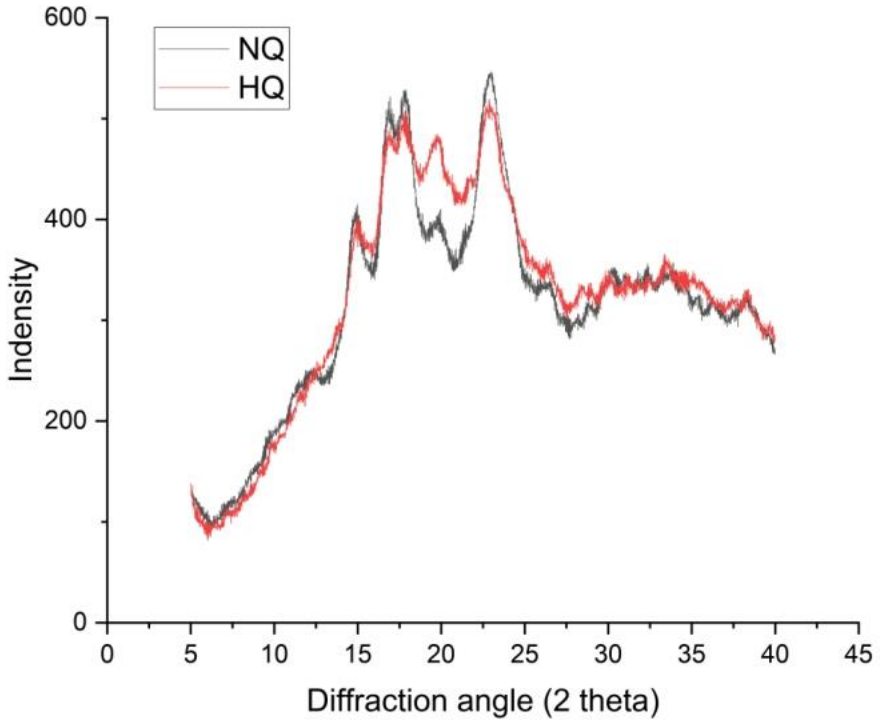

Figure 4.4.1. X-ray diffractograms of Native Quinoa Starch (NQ) and Heat-moisture treatment Quinoa Starch (HQ).

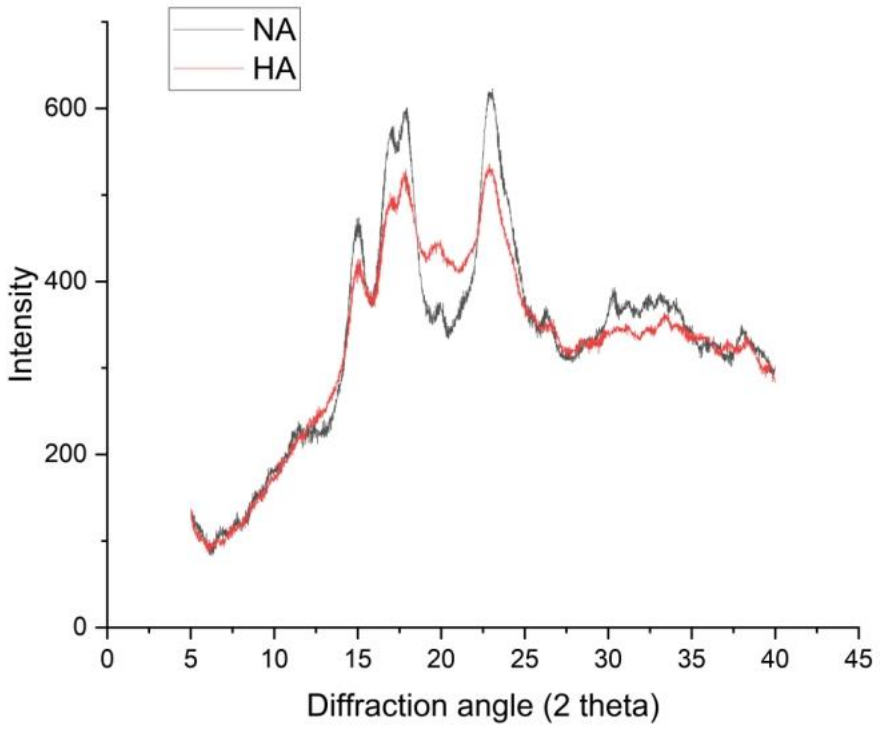

Figure 4.4.2. X-ray diffractograms of Native Amaranth Starch (NA) and Heat-moisture treatment Amaranth Starch (HA).

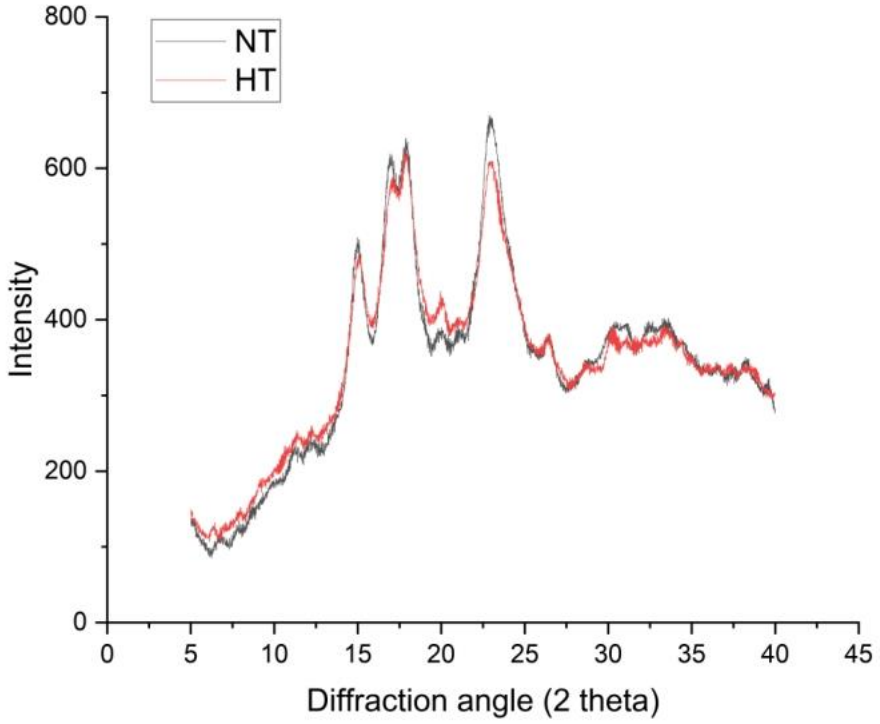

Figure 4.4.3. X-ray diffractograms of Native Taro Starch (NT) and Heat-moisture treatment Taro Starch (HT).

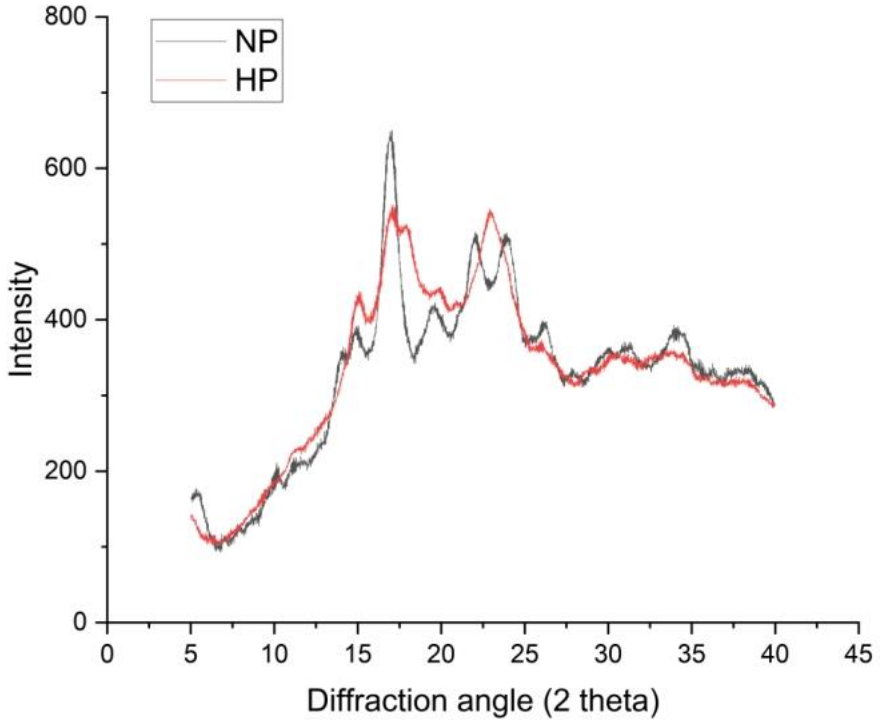

Figure 4.4.4. X-ray diffractograms of Native Potato Starch (NP) and Heat-moisture treatment Potato Starch (HP).

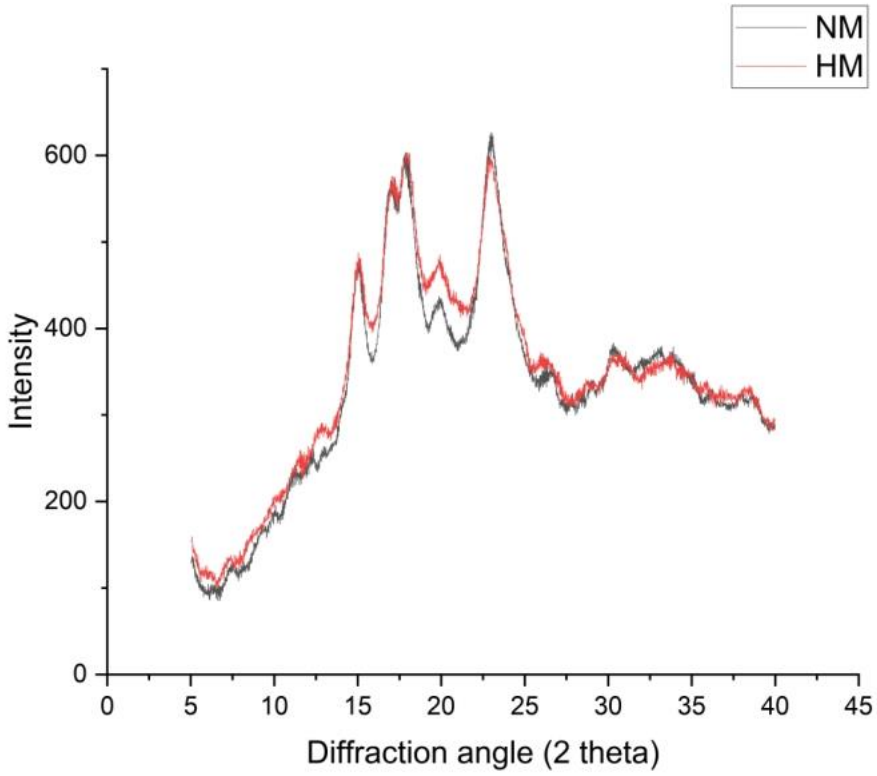

Figure 4.4.5. X-ray diffractograms of Native Maize Starch (NM) and Heat-moisture treatment Maize Starch (HM).

Table 4.4.1. Relative crystallinity of native starches and modified starches.

Sample	Relative Crystallinity (%)
NQ	22.5 ± 0.8 a
NA	24.1 ± 0.8 a
NT	24.2 ± 0.4 a
NP	19.1 ± 0.2 b
NM	21.8 ± 1.0 ba
HQ	21.5 ± 2.3 a
HA	20.5 ± 1.7 a
HT	21.3 ± 2.4 a
HP	22.3 ± 1.5 a
HM	27.0 ± 1.9 a

* NQ, Native Quinoa; NA, Native Amaranth; NT, Native Taro; NP, Native Potato; NM, Native Maize; HQ, HMT Quinoa; HA, HMT Amaranth; HT, HMT Taro; HP, HMT Potato; HM, HMT Maize. Values in the same column with the different letters differ significantly ($p < 0.05$).

Due to the principle of XRD, the atoms of the incident beam and the selected starch will interact with the electrons; thus, the starch can be distinguished into A, B, C, and V types (Purohit et al., 2019; Schafranski et al., 2021). According to Figures 4.4.1, 4.4.2, 4.4.3 and 4.4.5, the four selected natural starches (quinoa, amaranth, taro and corn) all exhibit typical type A starches. The patterns obtained from most grain starches and some tuber starches are typical A-type diffraction patterns, and the diffraction angles of their X-ray patterns at 2θ show peaks at 15.3°, 17.1°, 18.2° and 23.5° (Schafranski et al., 2021). Among them, the diffraction patterns of the natural and treated starches were mainly reflected at 15°, 17°, 18° and 23° of 2θ, resulting in peak intensity. Compared with natural starch, HMT starch had no changes in the crystal types of these four kinds of starch. This conclusion is the same as that of sweet potato starch treated by Trung et al. (2017) and mango seed starch studied by

Bharti, Singh and Saxena (2019). HMT treatment does not change the crystal structure of the selected natural starch. Moreover, the X-ray diffraction pattern remained unchanged after treatment. However, it can be seen from Figure 4.4.4 that the 2θ of the X-ray diffraction pattern of natural potato starch shows maximum intensity peaks at (almost equal to) 5.6°, 14.4°, 17.2°, 22.2° and 24°. This characteristic fits the typical amylose-rich grain tuber diffraction pattern, also classified as a B-pattern diffraction pattern (Schafranski et al., 2021). At the same time, after heat-moisture treatment, the X-ray diffraction pattern of potato starch changed, the intensity of five peaks decreased to four, and the range of diffraction Angle changed to 15.3°, 17.1°, 18.2° and 23.5° at 2θ (typical A-type diffraction pattern). These results indicated that potato starch's crystal structure changed from B-type to A-type after HMT treatment. As Lee and Moon (2015) found after heat-moisture treatment of natural waxy potato starch, the XRD image of natural waxy potato starch was a B-type diffraction image, which was transformed into a combination of B-type and A-type after HMT treatment. Hoover and Vasanthan (1994) changed the crystal form from B to A+B type after the heat-moisture treatment of common potato and yam starch. The reason for the change of the X-ray diffraction pattern of natural starch caused by HMT may be that the water molecules in the starch centre link were dehydrated during the heat-moisture treatment, which resulted in the relative movement of the double helix structure, which affected the formation of starch microcrystals or changed the orientation of the crystal (Gunaratne, 2018; Schafranski et al., 2021).

At the same time, the intensity of diffraction peak was observed, and it was found that HMT treatment could reduce the peak intensity of diffraction of some starch. The 2θ values of natural quinoa, natural amaranth and natural taro starch in the X-ray diffraction pattern were 15.3°, 17.1° and 23.5°, and the X-ray diffraction intensity of natural quinoa, natural amaranth and natural taro starch partially increased. The diffraction intensity decreases when the 2θ value is 18.2°. The peak strength of HMT corn starch did not change significantly except at 18.2°. The enhanced diffraction intensity caused by the heat-moisture treatment may be attributed to the formation of

new crystals during the heat-moisture treatment or changes in the extent or amount of starch crystallization areas (Kaur & Singh, 2019). Kaur and Singh (2019) study found that oat starch modification in damp and hot processing, the diffraction peak of 2 theta at 15.3° and 17.1° when there has been a marked increase. This phenomenon is similar to the experimental results.

It can be found in Table 4.4.1 that the relative crystallinity (RC) of natural starch changes in different degrees before and after treatment, among which small grain starch and large grain starch show different changing trends. Compared with natural quinoa starch, HMT quinoa starch had no significant change in RC value. Compared with the untreated starch, the RC values of amaranth starch and taro starch decreased significantly (amaranth starch decreased from 24.1 ± 0.8 to 20.5 ± 1.7; taro starch decreased from 24.2 ± 0.4 to 21.3 ± 2.4). Park et al. (2018) found that the RC value of waxy corn starch after HMT treatment also decreased significantly, especially after a long time of HMT, the RC value would decrease significantly. This reason can be attributed to the destruction of crystallization during HMT treatment, which further limits the accumulation of starch double helix structures (Park et al., 2018). Meanwhile, Gunaratne and Hoover (2002) attributed the decrease of crystallinity caused by HMT modification to the decrease of semi-crystallinity or the increase of amorphous area. However, the reduction of RC value caused by HMT modification also occurred in the HMT-treated red bean starch (Wang et al., 2017), cassava starch (Dudu et al., 2019) and sweet potato (Huang et al., 2016). The reduction can be attributed to the disintegration of the crystallite conformations after the double helix structure. More Oyeyinka & Oyeyinka (2018); Pratiwi et al. (2018) believed that in the process of heat-moisture treatment, the amorphous region and crystallization region in starch increased together, and since the RC value represents the ratio of the area of crystallization region to the sum of the total area of the amorphous region and the crystallization region in the X-ray diffraction pattern, this lamellar imbalance phenomenon led to the decrease of the RC value. In addition, Q. Wang et al. (2021) found that after the physical modification of cereal starch by HMT, the partial hydrogen

bonds that maintain starch stability would also decompose, and this structural instability may also lead to the reduction of RC value.

However, Table 4.4.1 also shows that the RC value of HMT potato starch increased from 19.1 ± 0.2% to 22.3 ± 1.5%, and HMT corn starch increased from 21.8 ± 1.0% to 27.0 ± 1.9%. Dudu et al. (2019) believed that the increase in RC value of natural starch after HMT modification was due to the recrystallization of the small crystalline region in natural starch under the influence of hot and humid treatment and the improvement of the crystallization region. This result correlates increased RC values with moisture and temperature. As for the influence of moisture and temperature on the increase of RC value in the process of moisture-heat treatment, K. Liu et al. (2019) found that with the continuous increase of moisture content in the modification process of natural highland barley starch, the increase of crystallinity of the treated highland barley starch would also increase. However, when the level of treated water reaches the high-water phase, the oil in the microcrystalline region appears to have an obvious disintegration phenomenon (K. Liu et al., 2019). This also shows that moisture is a crucial factor affecting RC value. More importantly, regarding the increased RC value of the modified lake after HMT, Schafranski et al., 2021 linked this phenomenon to the previously mentioned change in the crystal pattern of X-ray diffraction patterns caused by HMT. Under the dual factors of water treatment and heat treatment, the amorphous amylose in the starch was partially transformed into the crystal, which led to the change of crystal shape. However, the increased RC indicates that the starch double helix chain moves in the crystal to form a more orderly crystallization mechanism.

In conclusion, it can be seen that many studies have shown the changes in the X-ray diffraction pattern of starch after HMT treatment, as well as the changes in RC value, which are similar to the conclusions in this study. This also proves that the XRD results seem unrelated to the size of the natural starch particles and related to the parameters in the heat-moisture treatment process and the type of starch.

4.5 Pasting properties of starch

In this part, gelatinization performance measured by MCR 301 Rheometer is shown In Figure 4.5.1 and Table 4.5.2. Pasting analyses as a critical factor to evaluate the properties of different starches, some techniques have been applied, especially the RVA analyzer and RVA analysis chart, which can intuitively simulate the shear resistance of starches from heating to cooling (Schafranski et al., 2021). The specific parameters before and after starch treatment are shown in the table. The results showed that the size of starch and the structure of starch might affect the change of starch adhesion property after HMT modification. At the same time, starch pasting parameters were significantly affected by HMT treatment.

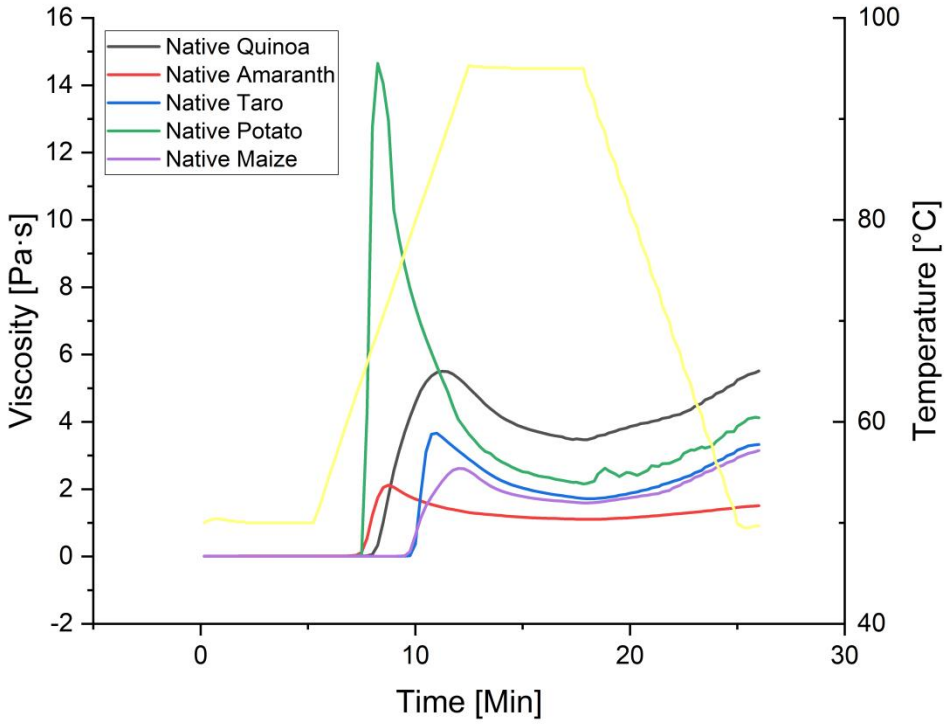

Figure 4.5.1. Pasting properties of native starch samples.

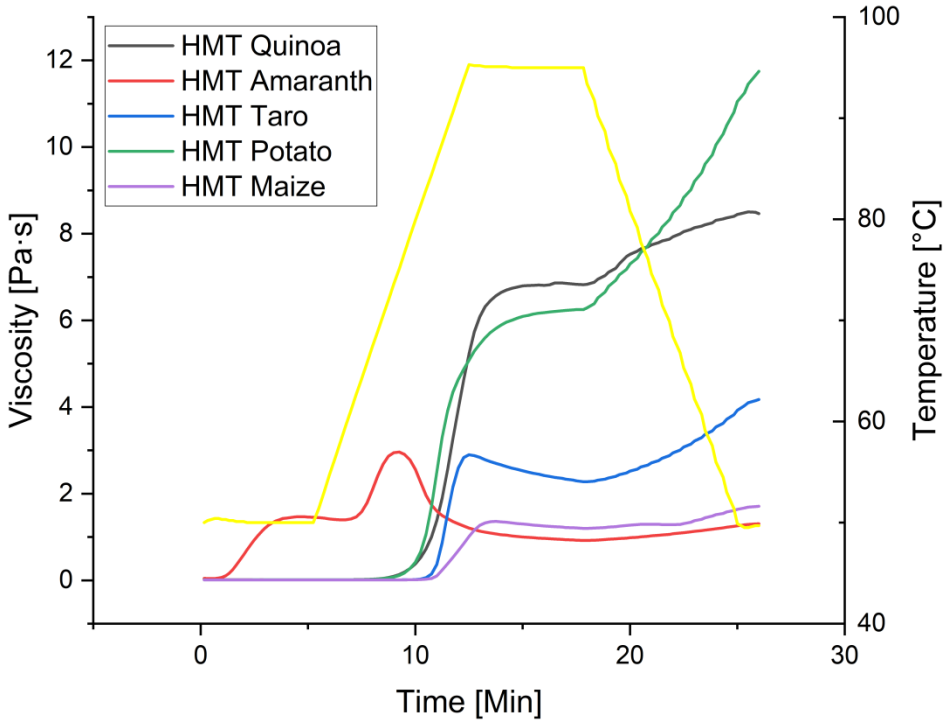

Figure 4.5.2. Pasting properties of HMT starch samples.

Table 4.5. Pasting properties of starches.

Sample	PT (°C)	PV (Pa·s)	HPV (Pa·s)	CPV (Pa·s)	BD (Pa·s)	SB (Pa·s)
NQ	65.80 ± 0.00 c	5.51 ± 0.01 b	3.45 ± 0.07 a	5.52 ± 0.04 a	2.06 ± 0.08 b	2.07 ± 0.11 a
NA	61.10 ± 0.00 e	2.12 ± 0.00 e	1.11 ± 0.02 e	1.51 ± 0.01 d	1.02 ± 0.02 d	0.41 ± 0.01 c
NT	78.30 ± 0.00 a	3.65 ± 0.02 c	1.73 ± 0.02 c	3.33 ± 0.04 C	1.94 ± 0.00 c	1.61 ± 0.02 b
NP	64.30 ± 0.00 d	14.60 ± 0.07 a	2.16 ± 0.02 b	4.14 ± 0.22 b	12.5 ± 0.05 a	1.98 ± 0.20 a
NM	76.80 ± 0.10 b	2.61 ± 0.01 d	1.59 ± 0.03 d	3.15 ± 0.00 C	1.03 ± 0.02 d	1.56 ± 0.03 b
HQ	66.60 ± 1.13 b	6.46 ± 0.25 a	6.41 ± 0.24 a	7.93 ± 0.01 b	0.04 ± 0.01 e	1.52 ± 0.25 c
HA	32.00 ± 1.27 c	2.95 ± 0.03 b	0.94 ± 0.04 d	1.32 ± 0.02 e	2.03 ± 0.01 a	0.38 ± 0.01 d
HT	81.30 ± 0.00 a	2.86 ± 0.06 b	2.28 ± 0.01 c	4.18 ± 0.06 c	0.63 ± 0.05 b	1.90 ± 0.06 b
HP	67.40 ± 0.00 b	6.22 ± 0.04 a	6.01 ± 0.00 b	11.7 ± 0.00 a	0.24 ± 0.04 c	5.69 ± 0.00 a
HM	82.90 ± 0.00 a	1.36 ± 0.03 c	1.20 ± 0.03 d	1.71 ± 0.01 d	0.16 ± 0.00 d	0.51 ± 0.01 d

*NQ, Native Quinoa; NA, Native Amaranth; NT, Native Taro; NP, Native Potato; NM, Native Maize; HQ, HMT Quinoa; HA, HMT Amaranth; HT, HMT Taro; HP, HMT Potato; HM, HMT Maize. PT: peak temperature; PV: peak viscosity; HPV: hot paste viscosity; CPV: cool paste viscosity; BD: breakdown; SD: setback viscosity. Values in the same column with the different letters differ significantly ($p < 0.05$).

It could be found that the pasting properties of the five native starches before treatment are different, and the size of the particle size seems to influence the pasting results of the native starch. As found by (Chandla et al., 2017; Kong et al., 2009), changes in amylose content and particle size change the starch gelatinization curve. The transformation curves varied with amylose content and particle size. Although Lindeboom et al. (2004) found that generally, small granule starch has a smaller gelatinization temperature. Comparing the PT of the native starch in table 4.3, it would be found that the temperature when the granule of small granule starch is dispersed will also be higher, which means it has a higher PT. Compared with large granule starch, the PT of natural quinoa and taro starch is higher than that of potato starch; the PT of natural taro starch is higher than that of maize starch. This phenomenon may be attributed to the enhanced water absorption caused by the low crystallinity of some small-granular starches, resulting in more significant swelling.

Among them, in the heating stage in the image, it can be found that the viscosity of starch gradually increases with the temperature increase. This phenomenon is due to the precipitation of amylose molecules of starch granules from the starch granules, and the peak viscosity represents the bulk swelling of the starch granules (Schafranski et al., 2021). At the same time, starch swells during the heating stage due to water absorption, which is also related to the water swell of starch (Hoover, 2010). Therefore, the PV value is not only related to the structure of starch granules but also related to their water absorption. Moreover, a retrograde phenomenon occurs during the cooling phase of the image, when starch molecules recombine, and there is a slight trend of increase in viscosity (Balet et al., 2019). Therefore, the effect of HMT on starch can be analyzed by different parameters for each stage.

Firstly, the average pasting temperature (PT) of natural quinoa starch is slightly more than that of potato starch; meanwhile, the PT of taro starch is higher than maize starch, and the average pasting temperature of taro starch is the highest. This result

seems to be similar to the study of Deka and Sit (2016). Due to the wide variety of taro, the gelatinization performance of different types of taro starch is quite different, especially in Figure.3 (Deka & Sit, 2016), the different results can be seen. The average pasting temperature of amaranth starch is the lowest among the five starches, only 61.1°C. At the same time, the values of PV, thermal past viscosity (HPV), CPV, BD and SB of amaranth starch are the smallest among the five natural starches, which is related to the characteristics of amaranth starch. According to Hoover et al. (1998); Kong et al. (2009); Marcone (2001) studies, since the amylose content of natural amaranth starch is only 3%-8%, this will significantly affect the thermal properties of amaranth starch.

Table 4.5 shows that the pasting temperature of HMT samples is higher than that of native starch, except for amaranth starch. This phenomenon is consistent with the results obtained by Chung et al. (2009). At the same time, Liu et al. (2016) also found that PT increased with the increase of HMT treatment temperature, and the paste temperature also increased significantly by increasing the water content during HMT modification. It would be indicated that HMT increased the thermal stability of native starch and also restricted starch gelatinization (Liu et al., 2016). This phenomenon will also be demonstrated in the following DSC results. By analyzing starches other than amaranth and comparing PT, it is found that the pasting temperature of HMT starch is higher than that of native starch. Nevertheless, it is found that the small granule starch (quinoa and taro) after HMT treatment does not increase as much as the large granule starch (potato and maize) for the pasting temperature by comparing the increase rate. This result might indicate that the particle size would affect the HMT and changes in starch gelatinization properties. Khatun et al. (2019) found that the small granular starches tend to leach more amylose and have lower gelatinization temperatures. This conclusion can explain the phenomenon shown in the table that the gelatinization temperature of amaranth starch decreases with HMT treatment. Another reason may be the less amylose content in this natural amaranth starch after

HMT treatment, and a higher degree of expansion cannot be expressed. As Hoover (2010) found, HMT treatment reduced starch granule swelling and increased amylose leaching in some cereal crops. Looking further at the effect of HMT on starch, it can be found that the pasting properties of amaranth are exceptional. Except for the PV and BD value, other parameters decreased to different degrees after modification. This phenomenon also occurs after the HMT treatment of waxy maize starch. No matter the treatment temperature and treated time setting, the setback value of the modified starch is lower than the natural starch; the other parameters also show that the HMT modification has very little influence or almost no influence on the gelatinization performance of waxy starch; the reason why is that waxy corn starch lacks amylose (Sui et al., 2015). At the same time, the properties of amaranth HMT are similar to waxy starch, which is also consistent with the purchased amaranth seeds being waxy, and it is proved that the amylose content will affect the influence of HMT on the thermal properties of starch.

In the heating stage, in addition to the change of PT, the viscosity is also constantly changing with temperature, and the PV is also affected by the HMT treatment. The increase in sticking is often due to the increased cross-linking of amylose and amylopectin in the amorphous region, resulting in increased stability and heat resistance of the starch structure, requiring more heat to destroy the starch resulting in gelatinization (Bharti et al., 2019). However, the increase in viscosity is often not entirely due to the cross-linking effect of linear amylopectin. During the heating stage of RVA, starch granules are processed under conditions of simultaneous action of a large amount of water, shear force and high temperature, so there may also be the influence of proteins and lipids in starch on it or the swelling between granules. Friction also affects starch PT (Bharti et al., 2019; Jane et al., 1999). In this study, with the heating, the RVA image presented by the HMT amaranth starch was different from the traditional gelatinized paste image. As shown in figure 4.5.2, the viscosity of amaranth starch rapidly increases in the initial heating stage. After maintaining

equilibrium, it continues to increase to the PV value. The reason for the initial increase in viscosity may not be due to water swelling of amaranth starch, but the complex phenomenon of protein and surface starch as studied by (Olkku & Rha, 1978), thus interfering with the normal exudation of starch granules, which in turn increases the viscosity. The growth of the latter stage should probably be the same as that of other types of starch, and there is a sharp decline trend after reaching PV, which is similar to the change of peak viscosity of rice starch treated by Arns (2015). At the end of the heating stage, as well as the temperature maintenance stage, according to Table 4.3, it can be found that the PV is greatly affected by the HMT treatment. Among them, HMT potato starch decreased from 14.60 ± 0.07 to 6.22 ± 0.04 Pa·s compared with natural potato starch, and both HMT corn starch and HMT taro starch decreased slightly (corn from 2.61 ± 0.01 to 1.36 ± 0.03 Pa·s; taro 3.65 ± 0.02 to 2.86 ± 0.06 Pa·s), which is similar to previous results (Arns, 2015; Schafranski et al., 2021), which confirm that HMT-modified starch has a reduced peak viscosity compared to native starch. However, the PV trends of HMT quinoa starch and amaranth starch differed. Compared with natural, HMT amaranth starch increased from 5.51 ± 0.01 to 6.46 ± 0.25; HMT amaranth increased from 2.12 ± 0.00 to 2.95 ± 0.03. Similar results were found in wheat starch made by Y. Liu et al. (2016) and corn starch made by Han & Hamaker (2002), both of which were affected by the increase of peak and final viscosity by related proteins in the particles.

By comparing other parameters, it can be found that the starch after HMT modification is often reduced. Among them, BD and SB decrease after heat treatment. The BD value of HMT potato starch decreased significantly from 12.5 ± 0.05 Pa·s to 0.24 ± 0.04 Pa·s. Except for amaranth starch, other kinds of starch decreased to different degrees. At the same time, the SB value of potato starch increased significantly (from 1.98 ± 0.20 to 5.69 ± 0.00), and other starches decreased to different degrees. The decrease of PV, BD and SB of starch after heat treatment is often because the amorphous region of starch particles is correlated with the change of crystallinity

under the influence of HMT. However, the increase in BD value and almost no significant decrease in SB value of amaranth starch may be due to the structure of selected amaranth starch. Sui et al. (2015) found that no matter how the HMT treatment parameters were controlled, the pulp performance of waxy corn starch hardly changed or did not decrease significantly, and the reason was that the waxy corn starch structure was caused by the lack of amylose. Therefore, amylose has a great influence on HMT modification methods.

Therefore, by exploring natural starch with different particle sizes under HMT modification, the treatment results seem unrelated to particle size but closely related to starch structure and type. HMT modification often improves the thermal stability and gelatinization characteristics of natural starch.

4.6 Swelling powder (SP) and water solubility index (WSI)

Due to the different structural forces inside different starches, different starches have different swelling and solubility curves (Deka & Sit, 2016a). The swelling power and water solubility index of natural starch and HMT starch at 85°C are shown in Table 4.6. The results show that HMT treatment of starch can significantly enhance starch's water absorption and swelling power. At the same time, the swelling power and solubility of different starch are different.

Table 4.6 Swelling power and solubility of different natural starches and HMT starches.

Sample	WSI	SP
NQ	44.9 ± 0.4 c	23.2 ± 0.3 c
NA	96.2 ± 0.5 a	44.4 ± 6.9 b
NT	44.0 ± 0.6 c	24.4 ± 0.2 c
NP	85.2 ± 3.0 b	62.1 ± 2.0 a
NM	12.7 ± 0.4 d	14.8 ± 0.3 d
HQ	3.2 ± 0.3 e	11.9 ± 0.8 c
HA	95.6 ± 0.5 a	26.3 ± 1.4 a
HT	12.4 ± 0.3 b	15.1 ± 0.3 b
HP	7.8 ± 0.5 d	14.5 ± 0.9 b
HM	9.3 ± 0.6 c	9.0 ± 0.2 d

* NQ, Native Quinoa; NA, Native Amaranth; NT, Native Taro; NP, Native Potato; NM, Native Maize; HQ, HMT Quinoa; HA, HMT Amaranth; HT, HMT Taro; HP, HMT Potato; HM, HMT Maize. Values in the same column with the different letters differ significantly ($p < 0.05$).

As a fundamental physicochemical property of starch, SP and WSI change with temperature. They would also be affected by the ratio of amylose to amylopectin, molecular weight and distribution, length of amylopectin, and phosphorus content (Hoover, 2001; Sujka & Jamroz, 2013). It can be seen from Table 4.6 that the SP and WSI of all selected samples decreased to varying degrees after HMT treatment. Moreover, for quinoa, taro and potato starches, the starch solubility was more pronounced by HMT treatment. Among them, for solubility, quinoa decreased from 44.9 ± 0.4 to 3.2 ± 0.3; taro decreased from 44.0 ± 0.6 to 12.4 ± 0.3; potato starch decreased from 85.2 ± 3.0 to 7.8 ± 0.5. The reduction in amaranth and maize starch was slightly lower, in which amaranth starch decreased from 96.2 ± 0.5 to 95.6 ± 0.5, which did not seem to change much. This phenomenon also appeared in the research from Sui et al. (2015) that after 30% moisture treatment content of the HMT starch. At the same time, after the modification of maize starch, it decreased from 12.7 ± 0.4 to 9.3 ± 0.6, and the decrease was also smaller. By comparing the changes of HMT starch swelling power, except for the SP of potato starch, which was greatly reduced (from 62.1 ± 2.0 to 14.5 ± 0.9), the swelling power of other HMT starches also decreased to some extent.

Kong et al. (2015) pointed out that the degree of change in swelling power and water solubility index was affected by moisture content. The decrease in swelling force was due to the increase in amylose-amylopectin (AM-AP) interaction and amylose-lipid complexes (Kong et al., 2015). These two factors would influence the starch SP and WSI. By observing Table 4.6, the swelling power of HMT starch is lower than that of native starch, which is consistent with the results from Adebowale & Lawal (2003); Das and Sit (2021); Deka & Sit (2016a, 2016b); Gunaratne et al. (2010); Li et al. (2011); Sui et al. (2015); Sun et al. (2014). As a characteristic of amylopectin, swelling behaviour is determined by the chain length distribution and pattern of amylopectin and the molecular weight of amylopectin. As the temperature increases, gelatinization begins, and amylose and amylopectin will change from precipitation in starch

granules (Sui et al., 2015). Therefore, the swelling power of starch modified by HMT decreased obviously. At the same time, comparing the decreasing trend of starch with different particle sizes, it could be found that the particle size of granule has no obvious effect on the swelling power of starch modified by HMT, just as in the conclusion of the pasting experiment, the gelatinization performance of starch modified by HMT is the main factor. The influencing factors are the content and function of different types of starch, its amylose, and amylopectin. Hoover and Manuel (1996) found that HMT modification results in cross-linking in the non-crystalline regions of starch. Some researchers were given a further explanation of the swelling behaviour of the starch structure. The reduction in swelling behaviour is due to the interaction between starch chains during HMT treatment, and the partial double helix structure will dissociate (Hoover & Manuel, 1996). Moreover, some studies have shown that the force that maintains the integration of starch granules is generally concentrated on the double helix structure, and the double helix is often unwound under the modification of HMT, so the stability and swelling force of the structure will be weakened (Cooke & Gidley, 1992; Varatharajan et al., 2011). For further analysis, Sui et al. (2015) found that the interaction of AM-AP chains and AP-AP chains enhances the mobility of linear chains and reduces hydrated hydroxyl groups. More studies have found that under the action of physical modification, a part of amylose will be assembled in the branched network structure, directly affecting amylopectin's water retention capacity (Das and Sit, 2021). So, the swelling power will decrease. In summary, tuber starch crystallization is disrupted under HMT modification of native starch; increased crystallinity; amylose-lipid interactions; AM-AM and AP-AP interactions; and B-to-A conversion form and B (polymorphic form), which lead to reduced swelling power and precipitation of amylose (Hoover, 2001). The above reasons may be why the HMT modification reduces the swelling power and solubility of the particles. The WSI of amaranth starch did not seem to be affected by HMT modification. At the same time, other starches decreased significantly, mainly potato starch. The WSI decreased from 85.2 ± 3.0 to 7.8 ± 0.5. The decrease in solubility, in

addition to the reasons mentioned above, Liu et al. (2016) pointed out that in addition to the strong bonds formed between AP molecules, both the novel crystallites and AM-lipid complexes formed during HMT treatment reduced the solubility. Although some studies have pointed out that starch after HMT treatment seems to have a slight increase in its solubility, there is not much evidence to support the reason. Deka and Sit (2016b) attributed the increase in starch solubility to autoclave Starch granules are weathered; Li et al. (2011) speculated that HMT modification might cause weak structure on the starch surface and lead to the expansion of the internal gap of starch, resulting in a decrease in solubility. Most cases are due to the apparent differences in the structure of different starches. At the same time, the decrease of SP value also indicated that HMT made the thermal stability of starch higher. They are greatly affected by the HMT treatment parameters, but the overall trend is, as Table shows, the solubility and swelling power of HMT starch compared with native starch both decreased the trend. And the degree of decline was independent of particle size.

4.7 Gel texture analysis native starches and HMT starches

The results of gel structural properties of different natural starch and HMT starch are shown in Table 4.7. Compared with natural starch, the structure and property parameters of HMT starch gel texture have different changes and are affected by the type of starch. However, the results did not show the effect of particle size on Gel texture property.

Table 4.7 Gel textural properties of native starches and HMT starches

Sample	Hardness (g)	Adhesiveness (g·s)	Cohesiveness	GUM (g)
NQ	16.00 ± 0.45 c	-169.74 ± 9.68 c	0.64 ± 0.00 a	10.23 ± 0.22 c
NA	2.47 ± 0.00 d	-22.88 ± 0.74 a	0.61 ± 0.01 b	1.51 ± 0.02 d
NT	17.37 ± 0.91 c	-115.87 ± 1.55 b	0.64 ± 0.01 a	11.17 ± 0.69 c
NP	54.17 ± 0.97 b	-321.74 ± 8.00 e	0.6 ± 0.01 b	32.25 ± 0.53 a
NM	66.43 ± 1.45 a	-210.28 ± 11.92 d	0.38 ± 0.02 c	25.29 ± 1.04 b
HQ	9.04 ± 0.59 c	-85.89 ± 2.33 b	0.62 ± 0.01 a	5.59 ± 0.31 c
HA	2.83 ± 0.04 d	-28.53 ± 1.33 a	0.59 ± 0.01 b	1.67 ± 0.04 d
HT	15.82 ± 1.07 b	-130.10 ± 0.19 c	0.55 ± 0.01 c	8.67 ± 0.47 b
HP	58.76 ± 3.86 a	-321.21 ± 17.03 d	0.46 ± 0.00 d	26.93 ± 1.75 a
HM	59.19 ± 1.35 a	-304.61 ± 17.26 d	0.45 ± 0.01 d	26.68 ± 1.36 a

* NQ, Native Quinoa; NA, Native Amaranth; NT, Native Taro; NP, Native Potato; NM, Native Maize; HQ, HMT Quinoa; HA, HMT Amaranth; HT, HMT Taro; HP, HMT Potato; HM, HMT Maize. Values in the same column with the different letters differ significantly ($p < 0.05$).

In Table 4.7, the gel texture properties of different natural starches showed significant differences. Among them, the hardness (2.47 ± 0.00) and adhesiveness (-22.88 ± 0.74) of natural amaranth starch were far lower than those of other kinds of starch. Natural corn starch has the highest hardness (66.43 ± 1.45), and natural potato starch has the highest adhesiveness (absolute value 321.74 ± 8.00). For gumminess, there are significant differences among the five natural starches ($p < 0.05$). The Gumminess value of natural amaranth starch was the lowest, which was 1.51 ± 0.02 g. the value of natural potato starch could be reached at 32.25 ± 0.53 g. These gel characteristics largely reflect the characteristics of food. Meanwhile, by comparing the gel characteristics of HMT starch, it can be found that different natural starches have different gel characteristics.

Firstly, the degree of amylose crystallization directly affects starch degradation, and the degradation phenomenon determines the hardness (Yu et al., 2012). It can be seen from Table 4.7 that the hardness of quinoa, taro and corn starch after HMT modification all decreased to different degrees. These results are consistent with Ariyantoro et al. (2022); Singh et al. (2005). The hardness of starch often depends on its structure of starch. Yu et al. (2009) found that the higher the amylose content and the longer the amylopectin chain, the higher the starch gel hardness would be. At the same time, Aaliya et al. (2021) pointed out that the hardness was determined by the hydrogen bonding between starch molecules and water, and the increase in starch viscosity caused by HMT modification was due to the cross-linking between intermolecular and intramolecular bonding which caused by physical modification. The increase of hardness can directly affect the enhancement of starch gel structure and prevent gel compression and rupture. However, according to Table 4.7, the hardness of HMT amaranth starch increased from 2.47 ± 0.00 g to 2.83 ± 0.04 g, while potato starch increased from 54.17 ± 0.97 g to 58.76 ± 3.86 g. The results indicated that amaranth and potato starch treated with HMT were more likely to retrograde and gel texture would be harden. This phenomenon was also confirmed in

the experiment by Adawiyah et al. (2017), in which HMT starch gel was more rigid than natural starch. Therefore, this may indirectly reflect the phenomenon that the amylose content in amaranth starch is low. It also indirectly proves that the influence of its straight chain branching content on pasting and swelling power is because of the low straight chain content.

Meanwhile, starch gel adhesion is the energy needed to overcome the attraction between starch gel and the gel contact surface; it is expressed through the negative force area in the TPA diagram (Aaliya et al., 2021). Therefore, based on the absolute value of adhesiveness (AD) in Table 4.7, it was found that natural potato starch had the highest AD value (321.74 ± 8.00 g·s), while amaranth starch had the lowest AD (22.88 ± 0.74 g·s). At the same time, it was found that the changing trend of starch AD under HMT modification seemed to be related to the type of starch. The AD of HMT quinoa starch decreased significantly (from 169.74 ± 9.68 g·s to 85.89 ± 2.33 g·s), while potato starch did not change (from 321.74 ± 8.0 g·s to 321.21 ± 17.03 g·s). However, other starches had different degrees of growth. Compared with natural starches, the adhesiveness of HMT amaranth starch increased slightly (from 22.88 ± 0.74 g·s to 28.53 ± 1.33 g·s), and both HMT taro starch and HMT corn starch increased significantly. Especially, the adhesiveness of HMT corn starch increased from 210.28 ± 11.92 g·s to 304.61 ± 17.26 g·s. Zhu (2017) pointed out that the influencing factors of AD value are similar to HD, both of which are related to the amylose content of starch. Furthermore, the less the content of amylose and lipid complex, the more amylose may form an elastic gel (Zhu, 2017). So that amylose content will significantly affect AD values.

Cohesiveness (CoH) determines the internal bond strength of the starch gel and shows the gel's bonding capacity (Aaliya et al., 2021). Among the natural starches, quinoa and taro starch had the highest CoH (0.64 ± 0.00), while corn starch had the lowest CoH (0.38 ± 0.02). By observing the cohesiveness of HMT starch, the

changing trend of cohesiveness was different from that of HD and AD. Only the CoH of maize starch showed a slight increase (from 0.38 ± 0.02 to 0.45 ± 0.01); the other four starches showed a small decrease. At the same time, the difference between HMT potato starch and HMT maize starch after treatment was low. In addition, according to Table 4.7, by comparing the starch after HMT modification with the natural starch before treatment, the viscosity of the other three kinds of starch decreased to different degrees, except that amaranth starch had a slight increase and maize starch seemed to have no change. The GUM values of HMT potato starch (26.93 ± 1.75) and HMT maize starch (26.68 ± 1.36 g) were similar, but the GUM values of three kinds of small grain starch were significantly different (quinoa starch, amaranth & taro starch; $p < 0.05$). As shown in the study, the gel properties of starch are greatly affected by the properties of starch (Zhu, 2017). At the same time, Kong et al. (2009) found that the gel properties of starch were somewhat related to the gelatinization properties of starch. Gelatinization parameters except BD were positively correlated with starch hardness, and the smaller the AD value of different types of starch, the larger the gelatinization parameters might be (Kong et al., 2009). However, by comparing Table 4.7 and Table 4.5, no significant correlation was found between starch granule gelatinization parameters and gel characteristics, which was the same as a result made by Li et al. (2016). At the same time, Li et al. (2016) also found that although the gelatinization characteristics of starch particles were unrelated to gelatinization parameters, the flour gels corresponding to starch showed a certain correlation with gelatinization characteristics due to the influence of other substances and the factors of low starch content.

Finally, the gel mechanical properties of starch are affected by the degradation of amylose content and amylopectin (Vandeputte et al., 2003; Yu et al., 2009). It is also affected by the rheology of proteins and lipids, as well as the interaction between the dispersed phase and the continuous phase of the gel (Li et al., 2016; Yu et al., 2012). Moreover, this study found that starch particle size did not seem to affect the gel

properties of HMT starch.

4.8 Thermal properties

According to the gelatinization characteristics of the five natural starches before and after treatment, as shown in Table 4.8.1 and Table 4.8.2, it can be found that the thermal parameters of the five natural starches before treatment are significantly different. At the same time, HMT treatment significantly affected starch gelatinization characteristics, and all thermal parameters of different varieties of HMT starch had apparent changes. At the same time, the gelatinization characteristics of the five starch samples after modification were also significantly different.

Table 4.8.1. Gelatinization property of native starches.

Sample	**T_O (℃)**	**T_P (℃)**	**T_C (℃)**	**ΔT (℃)**	**ΔH (J/g)**
NQ	55.14 ± 0.73 e	63.78 ± 0.14 d	73.41 ± 0.72 c	18.28 ± 1.45 a	11.58 ± 0.11 d
NA	56.79 ± 0.19 d	63.3 ± 0.43 d	73.30 ± 0.78 c	16.51 ± 0.59 a	12.54 ± 0.49 cd
NT	73.27 ± 0.04 a	76.77 ± 0.06 a	86.42 ± 0.01 a	13.15 ± 0.03 b	15.85 ± 0.78 b
NP	62.10 ± 0.20 c	66.30 ± 0.20 c	74.60 ± 0.50 c	12.50 ± 0.70 b	17.10 ± 0.50 a
NM	71.00 ± 0.10 b	74.30 ± 0.00 b	79.80 ± 0.10 b	8.80 ± 0.00 c	13.40 ± 0.20 c

*To, onset temperature; Tp peck temperature; Tc, conclusion temperature; ΔT (Tc-To), gelatinization temperature range; ΔH, gelatinization enthalpy. NQ, Native Quinoa; NA,

Native Amaranth; NT, Native Taro; NP, Native Potato; NM, Native Maize. Values in the same column with the different letters differ significantly ($p < 0.05$).

Table 4.8.2. Gelatinization property of HMT starches.

	Peak 1					Peak 2				
Sample	**T_O (℃)**	**T_P (℃)**	**T_C (℃)**	**ΔT (℃)**	**ΔH (J/g)**	**T_O (℃)**	**T_P (℃)**	**T_C (℃)**	**ΔT (℃)**	**ΔH (J/g)**
HQ	57.96 ± 0.04 d	67.37 ± 1.11 d	81.2 ± 2.31 ba	23.24 ± 2.35 a	3.44 ± 0.00 c	-	-	-	-	-
HA	61.16 ± 1.34 c	70.07 ± 0.86 c	86.5 ± 4.91 a	25.35 ± 3.57 a	4.59 ± 0.53 b	-	-	-	-	-
HT	74.99 ± 0.11 a	77.69 ± 0.10 a	82.05 ± 0.21 ba	7.06 ± 0.10 b	0.98 ± 0.08 d	83.25 ± 0.10 a	85.57 ± 0.01 a	87.77 ± 0.10 b	4.52 ± 0.00 c	0.29 ± 0.04 b
HP	44.26 ± 0.75 e	61.51 ± 0.02 a	70.93 ± 1.71 c	26.67 ± 2.46 a	5.70 ± 0.14 a	75.87 ± 0.44 c	85.33 ± 0.08 a	93.86 ± 0.44 a	17.99 ± 0.00 a	1.22 ± 0.10 a
HM	71.61 ± 0.12 b	74.33 ± 0.16 b	78.46 ± 0.49 b	6.85 ± 0.37 b	0.82 ± 0.08 d	81.42 ± 0.25 b	84.70 ± 0.21 b	87.63 ± 0.20 b	6.22 ± 0.05 b	1.38 ± 0.11 a

*To, onset temperature; Tp peck temperature; Tc, conclusion temperature; ΔT (Tc-To), gelatinization temperature range; ΔH, gelatinization enthalpy. HQ, HMT Quinoa; HA, HMT Amaranth; HT, HMT Taro; HP, HMT Potato; HM, HMT Maize. Values in the same column with the different letters differ significantly ($p < 0.05$).

First, it can be obtained from Table 4.8.1 that the natural quinoa starch has the lowest gelatinization temperature (To), which is 55.14 ± 0.73°C, while the natural taro starch, which is also a small-granular starch, has the highest gelatinization temperature (To = 73.27 ± 0.04°C). Among them, the thermal characteristics of natural quinoa starch are similar to those of natural amaranth starch. The thermal parameters, including gelatinization temperature, gelatinization range and gelatinization enthalpy change of gelatinization starch, are very close, similar to Wang et al. (2015); Zhu et al. (2017) obtained roughly the same results. The relative thermal parameters of these two natural starches are lower than those of other natural starches, and as found by Abugoch (2009), the ΔH of natural quinoa starch and amaranth starch gels are lower than that of natural corn starch.

At the same time, the thermal parameters are greatly affected by the starch structure. Kong et al. (2009), Marcone (2001), Stevenson et al. (2005), and Tattiyakul et al. (2007) found that the chain length distribution and average chain length of amylopectin can affect the starch thermal parameters. Meanwhile, Demeke et al. (1999); Stevenson et al. (2005) found that the content of amylose also affects the values of To, Tp and Tc. Therefore, the natural taro starch has the highest To (73.27 ± 0.04°C), Tp (76.77 ± 0.06°C) and Tc (86.42 ± 0.01°C), which indicates that the selected taro starch may have the highest amylose content, and the average amylopectin The chain length is also longer than the other starches chosen. This also proves that Kong et al. (2009) did research on the thermal properties of many different types of amaranth starch; the higher the amylose content and the longer the average chain length of the branched chain will increase the thermal properties and gelatinizing viscosity of the starch. Regarding the phenomenon of different To, Tp and Tc of different starches, Hoover & Ratnayake (2000); Vandeputte et al. (2003) also found that lipid complex amylose is one of the influencing factors. Therefore, according to the research of Deka and Sit (2016), the structure and gelatinization properties of different taro types are very different due to a large number of taro types.

It can also be obtained from table 4.8.1 that the thermal properties of selected taro starch and other starches are significantly different and appear to be independent of particle size. From table 4.8.1, comparing the ΔH of different types of natural starch selected, it can be obtained that the ΔH of natural potato starch is the largest (17.10 ± 0.50 J/g), and the natural quinoa starch is the smallest (11.58 ± 0.11 J/g). The ΔH of starch expresses the loss of the double helix structure of starch (Cooke & Gidley, 1992). According to the conclusion of Chung et al. (2009), the A chains of 6-12 in the natural starch structure with a small ΔH account for the ratio is higher, and the shorter A-type chain prevents it from forming a stable double helix. Therefore, the ΔH of quinoa starch and amaranth starch shown in Table 4.8.1 is smaller than that of other selected natural starches because of the chain pattern of quinoa starch and amaranth starch, which also explains the reason for the particular pasting property of amaranth starch.

When exploring the effect of HMT modification on starch, it can be obtained from Table 4.8.2 that compared with native starch, HMT starch has apparent differences in gelatinization properties. Especially the heat-moisture treatment taro, potato, and maize starch obtained from the DSC results showed two peaks, which were very special. For quinoa starch and amaranth starch, after HMT modification, the To, Tp, Tc, and ΔT of starch increased to different degrees, while ΔH decreased. This result is consistent with many studies that the To, Tc and Tp value increased significantly under HMT treatment (Huang et al., 2016; Sui et al., 2015; Xia et al., 2016). Moreover, Chen et al. (2017) found that by increasing the HMT treatment time, explored with the continuous increase of the HMT time, the To of starch will be transferred to a higher temperature. Moreover, that seems to be that the weak crystals in the starch are destroyed during HMT processing, making the starch form more perfect crystals (Chen et al., 2017). At the same time, Huang et al. (2016) conducted a study on starch forming more stable crystals in the process of HMT; and the results showed that with the progress of HMT treatment, the direct connection between starch chains

and the strengthening of chemical bonds within particles would lead to the continuous increase of To, Tc and Tp. And the association tends to get stronger over time (Huang et al., 2016). At the same time, due to the wide range of HMT treatment parameters and the large differences between different starches, that sweet potato starch treated with HMT showed higher gelatinization parameters, among which To, Tc, Tp, ΔT and ΔH all increased, and the reason for the increase of ΔH was attributed to the formation of large crystals caused by a high proportion of long-chain branched structures (Na et al., 2020). For the reasons for the change in gelatinization properties (To, Tp and Tc increase) of HMT starch compared to native starch, Schafranski et al. (2021) concluded that a new surface formed on the starch surface during heat treatment first layer will limit the penetration of water in starch granules, thus delaying the occurrence of swelling; at the same time, a more ordered crystalline structure will be formed under HMT modification, resulting in an increase in the gelatinization temperature (To, Tp & Tc); and because HMT is a kind of A physical modification method processed at high temperature, where the vapour pressure of the heating process causes gelatinization, phase separation of amylose and amylopectin, and shrinkage reactions of particulate matter.

Moreover, it can be found from Table 4.8.2 that the DSC gelatinization characteristic curve of native taro, potato and maize starch after HMT modification has a second peak. By analyzing it, another set of gelatinization parameters (To, Tp, Tc, ΔT and ΔH) was obtained. This phenomenon also appeared in the study conducted by Andrade et al. (2014) in the HMT physical modification of organic cassava starch (controlled moisture content of 10%, 20% and 30%, 120°C, for one-hour treatment), the DSC results showed that in addition to the main peak, another peak was displayed in the higher temperature range. And as the moisture content of the HMT treatment parameter is much higher, the second peak range is further back. That is, it appears in the higher temperature range. To explore the reason, Takaya et al. (2000) found that after HMT treatment of natural corn starch, the main peak of gelatinization was found

at about 67.8°C, and the second peak formed at 90.8°C was because of the decomposition of the amylose-lipid complex; it was also found that the first and second gelatinization peaks shifted to higher temperatures with increasing treatment temperature. And the peak width of cornstarch increased gradually under the increasing HMT treatment temperature (Takaya et al., 2000). Anderson et al. (2002) found that after the HMT treatment of wheat starch, DSC also showed a bimodal phenomenon, and the unimodal phase showed the difference in starch's heat absorption during the bimodal heating phase was probably due to some specific starch weights. Crystallization, or the formation of new crystals, in some cases, the starch granules may also lead to the formation of double peaks due to the perfection of small crystalline regions. Miyazaki & Morita (2005) also found the existence of the second peak for corn starch and its derivatives. Moisture heat treatment induces the appearance of new crystallites in the amorphous regions. Compared with native starch, To, Tp and Tc in the second peak of HMT taro, HMT potato and HMT maize starch were significantly increased. And the same as HMT quinoa and amaranth starch, its enthalpy value has a decreasing trend compared with the corresponding natural starch.

By comparing the thermal properties of HMT starch and natural starch, the thermal stability of treated starch was significantly increased, and the growing range and characteristics were determined by the type of starch. It seems that particle size is not a factor affecting HMT results. The HMT physical modification method not only promotes the mutual entanglement of amylose and amylopectin through intramolecular (or intermolecular) connection, promotes the intermolecular diffusion, and makes the swelling temperature higher, but also leads to the destruction of the crystallization domain (Schafranski et al., 2021). The increasing swelling temperature and crystallization domain destruction are interrelated (Schafranski et al., 2021). Therefore, based on this property, HMT, as a method that changes according to actual requirements, tends to increase the starch temperature range, increase gelatinization

temperature and increase starch stability (Zavareze & Dias, 2011).

4.9 Flow properties

This section shows the flow properties of native and HMT starch. The MCR 301 Rheometer and PP-50 mentioned in Chapter 3 were used for the experimental instruments, and the Herschel-Bulkley model fitted the experimental data. Because the Herschel-Bulkley rheological model can not only fit the flow curve between shear stress and a shear rate of the selected starch well but also has a high coefficient of determination R^2 (0.977-0.999) (Liao et al., 2019). The yield stress (σ0), consistency coefficient (K), flow behaviour index (n) and determination coefficient (R^2) in flow curves of each sample, including natural starch and HMT starch, were obtained from the fitted data (Tables 4.9.1 & 4.9.2). At the same time, the final results of the flow curves of each sample were described and drawn, and the changes in starch fluidity before and after HMT treatment were explored (Figure 4.9.1-4.9.4). The experimental data shows that the selected starch's flow properties are greatly affected by the type of starch, and the flow properties of different kinds of starch are different. At the same time, the effect of HMT physical modification on starch flow properties was different, but the overall effect was changed.

Table 4.9.1. Fitting parameters of Herschel-Bulkley model for flow curves of native and modified starches pastes (upward).

Upward				
Sample	σ0 (Pa)	K (Pa s n)	n	R2
NQ	89.8 ± 18.38 a	22.62 ± 5.8 c	0.38 ± 0.03 b	0.999
NA	3.75 ± 1.18 c	8.11 ± 0.34 d	0.51 ± 0.00 a	0.999
NT	40.99 ± 2.81 cb	39.64 ± 2.72 b	0.39 ± 0.01 b	0.999
NP	19.16 ± 9.49 cb	148.5 ± 0.43 a	0.39 ± 0.01 b	0.998
NM	59.49 ± 10.11 ba	5.16 ± 1.55 d	0.53 ± 0.02 a	0.977
HQ	1.5 ± 2.26 c	13.43 ± 0.73 b	0.42 ± 0 b	0.9999
HA	4.07 ± 0.15 c	5.81 ± 0.62 c	0.55 ± 0.02 a	0.99897
HT	19.48 ± 0.85 b	14.47 ± 1.16 b	0.52 ± 0.01 a	0.99797
HP	46.14 ± 6.52 a	33.71 ± 2.07 a	0.43 ± 0.00 b	0.99952
HM	4.17 ± 0.68 c	2.45 ± 0.18 c	0.51 ± 0.00 a	0.97652

* σ_0, yield stress; K, consistency coefficient; n, flow behaviour index; R^2 coefficient of determination; NQ, Native Quinoa; NA, Native Amaranth; NT, Native Taro; NP, Native Potato; NM, Native Maize; HQ, HMT Quinoa; HA, HMT Amaranth; HT, HMT Taro; HP, HMT Potato; HM, HMT Maize. Values in the same column with the different letters differ significantly ($p < 0.05$).

Table 4.9.2. Fitting parameters of Herschel-Bulkley model for flow curves of native and modified starches pastes (downward).

Downward				
Sample	σ0 (Pa)	K ($Pa^{-}s^{n}$)	n	R^2
NQ	26.97 ± 0.36 a	15.03 ± 0.40 b	0.45 ± 0.00 cb	1.000
NA	6.3 ± 0.12 c	10.52 ± 0.32 b	0.47 ± 0.00 b	1.000
NT	15.36 ± 0.25 b	7.22 ± 0.03 b	0.62 ± 0.00 a	0.999
NP	31.17 ± 2.05 a	41.71 ± 4.11 a	0.48 ± 0.01 b	1.000
NM	28.13 ± 3.71 a	12.04 ± 2.77 b	0.42 ± 0.02 c	0.996
HQ	1.96 ± 0.92 b	8.63 ± 0.93 b	0.48 ± 0.01 c	1.000
HA	1.96 ± 0.34 b	9.69 ± 0.06 b	0.47 ± 0.00 c	1.000
HT	8.59 ± 0.10 a	8.68 ± 0.14 b	0.58 ± 0.00 a	1.000
HP	5.33 ± 1.85 ba	40.71 ± 0.5 a	0.42 ± 0.01 d	1.000
HM	3.21 ± 0.39 c	2.28 ± 0.17 c	0.52 ± 0.00 b	0.999

* σ_0, yield stress; K, consistency coefficient; n, flow behaviour index; R^2 coefficient of determination; NQ, Native Quinoa; NA, Native Amaranth; NT, Native Taro; NP, Native

Potato; NM, Native Maize; HQ, HMT Quinoa; HA, HMT Amaranth; HT, HMT Taro; HP, HMT Potato; HM, HMT Maize. Values in the same column with the different letters differ significantly ($p < 0.05$).

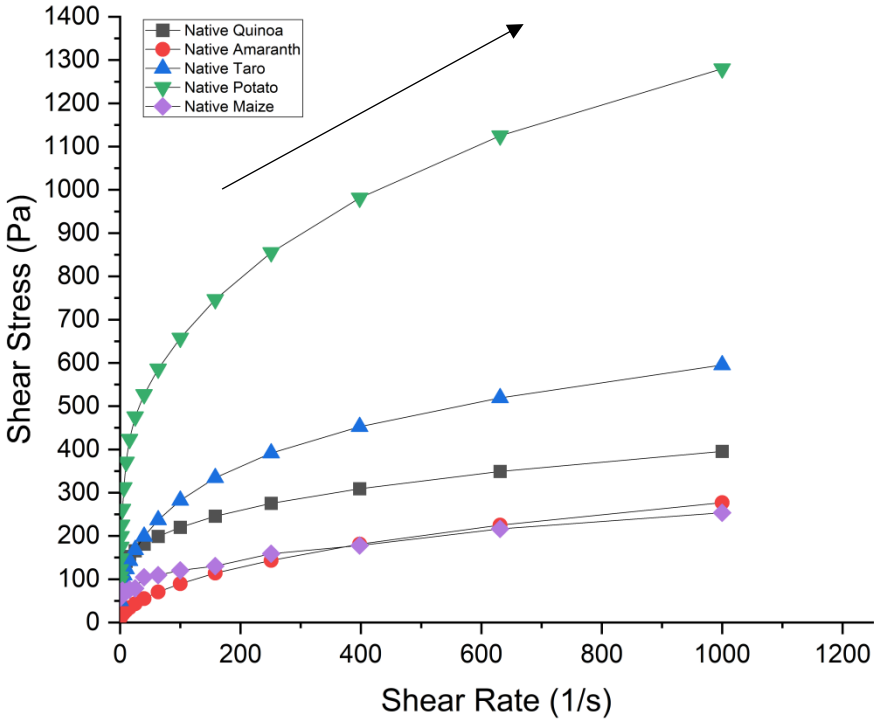

Figure 4.9.1. Upward flow curves of native starches.

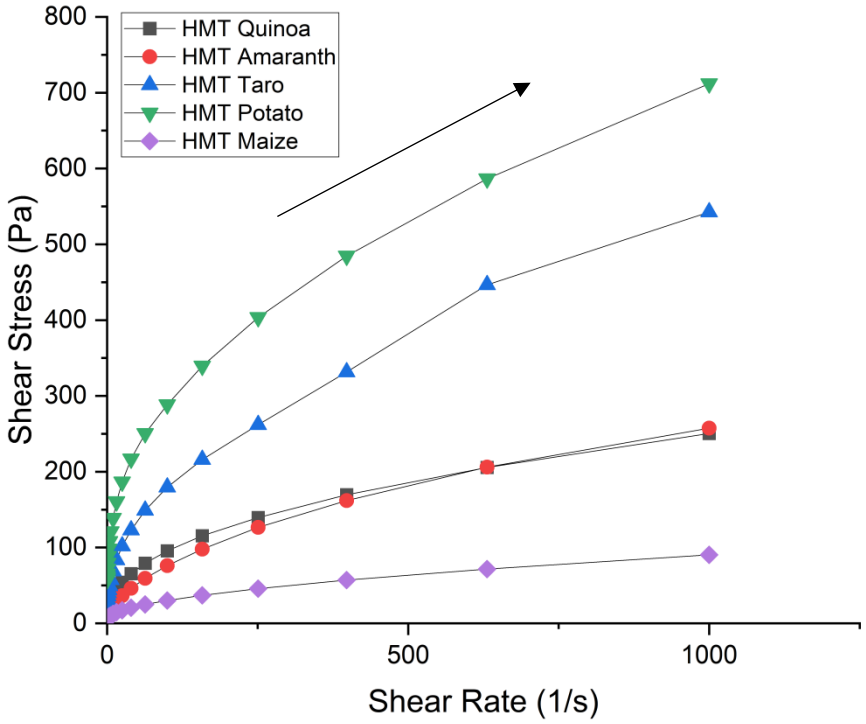

Figure 4.9.2. Upward flow curves of HMT starches.

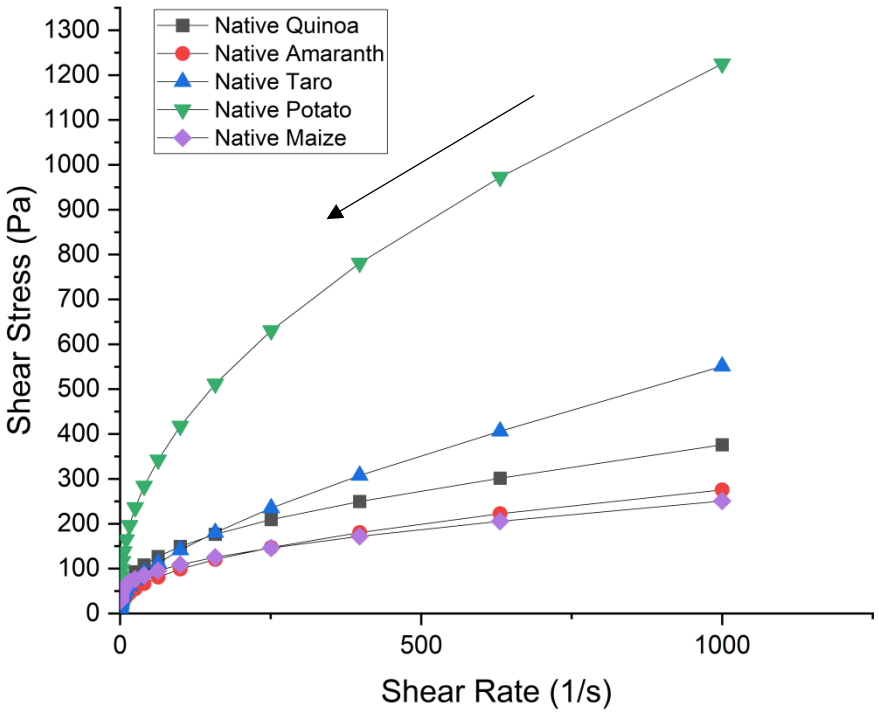

Figure 4.9.3. Downward flow curves of native starches.

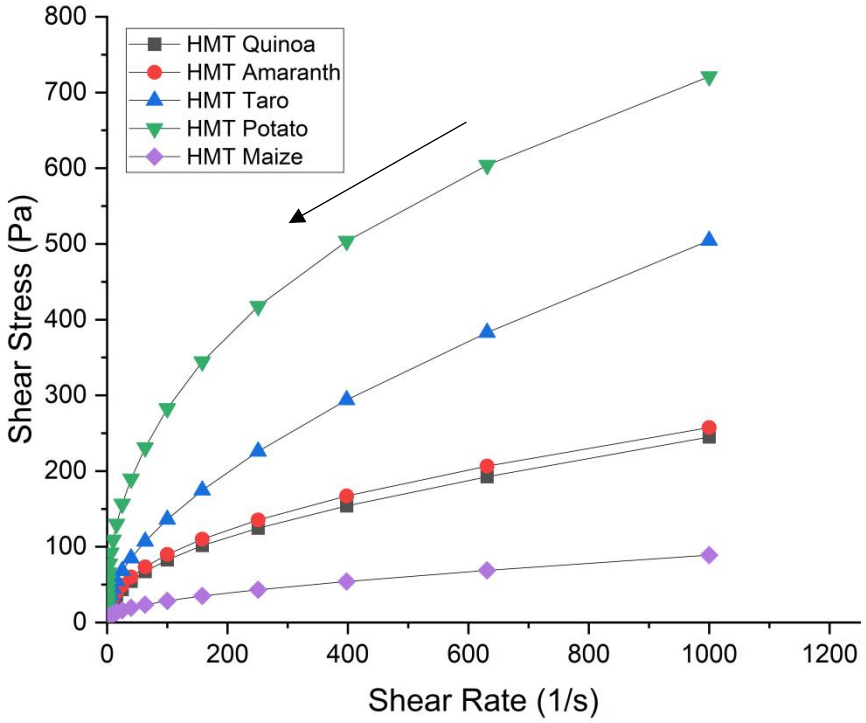

Figure 4.9.4. Downward flow curves of HMT starches.

In this study, whether natural starch or HMT modified starch, according to the description of the upward and downward shear process in Figure (4.9.1-4), it can be found that there is a nonlinear trend between shear stress and shear rate, and both of them exhibit non-Newtonian fluid characteristics. At the same time, the selected starch showed an increase in shear stress with an increasing shear rate before and after treatment. Hoover and Vasanthan (1994) came to the same conclusion by studying the gelatinized starch fluidity of natural wheat starch, oat starch, lentil starch and potato starch, all of which showed non-Newtonian shear thinning. For the natural starch, the natural potato starch showed the highest shear stress during the rising shear stage. Followed by taro starch and quinoa starch; at the same shear rate, natural amaranth and corn starch showed very similar shear stresses, and the five selected natural starches were the smallest. In the descending stage, it can be seen from Figure 4.9.3 that the shear stress of natural potato starch is much larger than that of the remaining four kinds of starch under the same shear rate. At the same time,

taro starch was larger than quinoa starch, and the flow curves of amaranth and corn starch were almost identical, indicating that the flow stress of natural amaranth and corn starch had the same trend of changing with shear rate. At the same time, it can be seen from the descending stage in Figure 4.9.2 & 4.9.4 that the flow curve gradually shifted from the process when the peak shear rate decreased to zero. Bao et al. (2011) believed that in the descending stage, the curve shifted from the approximate Newton fluid curve to the pseudoplastic fluid curve because amylopectin formed a stable network structure under the influence of shear force. Therefore, the change in the rheological curve in descending stage may be related to the change in amylopectin content. Comparing Figure 4.9.2 & 4.9.4, The effect of the HMT physical modification method on five kinds of natural starch can be obtained. The shear stresses of the five kinds of HMT starch were compared with the corresponding natural starch, and the corresponding shear stresses of HMT starch were lower than those of natural starch at the same shear rate, no matter in the ascending stage or the descending stage. This phenomenon is related to Hoover (2010); Liao et al. (2019) showed consistent results. In particular, the shear stress of starch modified by HMT with high moisture content would be significantly reduced. This result may be due to the intermolecular weakening in the selected starch paste, which was partially gelatinized under high moisture content (Liao et al., 2019). At the same time, potato starch still expressed the highest degree of shear stress, but the flow curve expressed by the remaining four kinds of starch changed somewhat. The flow curves of quinoa starch and amaranth starch after treatment were similar. Compared with the natural starch, the treated corn starch still had the smallest shear stress among the five kinds of starch (at the same shear rate), and the growth trend was lower than that of the natural corn starch. The descending process was similar to the ascending stage. Compared with the natural starch, the treated starch showed different shear stresses, but it still showed the characteristics of the pseudoplastic fluid.

Furthermore, a series of fluid property parameters were obtained by fitting the data

with the Herschel-Bulkley model. It can be seen from Table 4.9.1 that the fluid property parameters of different natural starches are quite different. In the ascending stage of natural starch, σ0 of quinoa starch was the highest (89.8 ± 18.38 Pa), while amaranth starch was the lowest (3.75 ± 1.18 Pa). The shear index (n) was corn starch > amaranth starch > taro starch > potato starch = quinoa starch, where the natural potato and taro starch at the end of the fitting showed the same shear index, indicating that they showed the same tendency to shear thinning. The n value of both natural starch and HMT starch was less than 1. This indicated that all starch paste samples showed pseudoplastic fluid behaviour. Where n less than 1 indicates shear thinning of the slurry system (Liao et al., 2019). Maize starch and amaranth starch have similar n values, and quinoa starch and taro starch have similar n values. Similar n values for different starches indicate that the expansion degree of the corresponding starch particles is almost the same (Hoover & Vasanthan, 1994). At the same time, Pearson's correlation coefficient should be considered when studying the difference in the n value of different starches according to the study (Y. Wang et al., 2018), and the n value is affected by starch composition. Among them, increasing amylose content in starch will increase the trend of starch thinning, whereas increasing amylopectin content will decrease this trend (Y. Wang et al., 2018). Therefore, the selected starch n value is affected by the internal structure of starch, which may also explain the higher n value of natural amaranth starch than other starches because of the higher amylopectin content in amaranth starch. This result is also consistent with the results of the previous sections. For the consistency index (K) of natural starch, the K value of natural potato starch was the highest (148.5 ± 0.43 $Pa^{-}S^{n}$), followed by natural taro starch and quinoa starch, and there was no significant difference between them. The smallest K was natural corn starch (5.16 ± 1.55 $Pa^{-}S^{n}$), similar to amaranth starch, with a K value of 8.11 ± 0.34 $Pa^{-}S^{n}$. The K value can express the viscosity of the corresponding starch paste in this fitting model (Zhou et al., 2017). For the characteristics of natural starch K value, Hoover and Vasanthan (1994) analyzed the correlation between flow property and swelling property of

various starches. They obtained that the contact degree between expanding particles would affect the K value after starch gelatinization and starch slurry (Hoover & Vasanthan, 1994). Moreover, the higher the value of K not only shows that the obtained starch paste has a more solid tendency but also indicates that the corresponding starch has higher amylose content. By observing Table 4.9.2, it can be seen that various parameters have changed to different degrees during the descent stage. Regarding the n value, taro starch had the largest value (0.62 ± 0.00), while the remaining starch had little difference and corn starch had the smallest value (0.42 ± 0.02). For the K value, the selected starch size was natural potato starch > quinoa > corn > amaranth > taro starch in order. The shear thinning process of starch paste in the selected starch was determined to have experienced rising and falling stages. The shear thinning in the second stage was the decrease in shear rate, and the properties of starch paste were greatly affected by the results of starch. (Feng et al., 2010) Except for the formation of the reticular structure of amylopectin during this period (Bao et al., 2011), its rheological parameters may be affected by short-term starch regeneration. Feng et al. (2010) found that short-term regeneration of amylose would produce gelation and crystallization formation, which greatly affected the viscosity and thixotropy of starch paste. For all kinds of natural starches, except amaranth starch, the rheological parameters of the other starches were significantly different in the upward and downward processes, and this variation trend indicated that the gel of the starch was not stable to shear force. At the same time, Zhu, Bertoft and Li (2016) found that the larger the particle size of natural starch, the higher the value of σ0 and K might be. It may be because there will be a residue of large particles after starch with large particle size forms paste, and the residue of large particles will lead to the higher shear resistance of the corresponding natural starch (Zhu, Bertoft & Li, 2016). This also well explains the curve change in potato starch's upward and downward shearing process in this experiment and the phenomenon that some parameters represent the largest.

By comparing Tables 4.4.1 and 4.4.2, it can be found that the parameters of starch physically modified by HMT have changed. In the rising stage, concerning the change of n value, except for HMT corn starch, which has a small decrease compared with natural starch, the other four starches all showed an upward trend. Especially HMT taro starch and HMT potato starch, HMT taro increased from 0.39 ± 0.01 to 0.52 ± 0.01, HMT potato starch increased from 0.39 ± 0.01 to 0.43 ± 0.00. The closer n is to 1, the closer the corresponding starch paste is Newtonian fluid (Hoover & Vasanthan, 1994), so the increase of the n value of some starch after HMT modification shows that this method promotes the transformation of starch from pseudoplastic fluid to Newtonian fluid, and also shows that the shear thinning tendency of starch is affected by increased by HMT. Liao et al. (2019) explored the rheological parameters of HMT sweet potato starch under different processing parameters and found that HMT samples of all experimental groups showed a higher shear thinning tendency than natural samples, and the n of HMT starch was higher; the results of this study are the same as the results of this experiment, and the reasons are more specifically explored. One possibility is that due to the short-term retrogradation, the high tendency of amylose makes the amylose paste and pre-agglomeration in the paste sample. Micellar clusters increased (Liao et al., 2019; Y. Wang et al., 2018). This starch modified by HMT has more particles in the starch slurry, leading to a higher degree of reorientation during the shearing process (Chen et al., 2017). Therefore, most starches modified by HMT show a higher degree of reorientation and high shear thinning tendency. However, it can be found from Table 4.9.1 that the n value of cornstarch after physical modification by HMT decreases. The weaker shearing tendency of corn starch after HMT treatment is similar to the findings of Bao et al. (2011). The reason for this phenomenon may be caused by the lower inherent viscosity of corn starch. The next step is to compare the K value affected by HMT. It can be found that in the process of the rising stage, the K value of HMT starch has decreased to varying degrees compared with the corresponding native starch. Among them, HMT potato starch showed the largest decline (from 148.5 ± 0.43 to 33.71 ±

2.07), while HMT amaranth starch and HMT maize starch showed similar declines (HMT amaranth starch: from 8.11 ± 0.34 to 5.81 ± 0.62; HMT cornstarch: decreased from 5.16 ± 1.55 to 2.45 ± 0.18). After physical modification by HMT, the K value of potato starch was still the highest, while corn starch was still the lowest. However, Liao et al. (2019) found that HMT may increase the K value of starch and correlated this phenomenon with the higher solid tendency caused by HMT. However, since only some starch samples expressed similar phenomena, this view may be based on the influence of the starch source. Hoover (2010) found that after several starch treatments, only the oat starch treated with HMT showed an increase, while the rest of the wheat, lentil and potato starches all significantly decreased K value under the influence of HMT. The decrease in K value is because granular starch is affected by HMT; its degree of swelling and leaching of amylose is reduced (Hoover, 2010; Hoover & Vasanthan, n.d.). It might also explain the decrease of the K value of different types of starch in this experiment, and the decrease range is also different due to the different structures of different starches. By comparing the σ0 in the upward stage, except that the potato starch increased from 19.16 ± 9.49 Pa to 46.14 ± 6.52 Pa, and the amaranth starch hardly changed, the σ0 of the other starches decreased after treatment. At the same time, further comparison found that both σ0 and K values showed a downward trend during the downward stage. In particular, the σ0 value dropped significantly after HMT. At the same time, by comparing the σ0 value, the K value and the n value are affected by HMT, and it is found that there are differences in their changes. The rheological parameters are affected by many factors. The rheological parameters of starch paste affected by HMT are affected by the change of particle volume, which changes the resistance of the particles to cope with the deformation during the gelatinization process, thus affecting the rheological parameters. At the same time, Li and Zhu (2017) found that the different rheological parameters are affected by many factors, such as non-starch other substances, molecular structure and genetic variation.

Finally, due to the numerous factors affecting the rheological properties of starch and particle size, it is also affected by other substances in the starch or starch structure. Therefore, the rheological parameters of five different starches cannot be directly determined by particle size or rheological parameters. At the same time, by comparing the rheological properties of starch modified by HMT, it can be concluded that the modification of HMT can generally lead to increased shear thinning and decreased consistency index. The changes in different trends may be affected by the structure and properties of the corresponding starch.

4.10 Oscillation of starch

In this part, the oscillatory properties of the selected starch samples were measured by the MCR 301 Rheometer with a PP-25 probe, as mentioned in the previous section. The energy storage modulus (G') and loss modulus (G") of the selected starch before and after treatment were obtained from the experimental data under different parameters. In addition, the data results are plotted to obtain the influence of temperature change and frequency change on G' and G" (Figures 4.10.1 to Figure 4.10.4). Different kinds of starch can be obtained through the image, showing different dynamic rheological properties. According to the temperature changes during the oscillation experiment, the oscillation curve can be divided into upward and downward temperature curves. For the record and analysis of the change of oscillation parameters under the temperature change, they are drawn in Tables 4.10.1 & 4.10.2. The experimental data are plotted for the influence of frequency variation on oscillation parameters.

4.10.1. Temperature sweep test

The 20% w/w concentration of natural starch and processing after the suspension heating and cooling process (40°C to 90°C, and then 90°C to 25°C), G' and G" change curve drawn into an image (Figure 4.10.1.1-4). It can be found that the temperature dependence of G' and G" of different natural starches are pretty different, and the G' and G" of HMT-modified starches have changed significantly. At the same time, all the data obtained from the experimental results were recorded, including the maximum value of G' and G" in the heating stage, the corresponding temperature when the maximum value was reached, and the maximum value of the damping factor (Tan) and the corresponding temperature when the damping factor reached the maximum value. The temperature scanning parameters of natural starch and HMT

starch were plotted in table 4.10.1. The values of G' and G'' were obtained at the beginning of cooling (90°C) and the end of cooling (25°C), and the corresponding damping factor (tan δ Max) at the end of cooling was recorded. The recorded data were used to plot the temperature scan parameter tables (4.10.2) for natural starch and HMT starch during the cooling process.

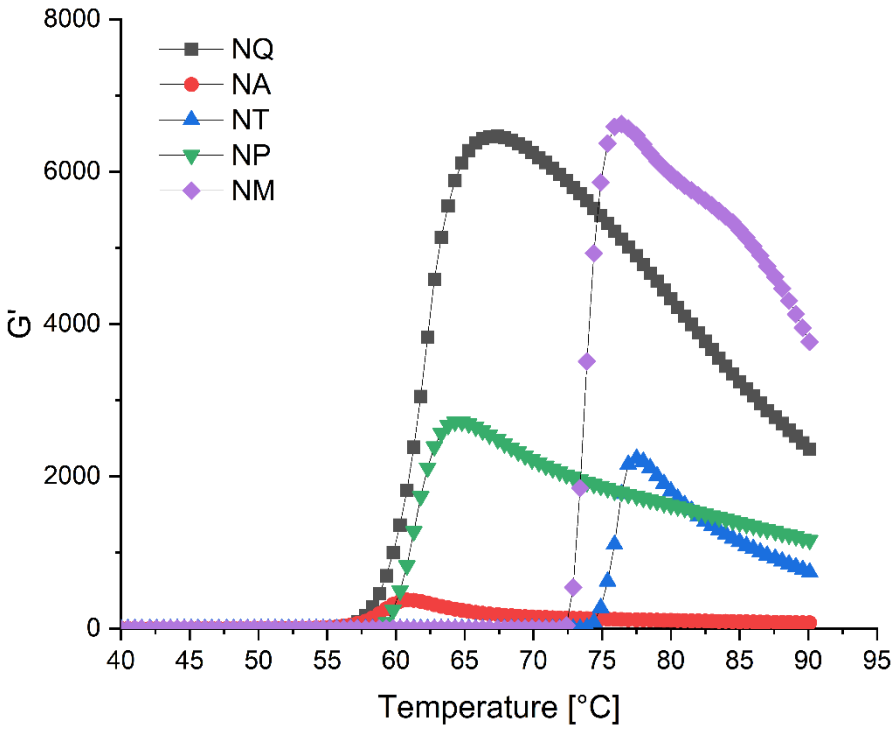

Figure 4.10.1.1. The change of G' of different varieties of native starch during heating.

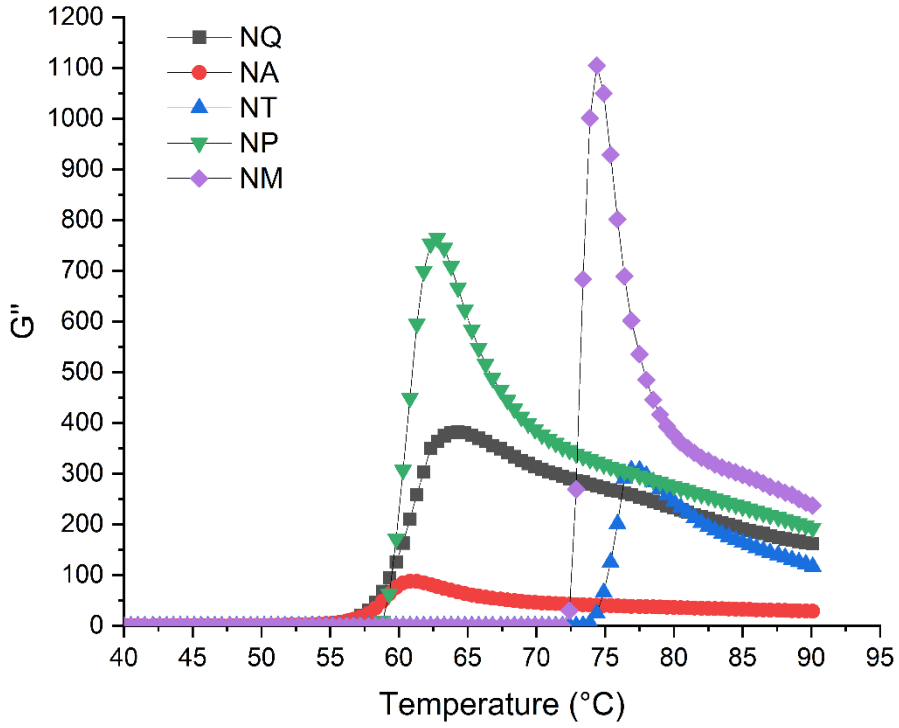

Figure 4.10.1.2. The change of G" of different varieties of native starch during heating.

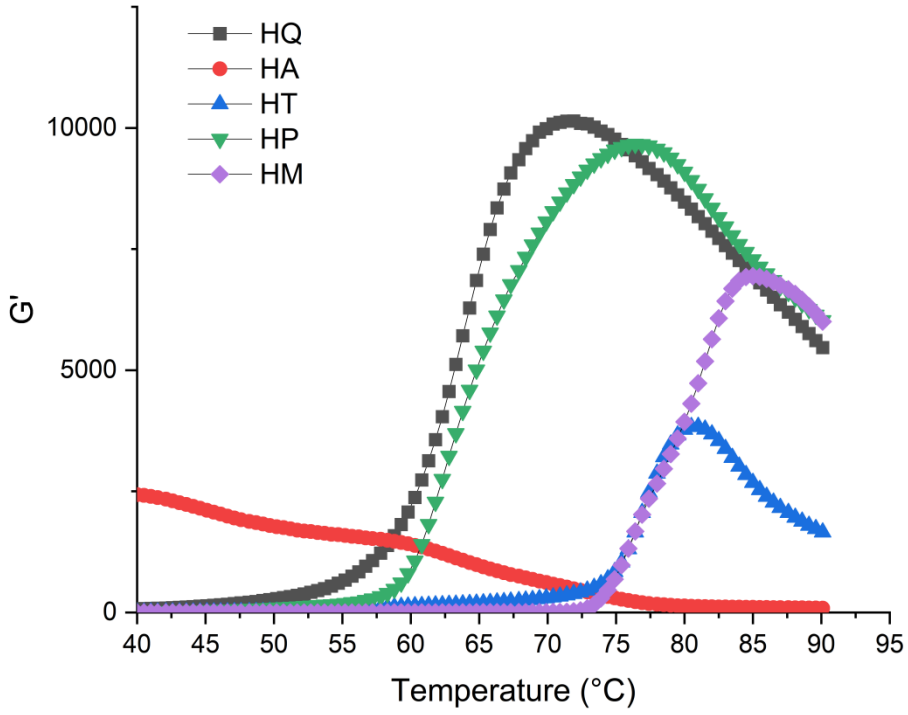

Figure 4.10.1.3. The change of G' of different varieties of HMT starch during heating.

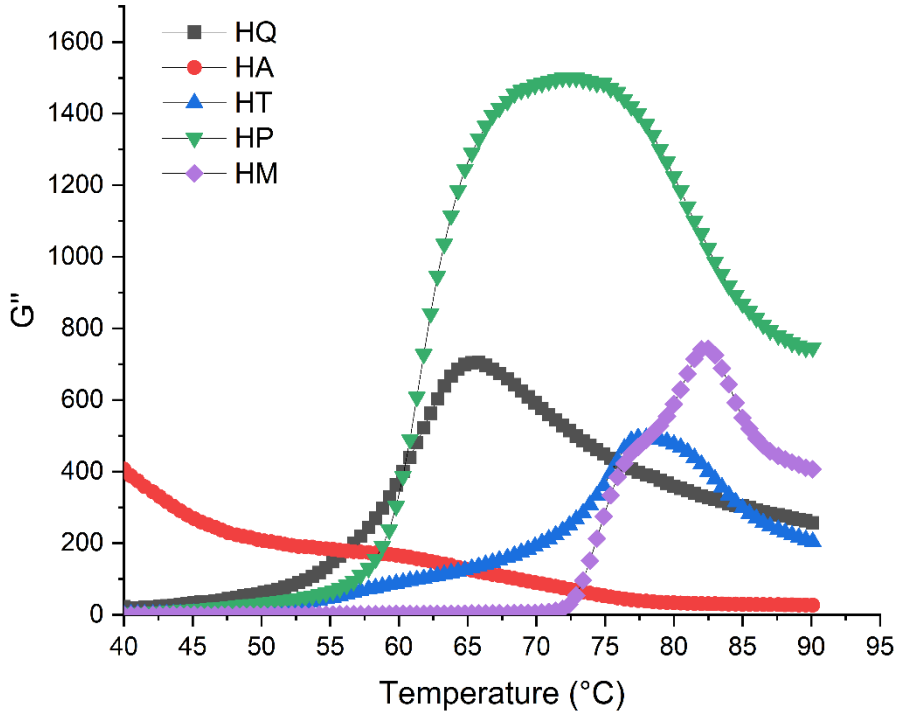

Figure 4.10.1.4. The change of G" of different varieties of HMT starch during heating.

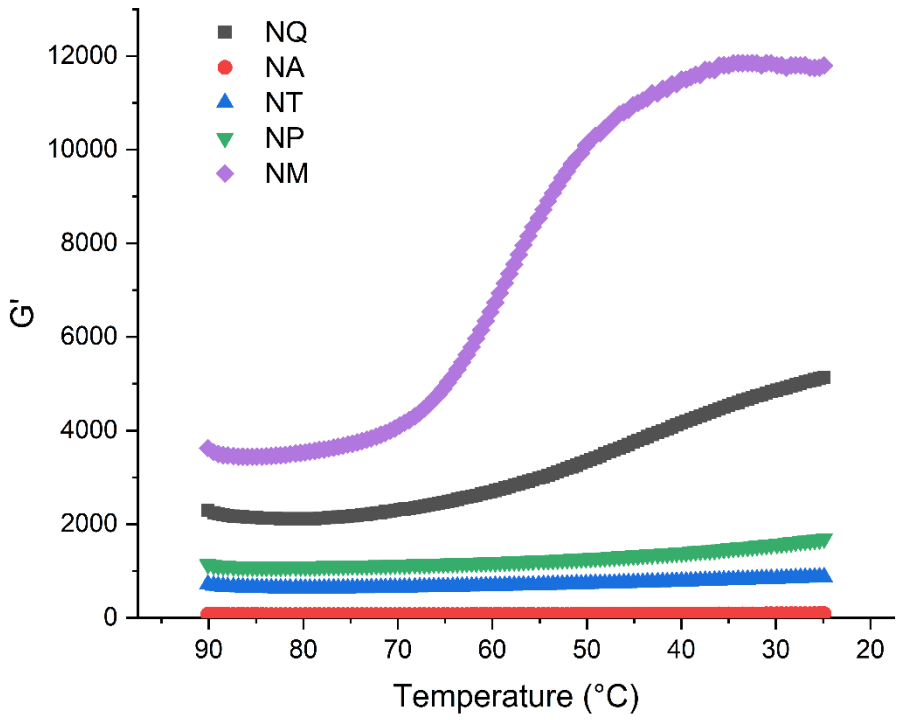

Figure 4.10.1.5. The change of G' of different varieties of native starch during cooling.

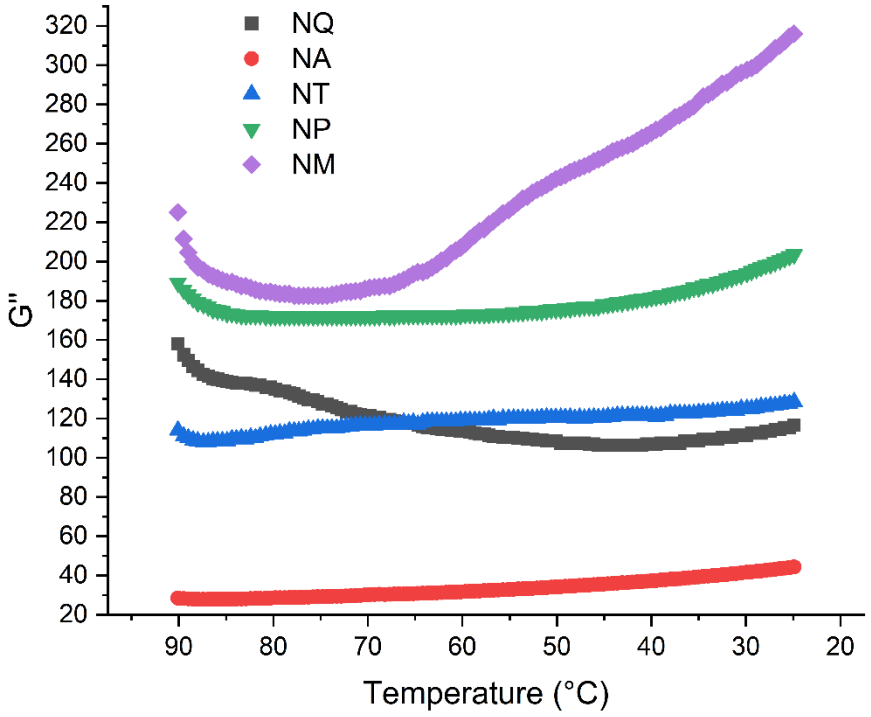

Figure 4.10.1.6. The change of G" of different varieties of native starch during cooling.

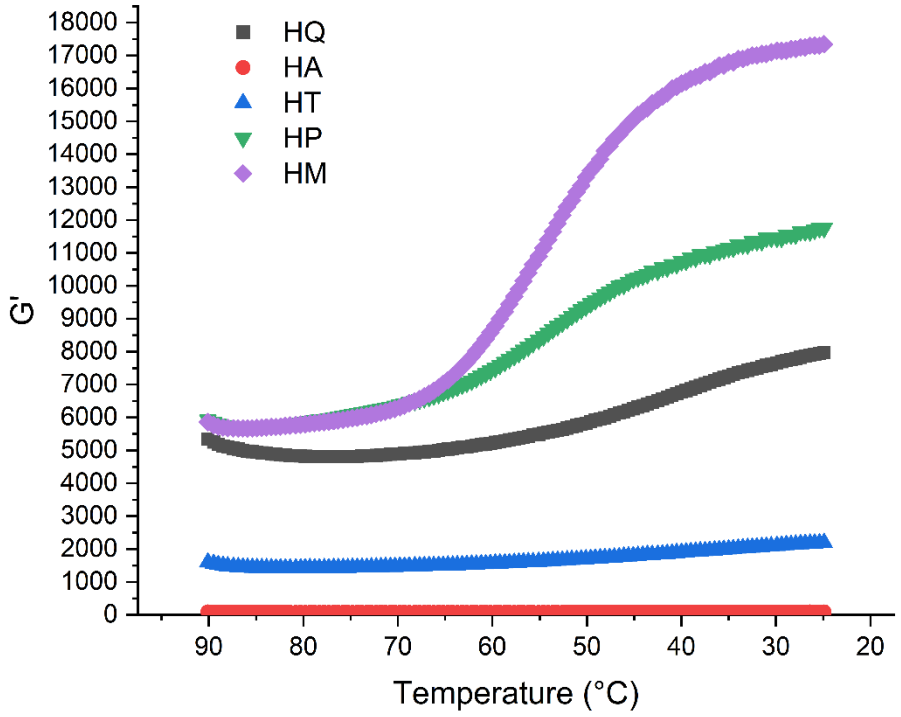

Figure 4.10.1.7. The change of G' of different varieties of HMT starch during cooling.

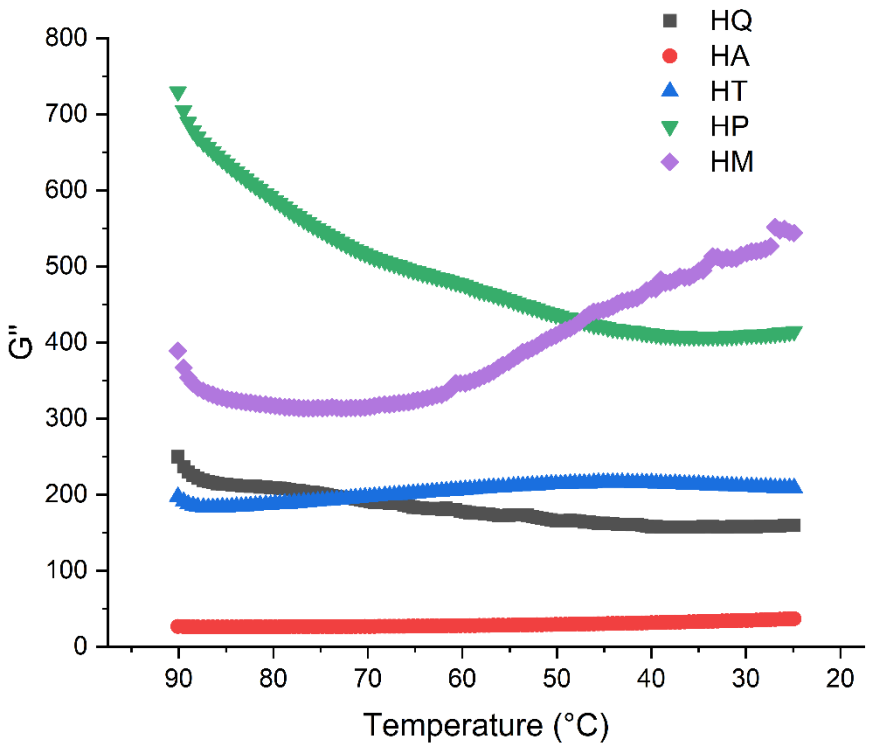

Figure 4.10.1.8. The change of G" of different varieties of HMT starch during cooling.

Table 4.10.1. Temperature sweep parameters of native starches and HMT starches (heating stage).

	Heating					
Sample code	**$T_{G'max}$**	**G'_{max}**	**$T_{G''max}$**	**G''_{max}**	**Ttan δ_{max}**	**tan δ_{max}**
NQ	67.10 ± 0.42 b	6465 ± 49.50 a	64.30 ± 0.00 c	383.00 ± 5.66 dc	54.45 ± 0.35 b	0.38 ± 0.01 b
NA	57.25 ± 5.02 c	375 ± 9.90 d	60.80 ± 0.00 e	88.05 ± 2.05 d	49.70 ± 0.71 b	0.43 ± 0.02 b
NT	77.40 ± 0.00 a	2235 ± 120.21 c	77.15 ± 0.35 a	309.50 ± 23.33 b	60.55 ± 2.47 a	0.96 ± 0.01 a
NP	64.30 ± 0.00 cb	2715 ± 21.21 b	62.80 ± 0.00 d	764.50 ± 12.02 cb	58.80 ± 0.00 a	0.95 ± 0.03 a
NM	76.40 ± 0.00 a	6625 ± 21.21 a	74.40 ± 0.00 b	1105.00 ± 7.07 a	71.90 ± 0.71 a	0.93 ± 0.04 a
HQ	71.15 ± 1.06 d	10145 ± 219.20 a	65.30 ± 0.71 d	708.50 ± 16.26 a	55.95 ± 1.06 c	0.22 ± 0.00 c
HA	40.50 ± 0.00 e	2415 ± 120.21 d	40.50 ± 0.00 e	388.50 ± 7.78 b	47.40 ± 1.84 d	0.12 ± 0.00 d
HT	80.75 ± 0.35 b	3835 ± 7.07 c	78.45 ± 1.48 b	510.50 ± 51.62 a	55.50 ± 2.55 a	0.72 ± 0.00 a
HP	76.40 ± 0.00 c	9665 ± 445.48 a	71.65 ± 0.35 c	1500.00 ± 84.85 a	57.50 ± 0.42 b	0.40 ± 0.00 b
HM	85.00 ± 0.00 a	6940 ± 169.71 b	82.50 ± 0.00 a	743.50 ± 20.51 a	58.80 ± 0.71 a	0.73 ± 0.00 a

*NQ, Native Quinoa; NA, Native Amaranth; NT, Native Taro; NP, Native Potato; NM, Native Maize; HQ, HMT Quinoa; HA, HMT Amaranth; HT, HMT Taro; HP, HMT Potato; HM, HMT Maize. Values in the same column with the different letters differ significantly ($p < 0.05$).

Table 4.10.2. Temperature sweep parameters of native starches and HMT starches (cooling stage).

	Cooling				
Sample Code	**G'_{90}**	**G''_{90}**	**G'_{25}**	**G''_{25}**	**tan δ_{25}**
NQ	2290 ± 7.07 b	158 ± 1.41 c	5140 ± 28.28 b	116.50 ± 0.71 c	0.02267 ± 0.0000 d
NA	72.60 ± 3.32 e	28.5 ± 0.85 e	87.50 ± 4.24 d	44.35 ± 1.77 d	0.50696 ± 0.0044 a
NT	736 ± 33.23 d	114 ± 7.07 d	871.50 ± 10.61 dc	128.50 ± 2.12 c	0.14744 ± 0.0006 b
NP	1140 ± 0.00 c	189 ± 1.41 b	1690 ± 14.14 c	203.50 ± 4.95 b	0.12041 ± 0.0019 c
NM	3610 ± 21.21 a	225 ± 2.83 a	11800 ± 707.11 a	316.00 ± 9.90 a	0.0268 ± 0.0008 d
HQ	5280 ± 84.85 b	250 ± 9.90 c	7980 ± 339.41 c	159.50 ± 4.95 c	0.01999 ± 0.0002 e
HA	89.50 ± 2.26 d	26.75 ± 0.49 d	87.40 ± 3.68 e	36.85 ± 1.48 d	0.42164 ± 0.0007 a
HT	1590 ± 7.07 c	197.5 ± 2.12 c	2195 ± 35.36 d	209.00 ± 2.83 c	0.09522 ± 0.0002 b
HP	6050 ± 176.78 a	729.50 ± 31.82 a	11750 ± 212.13 b	414.50 ± 13.44 b	0.03527 ± 0.0005 c
HM	5750 ± 155.56 a	389 ± 11.31 b	17350 ± 636.4 a	544.00 ± 31.11 a	0.03134 ± 0.0006 d

*NQ, Native Quinoa; NA, Native Amaranth; NT, Native Taro; NP, Native Potato; NM, Native Maize; HQ, HMT Quinoa; HA, HMT Amaranth; HT, HMT Taro; HP, HMT Potato; HM, HMT Maize. Values in the same column with the different letters differ significantly ($p < 0.05$).

According to Figure 4.10.1-2, the G' and G" of the selected natural starch suspension during heating are expressed as a function of temperature, respectively. The starch energy storage modulus, also known as elastic modulus (G'), represents the amount of energy stored during deformation (Liu et al., 2016). The loss modulus, also known as the viscous modulus (G"), is used as a parameter to measure dissipated energy (Marboh & Mahanta, 2021). According to the image, it can be found that the temperature oscillation curves obtained by different kinds of starch are different.

Due to the previous DSC experiment, various gelatinization temperatures of the selected starch were obtained (natural quinoa starch is about 55°C, natural amaranth starch is about 56°C, taro starch is about 73°C, potato starch is about 62°C, and corn starch is about 71°C. Combined with the obtained Figure (4.10.1-2), it can be found that G' and G" curves are relatively smooth at the beginning of heating. With the increase in temperature, the corresponding values of G' and G" do not change significantly. However, when the experimental temperature reached the corresponding gelatinization temperature of natural starch, the values of G' and G" increased sharply, and the curve increased significantly. This result is consistent with the results obtained by Li and Zhu (2018) in the temperature scanning test of different quinoa starches, which also found that the values of G' and G" would increase significantly before reaching G'_{Max}. After reaching the gelatinization temperature, the G' and G" values increased with the temperature increase. Sing et al. (2003) believed this phenomenon was caused by the precipitation of amylose in this process, which expanded at gelatinization temperature and generated a three-dimensional network structure. It can be found from Table 4.10.1 that the G'_{Max} of native quinoa selected in this experiment is 6465 ± 49.5, and the value of $T_{G' Max}$ is 54.45 ± 0.35 degrees. Li and Zhu (2018) found that the G'_{Max} of quinoa ranges from 3997Pa to 7510Pa, and the temperature range of $T_{G' Max}$ is from 57.7 degrees to 67.3 degrees. Therefore, the selected parameters of natural quinoa are within the range

of quinoa. At the same time, according to Table 4.10.1, there was no significant difference in G'_{Max} value between natural quinoa starch and natural corn starch. However, G' of corn starch was the highest among the five natural starches (6625 ± 21.21), and the remaining natural starch in descending order was quinoa starch> potato starch> taro starch>amaranth starch. The G' value of natural amaranth starch was minimal, only 375 ± 9.90. At the same time, the order of G''_{Max} values was consistent with the results of G'_{Max}, with the highest value of corn starch and the lowest value of amaranth starch. Both G'_{Max} and G''_{Max} of corn starch were higher than those of quinoa starch, which was consistent with the results obtained by Li and Zhu (2018). In addition, the higher the value of G'_{Max} and G''_{Max}, the less likely the corresponding starch to form a paste with lower viscosity at the concentration selected in the experiment (Li & Zhu, 2018). Therefore, according to this theory, among the five kinds of starch selected, natural amaranth starch is more likely to form a paste with lower viscosity at this concentration than the other four kinds of starch. As for the trend of G' value and G' with temperature change, Eliasson (1986) found that the initial increase of G' value was since starch particles were affected by temperature rise, expanding continuously and packing closely in the suspension, leading to a significant increase of G' value. Therefore, compared with the natural starch in Table 4.10.1, the $T_{G'max}$ values of HMT starch, except for amaranth starch, increased to different degrees. The modification of HMT increased quinoa starch from 67.10 to 71.15°C, taro starch from 77.40 to 80.75°C, potato starch from 64.30 to 76.40°C. And corn starch increased from 76.40 to 85.00°C. This phenomenon indicates that HMT treatment can delay starch granule expansion, which is consistent with the result of HMT treatment of rice starch by Takahashi et al. (2005). In addition, it can be found that the physical modification of HMT has similar effects on $T_{G''max}$ and $T_{G'max}$, among which the value of $T_{G'max}$ and $T_{G''max}$ decreased in amaranth starch. In brief, the modification of HMT resulted in the more likely expansion of amaranth starch particles and more likely accumulation in the suspension. It would also explain why the amaranth starch mentioned earlier is more

likely to form a paste with lower viscosity than the four starch types. Amaranth starch shows a unique phenomenon. Gunaratne & Corke (2007) believed that since the factor affecting starch particle expansion is soluble amylose leaching, while lack of amylose starch amaranth would show greater expansion after HMT modification. In addition, the reduction of amylose precipitation in the process of HMT modification jointly leads to a lower temperature when HMT amaranth starch reaches the peak energy storage modulus and loss modulus than natural starch. Combined with the above results and views, amaranth starch is more likely to expand at low temperatures than other selected starches. However, the rigidity of starch grain expansion is much weaker than other kinds of starch. By observing the dynamic oscillation temperature curve, it can be found that G' and G" rose to the maximum value and then began to decline. At the same time, comparing the values of various G'_{Max} and G''_{Max} before and after treatment, it can be found that the peak energy storage modulus and loss modulus of natural starch was increased by HMT modification. However, the G" of HMT maize starch was partially decreased (from 1105.00 ± 7.07 to 743.50 ± 20.51).

At the same time, the temperature cooled down from a peak of 90 °C until it returned to 25°C. During the period, G' and G" values increased again with the decrease in temperature. The comparison curve showed that the G' value of each starch in the cooling stage was maize starch > quinoa starch > potato starch > taro starch > amaranth starch. For G" value, maize starch was still the largest, followed by potato starch; Quinoa starch and taro starch showed similar trends, while amaranth starch was still the smallest. As for the growth range, it can be seen from Figure 4.10.1.7 and Table 4.10.1.2 that natural corn starch has the most extensive increasing range, with G' increasing from about 3610 ± 21.21 to 11800 ± 707.11. The value of natural quinoa starch increased from about 2290 ± 7.07 to 5140 ± 28.28. The growth of the remaining three starches was low. Amaranth starch had the lowest growth, from

72.60 ± 3.32 to 87.50 ± 4.24. As for the variation of G", except for natural quinoa starch, which decreased from 158 ± 1.41 to 116.50 ± 0.71, the G" value of the other four kinds of starch increased, and the increased range was relatively low. As for the characteristics that quinoa starch showed increased hardness and decreased starch molecular fluidity after cooling, Li and Zhu (2018) believed that it was because the amylose leached in the cooling process was reordered or affected by long-chain amylopectin. In addition, it can be seen from Figures 4.10.1.7 & 8 that the temperature curve of G' value changed during the cooling process for different starches after HMT modification. From the largest to the smallest, HMT maize starch>HMT potato Starch >HMT quinoa starch>HMT taro Starch >HMT amaranth. Compared with the G' curve of natural starch, the G' trend increased with the temperature decrease in the cooling stage. Among them, the G' of maize starch increased the most, and the natural potato starch had lower growth than others. Compared with natural starch, corn starch's value increased from 6050 ± 176.78 to 11750 ± 212.13 after HMT modification. At the same time, the growth of other starch was not only higher but also the value of G' was larger. For G" value, the modified starch also showed the same trend; that is, the HMT starch had a larger G" value. Therefore, it can be obtained that after HMT modification, the cooled starch gel shows higher hardness.

As for the damping factor, Rao (2014) believed that this parameter represented the elastic component of viscosity and some viscoelastic behaviours. The damping factor can generally be divided into four stages in the heating and cooling stages (Li & Zhu, 2018). These four stages express the elastic behaviour and the changes of elastic components during the gelation, starch particle breakage and rebound process of starch from room temperature to gelatinization temperature. There was no significant difference in the damping factors of natural starch, natural taro, potato and corn starch, and the remaining quinoa and amaranth starch were similar. The damping factor of taro starch was the highest (0.96 ± 0.01), while the damping factor

of natural amaranth starch was the lowest (49.70 ± 0.71). According to the theory of Li and Zhu (2018), taro starch paste is the most elastic among the selected starches, while amaranth starch paste is the least elastic. At the same time, it can be seen from Table 4.10.1 that the damping factors of starch modified by HMT all decreased. The damping factor of HMT potato starch decreased the most, from 0.95 ± 0.03 to 0.40 ± 0.00. These results indicated that compared with the natural starch, the gelatinized paste obtained by the physical modification of HMT was less elastic than that of the natural starch.

4.10.2. Frequency sweep measurement

The heated and cooled starch gel was scanned for frequency, and the data obtained were plotted in Figure. 4.10.2.1 - 4. The Figure records the changes of each starch's G' and G" values when the frequency increases from 0.1Hz to 40Hz.

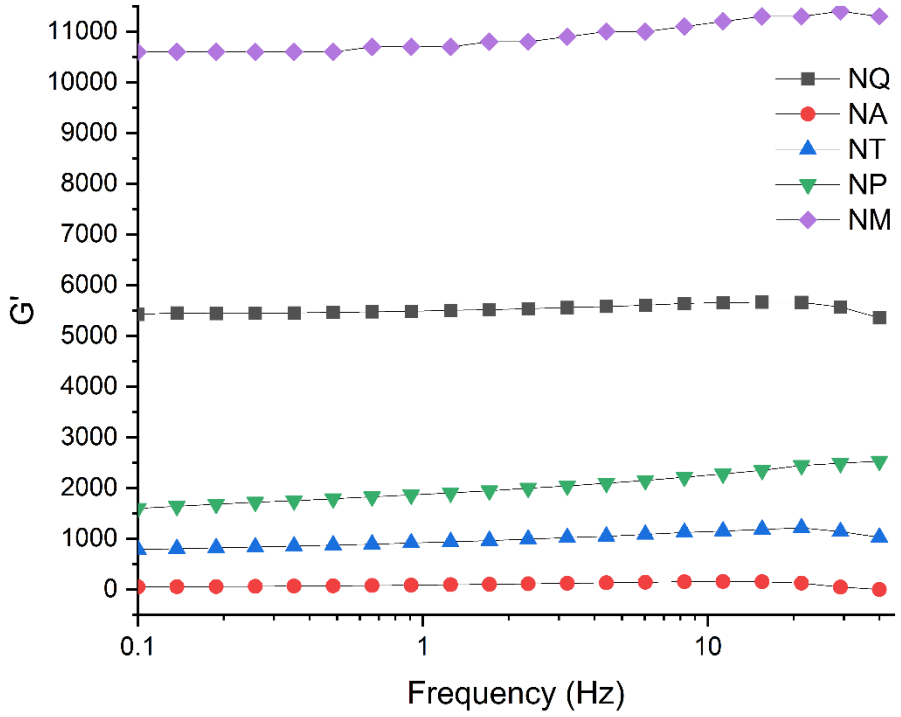

Figure 4.10.2.1. The change of G' of different varieties of native starch during frequency increasing.

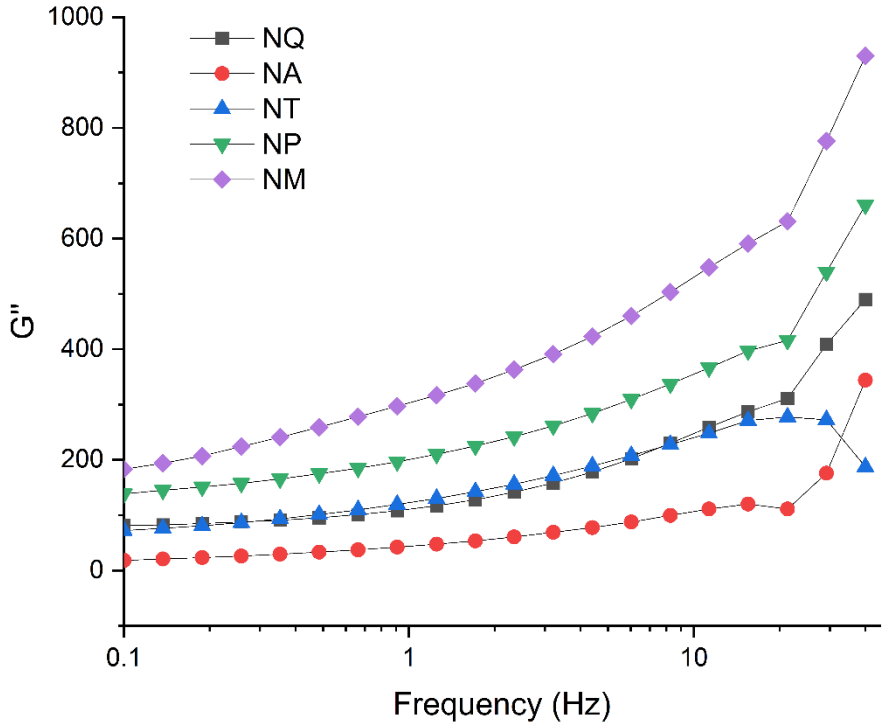

Figure 4.10.2.2. The change of G" of different varieties of native starch during frequency increasing.

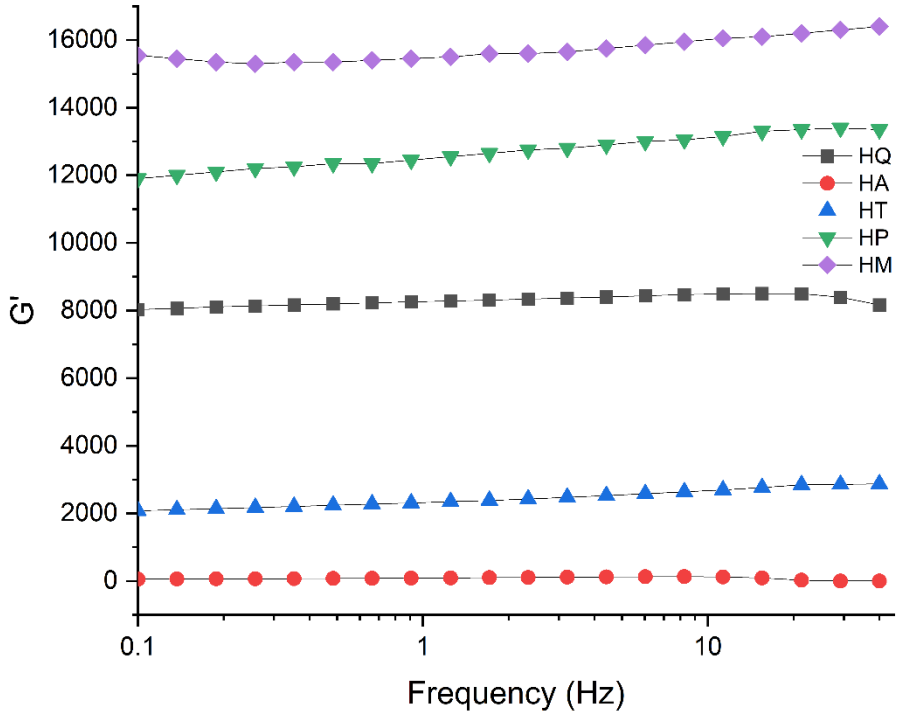

Figure 4.10.2.3. The change of G' of different varieties of HMT starch during frequency increasing.

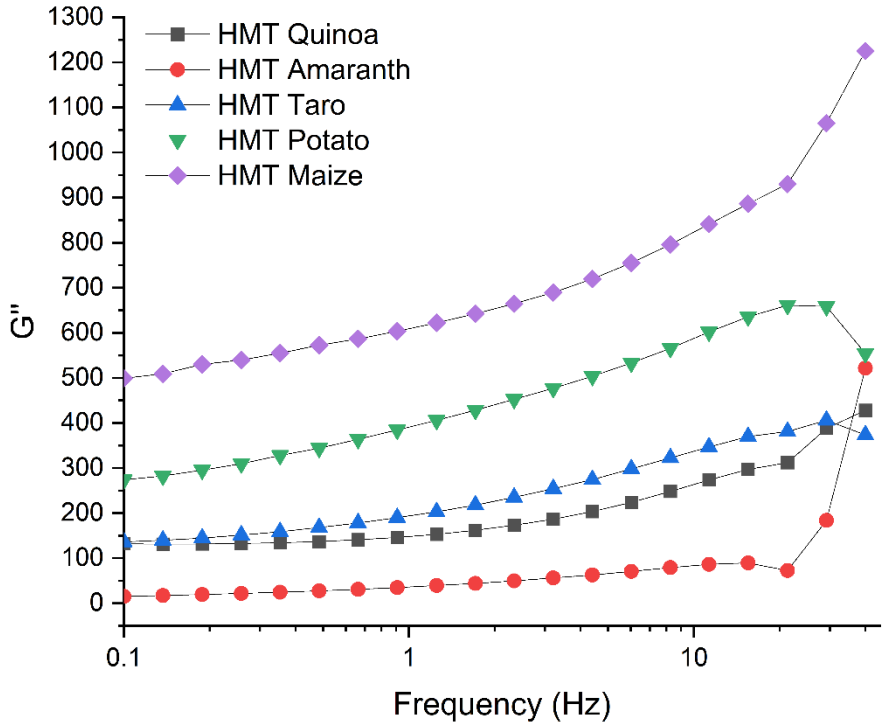

Figure 4.10.2.4. The change of G'' of different varieties of HMT starch during frequency increasing.

In Figure 4.10.2.1&2, G' and G'' values of different kinds of natural starches have different dependence on frequency. In terms of G' value, natural maize had the highest starch, followed by quinoa starch > potato starch > taro starch>amaranth starch. G' of the selected natural starch remained stable with the increase of experimental frequency. For the value of G'', the order of the size of the natural starch is maize starch> potato starch > quinoa starch > taro starch > amaranth. And with the increase of frequency, the value of G'' also increases, and the two are positively correlated. At the same time, the relationship between G' and G'' was observed. It was found that the value of G' was much higher than that of the corresponding starch sample in the frequency range. Moreover, that means that these curves do not intersect. This phenomenon indicates that because amylose in starch particles is reordered and a fixed amount of leaching is maintained, the gel

occupies the dominant range within the selected experimental frequency, thus expressing that the curves of G' and G'' do not coincide (Li & Zhu, 2018). It also shows that starch gels show more elastic characteristics rather than viscous characteristics. This conclusion is consistent with Munish et al. (2022). For the stability ability of gels at different frequencies, gels can often be distinguished into "true gels" and "weak gels" (Ikeda & Nishinari, 2001; Rao, 2014). At the same time, Mezger (2020) believed that G' in the low-frequency state could represent the degree of starch gel cross-linking, while in the high-frequency state, the stronger the starch cross-linking, the more stable the network structure, and the greater the corresponding G' value. Therefore, compared with the selected natural starches, the natural cornstarch gel had the strongest cross-linking degree and formed the most stable network structure, while the amaranth starch gel was the weakest. Li and Zhu (2018) believed that this phenomenon was caused by the low amylose content of amaranth starch. This phenomenon is similar to what we found with the gel texture in the previous section. Meanwhile, it can be seen from Figure 4.10.2.2 that the loss modulus (G'') of natural starch increases with the increase of frequency, which is consistent with the conclusion of amaranth starch made by Munish et al. (2022).

At the same time, comparing the starch G' and G'' curves after HMT treatment, it can be found that the value of the modified starch G' was significantly higher than that of the original starch. The results indicated that the physical modification of HMT enhanced the expression of the elastic ability of starch. At the same time, it was found from 4.10.2.3 that different HMT starches exhibited different levels of energy storage modulus at the same frequency. From large to small, maize starch>potato starch> quinoa starch> taro starch> amaranth starch. Among them, the granule size of maize starch and potato starch is much larger than the other three kinds of small grain starch. As for the influence of particle size on dynamic rheological properties, Li and Zhu (2018) explored the differences between quinoa starch with different particle sizes in frequency scanning measurement experiments and found that

quinoa starch with larger particle sizes exhibited much higher elasticity. The mean diameter of mass moment of particle size parameter (D [4,3]) is positively correlated with the obtained G'_{40Hz} and $G'_{0.1Hz}$. In addition, it was also reported that corn starch exhibited stronger elasticity in corn starch with larger particle sizes (Zhu et al., 2016). This conclusion is consistent with the results obtained above. Meanwhile, in the curve of G' and frequency, it can be found that the G' value of amaranth starch treated with HMT decreased slightly with the increase of frequency. For this phenomenon, Munish et al. (2022) believed that the modification of HMT might destroy the molecular order in starch particles. For the loss modulus, the modified starch with HMT showed a lower G" value than the natural starch. Due to this feature, Liu et al. (2016) believed that HMT treatment would reduce the deformation recovery rate and rheological resistance of starch so that the G" value of HMT starch was lower than that of the corresponding natural starch.

Finally, it could be found that in the experiment of dynamic starch rheology, with the change of temperature and frequency, various oscillatory parameters of different natural species are different. Moreover, HMT modification not only changes the properties of starch gel oscillation but also has some effects on the experimental results. In particular, the larger the selected starch particle size, the stronger the gel showed the elasticity, which was especially obvious in HMT starch. However, from the results of this experiment, the size of starch particles is not the only factor affecting the rheological properties. As Li and Zhu (2018) found, due to the particle morphology of different starch samples, the composition structure and chemical composition of amylopectin will affect the final rheological properties. And rheological quantification involves various factors and structural basis, which is a very complex system (Li & Zhu, 2018). Liu et al. (2016); Singh et al. (2005) found that the rheological properties of starch after HMT modification were also affected by protein-lipid complexes. Although the amylose content of selected starches is sometimes low, disruption of starch and protein-lipid interactions during HMT also

affects rheological properties; thus, both the energy storage and loss modulus change (Liu et al., 2016). Therefore, many factors affect the final rheological properties of starch.

Chapter 5 Conclusion and Future work

5.1 General conclusion

The effects of different particle sizes on the results of modified HMT were studied by analyzing and characterizing the physicochemical properties of five kinds of starch before and after heat-moisture treatment. Firstly, the results showed that HMT modification had different effects on the physicochemical properties of different starch. Secondly, after HMT modification, only part of the changes in properties was related to the particle size. For example, the morphology of starch particles and some dynamic oscillatory properties of starch gel showed an intuitive relationship with starch particles. However, the rest of the properties show the irrelevant relationship of the particle size.

Among them, the natural small granule starch is more accessible to aggregate than the large grain starch. At the same time, after heat-moisture treatment, the aggregation degree of small particles was much greater than that of large starch particles. That is, the modification of HMT enhanced the aggregation of small starch particles. At the same time, it can be seen from SEM results that the appearance of native small granule starch is relatively consistent, and most of it is irregular. After HMT modification, the surface of small starch particles and large starch particles did not have apparent depression and fracture, which indicates that HMT is relatively mild, and that the particle size has no influence on the change of particle surface after HMT modification. Moreover, scanning electron microscopy also showed the large area aggregation of small starch particles after modification. As for the crystal properties of starch, both relative crystallinity and X-ray diffraction patterns showed that the modified starch exhibited different properties independent of starch particle size. In particular, only the modified potato starch showed a change in crystal type. For gelatinization characteristics, DSC results and swelling characteristics, the

HMT-modified starch showed stronger thermal stability. The results also showed that these changes were independent of starch particle size. The gel properties showed that the effect of HMT modification on starch gels was related to the starch type and amylopectin content but had no direct correlation with particle size. Finally, the rheological properties of all starch samples showed pseudoplastic fluid and increased shear-thinning after HMT treatment. And both of them were not directly related to particle size. For the results of the frequency oscillation experiment, some data showed that the larger the particle size, the stronger the elasticity of the HMT-modified gel. However, combined with the overall experiment, particle size has no apparent effect on the results of dynamic oscillation.

Starch is a complex system, and most of its physicochemical properties are affected by many factors. This experimental conclusion verifies the conclusions of some studies to some extent. At the same time, the changes in small-particle starch after HMT modification can serve as a basis for future research.

5.2 Future work

The difference in physicochemical properties between small granule starch and large granule starch after HMT modification can be widely used in future research plans.

The results of this study are generally consistent with the changes in physicochemical parameters of starch modified by HMT before. However, due to the time limitation of this experiment, the specific contents of amylose and amylopectin of various starches could not be explored in depth. Moreover, the specific changes of the internal starch structure during HMT modification were not explored in depth, which limited finding the relationship between particle size and HMT physical

modification methods.

At the same time, as a large number of previous studies have found, although there is no significant difference in the particle size representation of the same kind of small starch, the final experimental results are often characterized by a significant difference in parameters due to the influence of growth conditions, growth environment, genotype, maturity and trace elements.

Although starch with different particle sizes shows roughly similar gelatinization characteristics, it can be combined and further studied according to some different properties they show to be used in production and processing.

References

Aaliya, B., Sunooj, K. V., Rajkumar, C. B., Navaf, M., Akhila, P. P., Sudheesh, C., George, J., & Lackner, M. (2021). Effect of thermal Pretreatments on phosphorylation of corypha umbraculifera L. Stem pith starch: A comparative study using dry-heat, heat-moisture and autoclave treatments. *Polymers*, 13(21), 3855. https://doi.org/10.3390/polym13213855

Abegunde, O. K., Mu, T., Chen, J., & Deng, F. (2013). Physicochemical characterization of sweet potato starches popularly used in Chinese starch industry. *Food Hydrocolloids*, 33(2), 169-177. https://doi.org/10.1016/j.foodhyd.2013.03.005

Aboubakar, Njintang, Y., Scher, J., & Mbofung, C. (2008). Physicochemical, thermal properties and microstructure of six varieties of Taro (Colocasia esculenta L. Schott) flours and starches. *Journal of Food Engineering*, 86(2), 294-305. https://doi.org/10.1016/j.jfoodeng.2007.10.006

Abugoch, J., & Lilian, E. (2009). Chapter 1 Quinoa (Chenopodium quinoa Willd.): Composition, Chemistry, Nutritional, and Functional Properties. *In Advances in food and nutrition research*. Academic Press.

Adawiyah, D. R., Akuzawa, S., Sasaki, T., & Kohyama, K. (2017). A comparison of the effects of heat moisture treatment (HMT) on rheological properties and amylopectin structure in Sago (Metroxylon Sago) and arenga (Arenga pinnata) starches. *Journal of Food Science and Technology*, 54(11), 3404-3410. https://doi.org/10.1007/s13197-017-2787-1

Adebowale, K. O., & Lawal, O. S. (2003). Microstructure, physicochemical properties and retrogradation behaviour of Mucuna bean (Mucuna pruriens) starch on heat moisture treatments. *Food Hydrocolloids*, 17(3), 265-272.

https://doi.org/10.1016/s0268-005x(02)00076-0

Ai, Y., & Jane, J. (2015). Gelatinization and rheological properties of starch. *Starch - Stärke*, 67(3-4), 213-224. https://doi.org/10.1002/star.201400201

Ambigaipalan, P., Hoover, R., Donner, E., & Liu, Q. (2014). Starch chain interactions within the amorphous and crystalline domains of pulse starches during heat-moisture treatment at different temperatures and their impact on physicochemical properties. *Food Chemistry*, 143, 175-184. https://doi.org/10.1016/j.foodchem.2013.07.112

Anderson, A. K., Guraya, H. S., James, C., & Salvaggio, L. (2002). Digestibility and pasting properties of rice starch heat-moisture treated at the melting temperature (Tm). *Starch - Stärke*, 54(9), 401-409. https://doi.org/10.1002/1521-379x(200209)54:9<401::aid-star401>3.0.co;2-z

Ariyantoro, A. R., Yulviatun, A., Affandi, D. R., & Septiarani, A. (2022). The effect of moisture content and time of heat moisture treatment (HMT) on the properties of Jack bean (Canavalia Ensiformis) starch. IOP Conference Series: *Earth and Environmental Science*, 1018(1), 012028. https://doi.org/10.1088/1755-1315/1018/1/012028

Arns, B., Bartz, J., Radunz, M., Evangelho, J. A., Pinto, V. Z., Zavareze, E. D., & Dias, A. R. (2015). Impact of heat-moisture treatment on rice starch, applied directly in grain Paddy rice or in isolated starch. *LWT - Food Science and Technology*, 60(2), 708-713. https://doi.org/10.1016/j.lwt.2014.10.059

Balet, S., Guelpa, A., Fox, G., & Manley, M. (2019). Rapid Visco analyser (RVA) as a tool for measuring starch-related physiochemical properties in cereals: A review. *Food Analytical Methods*, 12(10), 2344-2360. https://doi.org/10.1007/s12161-019-01581-w

Bao, J., Kong, X., Xie, J., & Xu, L. (2004). Analysis of genotypic and environmental effects on rice starch. 1. Apparent Amylose content, pasting viscosity, and gel texture. *Journal of Agricultural and Food Chemistry*, 52(19), 6010-6016. https://doi.org/10.1021/jf049234i

Bartz, J., Da Rosa Zavareze, E., & Dias, A. R. (2017). Study of heat-moisture treatment of potato starch granules by chemical surface gelatinization. *Journal of the Science of Food and Agriculture*, 97(10), 3114-3123. https://doi.org/10.1002/jsfa.8153

Beleia, A., Miller, R. A., & Hoseney, R. C. (1996). Starch gelatinization in sugar solutions. *Starch - Starke*, 48(7-8), 259-262. https://doi.org/10.1002/star.19960480705

Belitz, H., Grosch, W., & Schieberle, P. (2007). Lehrbuch Der Lebensmittelchemie. *Springer*.

Bet, C. D., De Oliveira, C. S., Colman, T. A., Marinho, M. T., Lacerda, L. G., Ramos, A. P., & Schnitzler, E. (2018). Organic amaranth starch: A study of its technological properties after heat-moisture treatment. *Food Chemistry*, 264, 435-442. https://doi.org/10.1016/j.foodchem.2018.05.021

Bharti, I., Singh, S., & Saxena, D. (2019). Exploring the influence of heat moisture treatment on physicochemical, pasting, structural and morphological properties of mango kernel starches from Indian cultivars. *LWT*, 110, 197-206. https://doi.org/10.1016/j.lwt.2019.04.082

Bian, L., & Chung, H. (2016). Molecular structure and physicochemical properties of starch isolated from hydrothermally treated brown rice flour. *Food Hydrocolloids*, 60, 345-352. https://doi.org/10.1016/j.foodhyd.2016.04.008

Biliaderis, C. G. (2009). Structural transitions and related physical properties of

starch. *Starch*, 293-372. https://doi.org/10.1016/b978-0-12-746275-2.00008-2

Chandla, N. K., Saxena, D., & Singh, S. (2017). Processing and evaluation of heat moisture treated (HMT) amaranth starch noodles; An inclusive comparison with corn starch noodles. *Journal of Cereal Science*, 75, 306-313. https://doi.org/10.1016/j.jcs.2017.05.003

Charles, A. L., Chang, Y. H., Ko, W. C., Sriroth, K., & Huang, T. C. (2005). Influence of Amylopectin structure and Amylose content on the gelling properties of five cultivars of cassava starches. *Journal of Agricultural and Food Chemistry*, 53(7), 2717-2725. https://doi.org/10.1021/jf048376+

Chatpapamon, C., Wandee, Y., Uttapap, D., Puttanlek, C., & Rungsardthong, V. (2019). Pasting properties of cassava starch modified by heat-moisture treatment under acidic and alkaline pH environments. *Carbohydrate Polymers*, 215, 338-347. https://doi.org/10.1016/j.carbpol.2019.03.089

Chen, Y., Yang, Q., Xu, X., Qi, L., Dong, Z., Luo, Z., Lu, X., & Peng, X. (2017). Structural changes of waxy and normal maize starches modified by heat moisture treatment and their relationship with starch digestibility. *Carbohydrate Polymers*, 177, 232-240. https://doi.org/10.1016/j.carbpol.2017.08.121

Chin, S. F., Pang, S. C., & Tay, S. H. (2011). Size controlled synthesis of starch nanoparticles by a simple nanoprecipitation method. *Carbohydrate Polymers*, 86(4), 1817-1819. https://doi.org/10.1016/j.carbpol.2011.07.012

Chmelík, J., Krumlová, A., Budinská, M., Kruml, T., Psota, V., Bohačenko, I., Mazal, P., & Vydrová, H. (2001). Comparison of size characterization of Barley starch granules determined by electron and optical microscopy, low angle

laser light scattering and gravitational field-flow fractionation. *Journal of the Institute of Brewing*, 107(1), 11-17. https://doi.org/10.1002/j.2050-0416.2001.tb00074.x

Chung, H., Liu, Q., & Hoover, R. (2009). Impact of annealing and heat-moisture treatment on rapidly digestible, slowly digestible and resistant starch levels in native and gelatinized corn, pea and lentil starches. *Carbohydrate Polymers*, 75(3), 436-447. https://doi.org/10.1016/j.carbpol.2008.08.006

Collado, L. (1999). Heat-moisture treatment effects on sweetpotato starches differing in amylose content. *Food Chemistry*, 65(3), 339-346. https://doi.org/10.1016/s0308-8146(98)00228-3

Cooke, D., & Gidley, M. J. (1992). Loss of crystalline and molecular order during starch gelatinisation: Origin of the enthalpic transition. *Carbohydrate Research*, 227, 103-112. https://doi.org/10.1016/0008-6215(92)85063-6

Dai, L., Zhang, J., & Cheng, F. (2019). Succeeded starch nanocrystals preparation combining heat-moisture treatment with acid hydrolysis. *Food Chemistry*, 278, 350-356. https://doi.org/10.1016/j.foodchem.2018.11.018

Das, A., & Sit, N. (2021). Modification of Taro starch and starch nanoparticles by various physical methods and their characterization. *Starch - Stärke*, 73(5-6), 2000227. https://doi.org/10.1002/star.202000227

De Oliveira, C. S., Bet, C. D., Bisinella, R. Z., Waiga, L. H., Colman, T. A., & Schnitzler, E. (2018). Heat-moisture treatment (HMT) on blends from potato starch (PS) and sweet potato starch (SPS). *Journal of Thermal Analysis and Calorimetry*, 133(3), 1491-1498. https://doi.org/10.1007/s10973-018-7196-9

Deka, D., & Sit, N. (2016). Dual modification of Taro starch by microwave and other heat moisture treatments. *International Journal of Biological Macromolecules*,

92, 416-422. https://doi.org/10.1016/j.ijbiomac.2016.07.040

Demeke, T., Hucl, P., Abdel-Aal, E. M., Båga, M., & Chibbar, R. N. (1999). Biochemical characterization of the wheat waxy a protein and its effect on starch properties. *Cereal Chemistry Journal*, 76(5), 694-698. https://doi.org/10.1094/cchem.1999.76.5.694

Dickinson, E. (2017). Biopolymer-based particles as stabilizing agents for emulsions and foams. *Food Hydrocolloids*, 68, 219-231. https://doi.org/10.1016/j.foodhyd.2016.06.024

Dudu, O. E., Li, L., Oyedeji, A. B., Oyeyinka, S. A., & Ma, Y. (2019). Structural and functional characteristics of optimised dry-heat-moisture treated cassava flour and starch. *International Journal of Biological Macromolecules*, 133, 1219-1227. https://doi.org/10.1016/j.ijbiomac.2019.04.202

Eerlingen, R. C., Jacobs, H., Block, K., & Delcour, J. A. (1997). Effects of hydrothermal treatments on the rheological properties of potato starch. *Carbohydrate Research*, 297(4), 347-356. https://doi.org/10.1016/s0008-6215(96)00279-0

ELIASSON, A. (1986). Viscoelastic behaviour during the gelatinization of starch I. Comparison of wheat, maize, potato and WAXY-Barley starches. J*ournal of Texture Studies*, 17(3), 253-265. https://doi.org/10.1111/j.1745-4603.1986.tb00551.x

Espinosa-Solis, V., Sanchez-Ambriz, S. L., Hamaker, B. R., & Bello-Pérez, L. A. (2011). Fine structural characteristics related to digestion properties of acid-treated fruit starches. *Starch - Stärke*, 63(11), 717-727. https://doi.org/10.1002/star.201100050

Evžen, Š., & Václav, D. (2017). Biosynthesis of waxy starch – a review. *Plant, Soil*

and Environment, 63(No. 8), 335-341. https://doi.org/10.17221/324/2017-pse

Fadimu, G., Adenekan, M., Akinlua, O., Al Juhaimi, F., Ghafoor, K., & Babiker, E. (2018). Effect of heat moisture treatment and partial acid hydrolysis on the morphological, functional and pasting properties of sweet potato starch. *Quality Assurance and Safety of Crops & Foods*, 10(4), 423-430. https://doi.org/10.3920/qas2018.1352

Feng, T., Gu, Z., Jin, Z., & Zhuang, H. (2010). Rheological properties of cereal starch gels and Mesona Blumes gum mixtures. *Starch - Stärke*, 62(9), 480-488. https://doi.org/10.1002/star.201000008

Frontmatter. (2020). *The Rheology Handbook*, 1-3. https://doi.org/10.1515/9783748603702-fm

Gani, A., Jan, A., Shah, A., Masoodi, F., Ahmad, M., Ashwar, B. A., Akhter, R., & Wani, I. A. (2016). Physico-chemical, functional and structural properties of RS3/RS4 from kidney bean (Phaseolus vulgaris) cultivars. International *Journal of Biological Macromolecules*, 87, 514-521. https://doi.org/10.1016/j.ijbiomac.2016.03.017

Gałkowska, D., Długosz, M., & Juszczak, L. (2013). Effect of high methoxy pectin and sucrose on pasting, rheological, and textural properties of modified starch systems. *Starch - Stärke*, 65(5-6), 499-508. https://doi.org/10.1002/star.201200148

Gong, B., Xu, M., Li, B., Wu, H., Liu, Y., Zhang, G., Ouyang, S., & Li, W. (2017). Repeated heat-moisture treatment exhibits superiorities in modification of structural, physicochemical and digestibility properties of red adzuki bean starch compared to continuous heat-moisture way. *Food Research*

International, 102, 776-784. https://doi.org/10.1016/j.foodres.2017.09.078

GREENWOOD, C. (1979). Observations on the structure of the starch granule. *Polysaccharides in Food*, 129-138. https://doi.org/10.1016/b978-0-408-10618-4.50013-5

Gunaratne, A. (2002). Effect of heat–moisture treatment on the structure and physicochemical properties of tuber and root starches. *Carbohydrate Polymers*, 49(4), 425-437. https://doi.org/10.1016/s0144-8617(01)00354-x

Gunaratne, A. (2018). Heat-moisture treatment of starch. *Physical Modifications of Starch*, 15-36. https://doi.org/10.1007/978-981-13-0725-6_2

Gunaratne, A., & Corke, H. (2007). Gelatinizing, pasting, and gelling properties of potato and amaranth starch mixtures. *Cereal Chemistry Journal*, 84(1), 22-29. https://doi.org/10.1094/cchem-84-1-0022

Gunaratne, A., Kong, X., & Corke, H. (2010). Functional properties and retrogradation of heat-moisture treated wheat and potato starches in the presence of Hydroxypropyl β-cyclodextrin. *Starch - Stärke*, 62(2), 69-77. https://doi.org/10.1002/star.200900193

Han, X., & Hamaker, B. R. (2002). Partial leaching of granule-associated proteins from rice starch during alkaline extraction and subsequent gelatinization. *Starch - Stärke*, 54(10), 454-460. https://doi.org/10.1002/1521-379x(200210)54:10<454::aid-star454>3.0.co;2-m

He, W., & Wei, C. (2017). Progress in C-type starches from different plant sources. *Food Hydrocolloids*, 73, 162-175. https://doi.org/10.1016/j.foodhyd.2017.07.003

Hoover, R. (2001). Composition, molecular structure, and physicochemical

properties of tuber and root starches: A review. *Carbohydrate Polymers*, 45(3), 253-267. https://doi.org/10.1016/s0144-8617(00)00260-5

Hoover, R. (2010). The impact of heat-moisture treatment on molecular structures and properties of starches isolated from different botanical sources. *Critical Reviews in Food Science and Nutrition*, 50(9), 835-847. https://doi.org/10.1080/10408390903001735

Hoover, R., & Manuel, H. (1996). The effect of heat–moisture treatment on the structure and physicochemical properties of normal maize, waxy maize, dull waxy maize and Amylomaize V starches. *Journal of Cereal Science*, 23(2), 153-162. https://doi.org/10.1006/jcrs.1996.0015

Hoover, R., & Ratnayake, W. (2002). Starch characteristics of black bean, chick pea, lentil, navy bean and Pinto bean cultivars grown in Canada. *Food Chemistry*, 78(4), 489-498. https://doi.org/10.1016/s0308-8146(02)00163-2

Hoover, R., Sinnott, A. W., & Perera, C. (1998). Physicochemical characterization of starches from amaranthus Cruentus grains. *Starch - Stärke*, 50(11-12), 456-463. https://doi.org/10.1002/(sici)1521-379x(199812)50:11/12<456::aid-star456>3.0.co;2-4

Hoover, R., & Vasanthan, T. (1994). Effect of heat-moisture treatment on the structure and physicochemical properties of cereal, legume, and tuber starches. *Carbohydrate Research*, 252, 33-53. https://doi.org/10.1016/0008-6215(94)90004-3

Hormdok, R., & Noomhorm, A. (2007). Hydrothermal treatments of rice starch for improvement of rice noodle quality. *LWT - Food Science and Technology*, 40(10), 1723-1731. https://doi.org/10.1016/j.lwt.2006.12.017

Huang, T., Zhou, D., Jin, Z., Xu, X., & Chen, H. (2016). Effect of repeated heat-moisture treatments on digestibility, physicochemical and structural properties of sweet potato starch. *Food Hydrocolloids*, 54, 202-210. https://doi.org/10.1016/j.foodhyd.2015.10.002

Ikeda, S., & Nishinari, K. (2001). “Weak gel”-type rheological properties of aqueous dispersions of Nonaggregated κ-carrageenan helices. *Journal of Agricultural and Food Chemistry*, 49(9), 4436-4441. https://doi.org/10.1021/jf0103065

Jane, J., Chen, Y. Y., Lee, L. F., McPherson, A. E., Wong, K. S., Radosavljevic, M., & Kasemsuwan, T. (1999). Effects of Amylopectin branch chain length and Amylose content on the gelatinization and pasting properties of starch. *Cereal Chemistry Journal*, 76(5), 629-637. https://doi.org/10.1094/cchem.1999.76.5.629

Jane, J., Kasemsuwan, T., Leas, S., Zobel, H., & Robyt, J. F. (1994). Anthology of starch granule morphology by scanning electron microscopy. *Starch - Stärke*, 46(4), 121-129. https://doi.org/10.1002/star.19940460402

Kaur, M., & Singh, S. (2019). Influence of heat-moisture treatment (HMT) on physicochemical and functional properties of starches from different Indian oat (Avena sativa L.) cultivars. *International Journal of Biological Macromolecules*, 122, 312-319. https://doi.org/10.1016/j.ijbiomac.2018.10.197

Khatun, A., Waters, D. L., & Liu, L. (2019). A review of rice starch digestibility: Effect of composition and heat-moisture processing. *Starch - Stärke*, 71(9-10), 1900090. https://doi.org/10.1002/star.201900090

Kittipongpatana, O. S., & Kittipongpatana, N. (2015). Resistant starch contents of native and heat-moisture treated Jackfruit seed starch. *The Scientific World*

Journal, 2015, 1-10. https://doi.org/10.1155/2015/519854

Kohyama, K., & Nishinari, K. (1991). Effect of soluble sugars on gelatinization and retrogradation of sweet potato starch. *Journal of Agricultural and Food Chemistry*, 39(8), 1406-1410. https://doi.org/10.1021/jf00008a010

Kong, X., Bao, J., & Corke, H. (2009). Physical properties of amaranthus starch. *Food Chemistry*, 113(2), 371-376. https://doi.org/10.1016/j.foodchem.2008.06.028

Kong, X., Kasapis, S., Bertoft, E., & Corke, H. (2010). Rheological properties of starches from grain amaranth and their relationship to starch structure. *Starch - Stärke*, 62(6), 302-308. https://doi.org/10.1002/star.200900235

Kong, X., Qiu, D., Ye, X., Bao, J., Sui, Z., Fan, J., & Xiang, W. (2014). Physicochemical and crystalline properties of heat-moisture-treated rice starch: Combined effects of moisture and duration of heating. *Journal of the Science of Food and Agriculture*, 95(14), 2874-2879. https://doi.org/10.1002/jsfa.7028

Lawal, O. S. (2005). Studies on the hydrothermal modifications of new cocoyam (Xanthosoma sagittifolium) starch. *International Journal of Biological Macromolecules*, 37(5), 268-277. https://doi.org/10.1016/j.ijbiomac.2005.12.016

Lee, C. J., & Moon, T. W. (2015). Structural characteristics of slowly digestible starch and resistant starch isolated from heat–moisture treated waxy potato starch. *Carbohydrate Polymers*, 125, 200-205. https://doi.org/10.1016/j.carbpol.2015.02.035

Li, G., Wang, S., & Zhu, F. (2016). Physicochemical properties of quinoa starch. *Carbohydrate Polymers*, 137, 328-338.

https://doi.org/10.1016/j.carbpol.2015.10.064

Li, G., & Zhu, F. (2017). Amylopectin molecular structure in relation to physicochemical properties of quinoa starch. *Carbohydrate Polymers*, 164, 396-402. https://doi.org/10.1016/j.carbpol.2017.02.014

Li, G., & Zhu, F. (2018). Rheological properties in relation to molecular structure of quinoa starch. *International Journal of Biological Macromolecules*, 114, 767-775. https://doi.org/10.1016/j.ijbiomac.2018.03.039

Li, G., & Zhu, F. (2018). Quinoa starch: Structure, properties, and applications. *Carbohydrate Polymers*, 181, 851-861. https://doi.org/10.1016/j.carbpol.2017.11.067

Li, S., Ward, R., & Gao, Q. (2011). Effect of heat-moisture treatment on the formation and physicochemical properties of resistant starch from mung bean (Phaseolus radiatus) starch. *Food Hydrocolloids*, 25(7), 1702-1709. https://doi.org/10.1016/j.foodhyd.2011.03.009

Liao, L., Liu, H., Gan, Z., & Wu, W. (2019). Structural properties of sweet potato starch and its vermicelli quality as affected by heat-moisture treatment. *International Journal of Food Properties*, 22(1), 1122-1133. https://doi.org/10.1080/10942912.2019.1626418

Lim, S., Lee, J., Shin, D., & Lim, H. S. (1999). Comparison of protein extraction solutions for rice starch isolation and effects of residual protein content on starch pasting properties. *Starch - Stärke*, 51(4), 120-125. https://doi.org/10.1002/(sici)1521-379x(199904)51:4<120::aid-star120>3.0.co;2-a

Lindeboom, N., Chang, P. R., & Tyler, R. T. (2004). Analytical, biochemical and physicochemical aspects of starch granule size, with emphasis on small

granule starches: A review. *Starch - Stärke*, 56(34), 89-99. https://doi.org/10.1002/star.200300218

Liu, H., Guo, X., Li, W., Wang, X., Lv, M., Peng, Q., & Wang, M. (2015). Changes in physicochemical properties and in vitro digestibility of common buckwheat starch by heat-moisture treatment and annealing. *Carbohydrate Polymers*, 132, 237-244. https://doi.org/10.1016/j.carbpol.2015.06.071

Liu, H., Lv, M., Peng, Q., Shan, F., & Wang, M. (2015). Physicochemical and textural properties of Tartary buckwheat starch after heat-moisture treatment at different moisture levels. *Starch - Stärke*, 67(3-4), 276-284. https://doi.org/10.1002/star.201400143

Liu, H., Lv, M., Wang, L., Li, Y., Fan, H., & Wang, M. (2016). Comparative study: How annealing and heat-moisture treatment affect the digestibility, textural, and physicochemical properties of maize starch. *Starch - Stärke*, 68(11-12), 1158-1168. https://doi.org/10.1002/star.201500268

Liu, K., Zhang, B., Chen, L., Li, X., & Zheng, B. (2019). Hierarchical structure and physicochemical properties of Highland Barley starch following heat moisture treatment. *Food Chemistry*, 271, 102-108. https://doi.org/10.1016/j.foodchem.2018.07.193

Liu, X., Wu, J., Xu, J., Mao, D., Yang, Y., & Wang, Z. (2016). The impact of heat-moisture treatment on the molecular structure and physicochemical properties of Coix seed starches. *Starch - Stärke*, 68(7-8), 662-674. https://doi.org/10.1002/star.201500290

Liu, Y., Peñuelas-Rivas, C. G., Tenorio-Borroto, E., Rivas-Guevara, M., Buendía-Rodríguez, G., Tan, Z., & González-Díaz, H. (2016). Chemometric approach to fatty acid metabolism-distribution networks and methane

production in ruminal microbiome. *Chemometrics and Intelligent Laboratory Systems*, 151, 1-8. https://doi.org/10.1016/j.chemolab.2015.11.008

Lorenz, K. (1990). Quinoa (Chenopodium quinoa) starch — physico-chemical properties and functional characteristics. *Starch - Stärke*, 42(3), 81-86. https://doi.org/10.1002/star.19900420302

Marboh, V., & Mahanta, C. L. (2021). Physicochemical and rheological properties and in vitro digestibility of heat moisture treated and annealed starch of sohphlang (Flemingia vestita) tuber. *International Journal of Biological Macromolecules*, 168, 486-495. https://doi.org/10.1016/j.ijbiomac.2020.12.065

Marcone, M. F. (2001). Starch properties of amaranthus pumilus (seabeach amaranth): A threatened plant species with potential benefits for the breeding/amelioration of present amaranthus cultivars. *Food Chemistry*, 73(1), 61-66. https://doi.org/10.1016/s0308-8146(00)00285-5

Marta, H., Cahyana, Y., Arifin, H. R., & Khairani, L. (2019). Comparing the effect of four different thermal modifications on physicochemical and pasting properties of breadfruit (Artocarpus altilis) starch. *International Food Research Journal*, 26(1), 269-276. https://www.proquest.com/docview/2224303124/citation/2A49ABCBE1424680PQ/1

Mezger, T. (2020). The rheology handbook: For users of rotational and oscillatory rheometers. *European Coatings*.

Miyazaki, M., & Morita, N. (2005). Effect of heat-moisture treated maize starch on the properties of dough and bread. *Food Research International*, 38(4), 369-376. https://doi.org/10.1016/j.foodres.2004.10.015

Na, J. H., Kim, H. R., Kim, Y., Lee, J. S., Park, H. J., Moon, T. W., & Lee, C. J. (2020). Structural characteristics of low-digestible sweet potato starch prepared by heat-moisture treatment. *International Journal of Biological Macromolecules*, 151, 1049-1057. https://doi.org/10.1016/j.ijbiomac.2019.10.146

Namazi, H., Fathi, F., & Dadkhah, A. (2011). Hydrophobically modified starch using long-chain fatty acids for preparation of nanosized starch particles. *Scientia Iranica*. https://doi.org/10.1016/j.scient.2011.05.006

Nashed, G., Rutgers, R. P., & Sopade, P. A. (2003). The Plasticisation effect of glycerol and water on the gelatinisation of wheat starch. *Starch - Stärke*, 55(34), 131-137. https://doi.org/10.1002/star.200390027

Nwokocha, L. M., & Williams, P. A. (2011). Comparative study of physicochemical properties of breadfruit (Artocarpus altilis) and white yam starches. *Carbohydrate Polymers*, 85(2), 294-302. https://doi.org/10.1016/j.carbpol.2011.01.050

Oliveira, L. C., & Torres, G. A. (2018). Plant centromeres: Genetics, epigenetics and evolution. *Molecular Biology Reports*, 45(5), 1491-1497. https://doi.org/10.1007/s11033-018-4284-7

Olkku, J., & Rha, C. (1978). Gelatinisation of starch and wheat flour starch—A review. *Food Chemistry*, 3(4), 293-317. https://doi.org/10.1016/0308-8146(78)90037-7

Oyeyinka, S. A., & Oyeyinka, A. T. (2018). A review on isolation, composition, physicochemical properties and modification of Bambara groundnut starch. *Food Hydrocolloids*, 75, 62-71. https://doi.org/10.1016/j.foodhyd.2017.09.012

Park, E. Y., Ma, J., Kim, J., Lee, D. H., Kim, S. Y., Kwon, D., & Kim, J. (2018). Effect

of dual modification of HMT and crosslinking on physicochemical properties and digestibility of waxy maize starch. *Food Hydrocolloids*, 75, 33-40. https://doi.org/10.1016/j.foodhyd.2017.09.017

Piecyk, M., Drużyńska, B., Ołtarzewska, A., Wołosiak, R., Worobiej, E., & Ostrowska-Ligęza, E. (2018). Effect of hydrothermal modifications on properties and digestibility of grass pea starch. *International Journal of Biological Macromolecules*, 118, 2113-2120. https://doi.org/10.1016/j.ijbiomac.2018.07.063

Pinto, V. Z., Moomand, K., Vanier, N. L., Colussi, R., Villanova, F. A., Zavareze, E. R., Lim, L., & Dias, A. R. (2014). Molecular structure and granule morphology of native and heat-moisture-treated pinhão starch. *International Journal of Food Science & Technology*, 50(2), 282-289. https://doi.org/10.1111/ijfs.12608

Pinto, V. Z., Vanier, N. L., Deon, V. G., Moomand, K., El Halal, S. L., Zavareze, E. D., Lim, L., & Dias, A. R. (2015). Effects of single and dual physical modifications on pinhão starch. *Food Chemistry*, 187, 98-105. https://doi.org/10.1016/j.foodchem.2015.04.037

Pratiwi, M., Faridah, D. N., & Lioe, H. N. (2017). Structural changes to starch after acid hydrolysis, debranching, autoclaving-cooling cycles, and heat moisture treatment (HMT): A review. *Starch - Stärke*, 70(1-2), 1700028. https://doi.org/10.1002/star.201700028

Purohit, S. R., Jayachandran, L. E., Raj, A. S., Nayak, D., & Rao, P. S. (2019). X-ray diffraction for food quality evaluation. *Evaluation Technologies for Food Quality*, 579-594. https://doi.org/10.1016/b978-0-12-814217-2.00022-6

Pérez, E., Gibert, O., Rolland-Sabaté, A., Jiménez, Y., Sánchez, T., Giraldo, A.,

Pontoire, B., Guilois, S., Lahon, M., Reynes, M., & Dufour, D. (2010). Physicochemical, functional, and macromolecular properties of waxy yam starches discovered from “Mapuey” (Dioscorea trifida) genotypes in the Venezuelan Amazon. *Journal of Agricultural and Food Chemistry*, 59(1), 263-273. https://doi.org/10.1021/jf100418r

Raeker, M. Ö., Gaines, C. S., Finney, P. L., & Donelson, T. (1998). Granule size distribution and chemical composition of starches from 12 soft wheat cultivars. *Cereal Chemistry Journal*, 75(5), 721-728. https://doi.org/10.1094/cchem.1998.75.5.721

Rafiq, S. I., Singh, S., & Saxena, D. C. (2016). Effect of heat-moisture and acid treatment on physicochemical, pasting, thermal and morphological properties of horse chestnut (Aesculus indica) starch. *Food Hydrocolloids*, 57, 103-113. https://doi.org/10.1016/j.foodhyd.2016.01.009

Ragheb, A. A., Abdel-Thalouth, I., & Tawfik, S. (1995). Gelatinization of starch in aqueous alkaline solutions. *Starch - Stärke*, 47(9), 338-345. https://doi.org/10.1002/star.19950470904

Rao, M. A. (2013). Rheological behavior of food gels. *Food Engineering Series*, 331-390. https://doi.org/10.1007/978-1-4614-9230-6_6

Ratnayake, W. S., & Jackson, D. S. (2008). Chapter 5 starch gelatinization. *Advances in Food and Nutrition Research*, 221-268. https://doi.org/10.1016/s1043-4526(08)00405-1

Ratnayake, W. S., Otani, C., & Jackson, D. S. (2009). DSC enthalpic transitions during starch gelatinisation in excess water, dilute sodium chloride and dilute sucrose solutions. *Journal of the Science of Food and Agriculture*, 89(12), 2156-2164. https://doi.org/10.1002/jsfa.3709

Roa, D. F., Santagapita, P. R., Buera, M. P., & Tolaba, M. P. (2014). Ball Milling of amaranth starch-enriched fraction. Changes on particle size, starch crystallinity, and functionality as a function of Milling energy. *Food and Bioprocess Technology*, 7(9), 2723-2731. https://doi.org/10.1007/s11947-014-1283-0

Sandhu, K. S., Siroha, A. K., Punia, S., & Nehra, M. (2020). Effect of heat moisture treatment on rheological and in vitro digestibility properties of pearl millet starches. *Carbohydrate Polymer Technologies and Applications*, 1, 100002. https://doi.org/10.1016/j.carpta.2020.100002

Schafranski, K., Ito, V. C., & Lacerda, L. G. (2021). Impacts and potential applications: A review of the modification of starches by heat-moisture treatment (HMT). *Food Hydrocolloids*, 117, 106690. https://doi.org/10.1016/j.foodhyd.2021.106690

Schirmer, M., Jekle, M., & Becker, T. (2014). Starch gelatinization and its complexity for analysis. *Starch - Stärke*, 67(1-2), 30-41. https://doi.org/10.1002/star.201400071

Shi, M., Gao, Q., & Liu, Y. (2018). Corn, potato, and wrinkled pea starches with heat-moisture treatment: Structure and digestibility. *Cereal Chemistry*, 95(5), 603-614. https://doi.org/10.1002/cche.10068

Simsek, S., & El, S. N. (2012). Production of resistant starch from Taro (Colocasia esculenta L. Schott) corm and determination of its effects on health by in vitro methods. *Carbohydrate Polymers*, 90(3), 1204-1209. https://doi.org/10.1016/j.carbpol.2012.06.039

Singh, J., Singh, N., & Saxena, S. (2002). Effect of fatty acids on the rheological properties of corn and potato starch. *Journal of Food Engineering*, 52(1),

9-16. https://doi.org/10.1016/s0260-8774(01)00078-4

Singh, N., Singh, J., Kaur, L., Singh Sodhi, N., & Singh Gill, B. (2003). Morphological, thermal and rheological properties of starches from different botanical sources. *Food Chemistry*, 81(2), 219-231. https://doi.org/10.1016/s0308-8146(02)00416-8

Singh, S., Raina, C., Bawa, A., & Saxena, D. C. (2006). Effect of heat-moisture treatment and acid modification on rheological, textural, and differential scanning calorimetry characteristics of Sweetpotato starch. *Journal of Food Science*, 70(6), e373-e378. https://doi.org/10.1111/j.1365-2621.2005.tb11441.x

Singla, D., Singh, A., Dhull, S. B., Kumar, P., Malik, T., & Kumar, P. (2020). Taro starch: Isolation, morphology, modification and novel applications concern - A review. *International Journal of Biological Macromolecules*, 163, 1283-1290. https://doi.org/10.1016/j.ijbiomac.2020.07.093

Siwatch, M., Yadav, R. B., & Yadav, B. S. (2022). Annealing and heat-moisture treatment of amaranth starch: Effect on structural, pasting, and rheological properties. *Journal of Food Measurement and Characterization*, 16(3), 2323-2334. https://doi.org/10.1007/s11694-022-01325-1

Stevenson, D., Domoto, P., & Jane, J. (2006). Structures and functional properties of Apple (Malus domestica Borkh) fruit starch. *Carbohydrate Polymers*, 63(3), 432-441. https://doi.org/10.1016/j.carbpol.2005.10.009

Stevenson, D. G., Doorenbos, R. K., Jane, J., & Inglett, G. E. (2006). Structures and functional properties of starch from seeds of three soybean (Glycine Max (L.) Merr.) varieties*. *Starch - Stärke*, 58(10), 509-519. https://doi.org/10.1002/star.200600534

STEVENSON, D., YOO, S., HURST, P., & JANE, J. (2005). Structural and physicochemical characteristics of winter squash (D.) fruit starches at harvest. *Carbohydrate Polymers*, 59(2), 153-163. https://doi.org/10.1016/j.carbpol.2004.08.030

Sudheesh, C., Sunooj, K. V., Alom, M., Kumar, S., Sajeevkumar, V. A., & George, J. (2020). Effect of dual modification with annealing, heat moisture treatment and cross-linking on the physico-chemical, rheological and in vitro digestibility of underutilised kithul (Caryota urens) starch. *Journal of Food Measurement and Characterization*, 14(3), 1557-1567. https://doi.org/10.1007/s11694-020-00404-5

Sui, Z., Yao, T., Zhao, Y., Ye, X., Kong, X., & Ai, L. (2015). Effects of heat–moisture treatment reaction conditions on the physicochemical and structural properties of maize starch: Moisture and length of heating. *Food Chemistry*, 173, 1125-1132. https://doi.org/10.1016/j.foodchem.2014.11.021

Sujka, M., & Jamroz, J. (2013). Ultrasound-treated starch: SEM and TEM imaging, and functional behaviour. *Food Hydrocolloids*, 31(2), 413-419. https://doi.org/10.1016/j.foodhyd.2012.11.027

Sun, Q., Han, Z., Wang, L., & Xiong, L. (2014). Physicochemical differences between sorghum starch and sorghum flour modified by heat-moisture treatment. *Food Chemistry*, 145, 756-764. https://doi.org/10.1016/j.foodchem.2013.08.129

Sáez-Plaza, P., Michałowski, T., Navas, M. J., Asuero, A. G., & Wybraniec, S. (2013). An overview of the Kjeldahl method of nitrogen determination. Part I. Early history, chemistry of the procedure, and Titrimetric finish. *Critical Reviews in Analytical Chemistry*, 43(4), 178-223.

https://doi.org/10.1080/10408347.2012.751786

Takahashi, T., Miura, M., Ohisa, N., & Kobayashi, S. (2005). Modification of gelatinization properties of rice flour by heat-treatment. *Nihon Reoroji Gakkaishi*, 33(2), 81-85. https://doi.org/10.1678/rheology.33.81

Takaya, T. (2000). Thermal studies on the gelatinisation and retrogradation of heat–moisture treated starch. *Carbohydrate Polymers*, 41(1), 97-100. https://doi.org/10.1016/s0144-8617(99)00115-0

Tan, X., Li, X., Chen, L., Xie, F., Li, L., & Huang, J. (2017). Effect of heat-moisture treatment on multi-scale structures and physicochemical properties of breadfruit starch. *Carbohydrate Polymers*, 161, 286-294. https://doi.org/10.1016/j.carbpol.2017.01.029

Tattiyakul, J., Pradipasena, P., & Asavasaksakul, S. (2007). TaroColocasia esculenta (L.) Schott Amylopectin structure and its effect on starch functional properties. *Starch - Stärke*, 59(7), 342-347. https://doi.org/10.1002/star.200700620

Tester, R. F., Karkalas, J., & Qi, X. (2004). Starch—composition, fine structure and architecture. *Journal of Cereal Science*, 39(2), 151-165. https://doi.org/10.1016/j.jcs.2003.12.001

Tester, R., & Morrison, W. (1993). Swelling and gelatinization of cereal starches. I. Effects of Amylopectin, Amylose, and Lipids'. *Journal of Cereal Science*, 17(1), 7.

Trung, P. T., Ngoc, L. B., Hoa, P. N., Tien, N. N., & Hung, P. V. (2017). Impact of heat-moisture and annealing treatments on physicochemical properties and digestibility of starches from different colored sweet potato varieties. *International Journal of Biological Macromolecules*, 105, 1071-1078.

https://doi.org/10.1016/j.ijbiomac.2017.07.131

Van Hung, P., Huong, N. T., Phi, N. T., & Tien, N. N. (2017). Physicochemical characteristics and in vitro digestibility of potato and cassava starches under organic acid and heat-moisture treatments. *International Journal of Biological Macromolecules*, 95, 299-305. https://doi.org/10.1016/j.ijbiomac.2016.11.074

Vandeputte, G., Vermeylen, R., Geeroms, J., & Delcour, J. (2003). Rice starches. III. Structural aspects provide insight in amylopectin retrogradation properties and gel texture. *Journal of Cereal Science*, 38(1), 61-68. https://doi.org/10.1016/s0733-5210(02)00142-x

Varatharajan, V., Hoover, R., Li, J., Vasanthan, T., Nantanga, K., Seetharaman, K., Liu, Q., Donner, E., Jaiswal, S., & Chibbar, R. (2011). Impact of structural changes due to heat-moisture treatment at different temperatures on the susceptibility of normal and waxy potato starches towards hydrolysis by porcine pancreatic Alpha amylase. *Food Research International*, 44(9), 2594-2606. https://doi.org/10.1016/j.foodres.2011.04.050

Waduge, R., Hoover, R., Vasanthan, T., Gao, J., & Li, J. (2006). Effect of annealing on the structure and physicochemical properties of Barley starches of varying amylose content. *Food Research International*, 39(1), 59-77. https://doi.org/10.1016/j.foodres.2005.05.008

Wang, B., Wang, L., Li, D., Zhou, Y., & Özkan, N. (2011). Shear-thickening properties of waxy maize starch dispersions. *Journal of Food Engineering*, 107(3-4), 415-423. https://doi.org/10.1016/j.jfoodeng.2011.06.011

Wang, H., Wang, Z., Li, X., Chen, L., & Zhang, B. (2017). Multi-scale structure, pasting and digestibility of heat moisture treated red adzuki bean starch.

International Journal of Biological Macromolecules, 102, 162-169. https://doi.org/10.1016/j.ijbiomac.2017.03.144

Wang, H., Zhang, B., Chen, L., & Li, X. (2016). Understanding the structure and digestibility of heat-moisture treated starch. *International Journal of Biological Macromolecules*, 88, 1-8. https://doi.org/10.1016/j.ijbiomac.2016.03.046

Wang, L., & Wang, Y. (2004). Rice starch isolation by neutral protease and high-intensity ultrasound. *Journal of Cereal Science*, 39(2), 291-296. https://doi.org/10.1016/j.jcs.2003.11.002

Wang, Q., Li, L., & Zheng, X. (2021). Recent advances in heat-moisture modified cereal starch: Structure, functionality and its applications in starchy food systems. *Food Chemistry*, 344, 128700. https://doi.org/10.1016/j.foodchem.2020.128700

Wang, S., Opassathavorn, A., & Zhu, F. (2015). Influence of quinoa flour on quality characteristics of cookie, bread and Chinese steamed bread. *Journal of Texture Studies*, 46(4), 281-292. https://doi.org/10.1111/jtxs.12128

Wang, Y., Ye, F., Liu, J., Zhou, Y., Lei, L., & Zhao, G. (2018). Rheological nature and dropping performance of sweet potato starch dough as influenced by the binder pastes. *Food Hydrocolloids*, 85, 39-50. https://doi.org/10.1016/j.foodhyd.2018.07.001

Wankhede, D. B., Gunjal, B. B., Sawate, R. A., Patil, H. B., Bhosale, M. B., Gahilod, A. T., & Walde, S. G. (1989). Studies on isolation and characterization of starch from Rajgeera grains (Amaranthus paniculatus Lin.). *Starch - Stärke*, 41(5), 167-171. https://doi.org/10.1002/star.19890410503

Watcharatewinkul, Y., Puttanlek, C., Rungsardthong, V., & Uttapap, D. (2009).

Pasting properties of a heat-moisture treated canna starch in relation to its structural characteristics. *Carbohydrate Polymers*, 75(3), 505-511. https://doi.org/10.1016/j.carbpol.2008.08.018

Whistler, R. L., BeMiller, J. N., & Paschall, E. F. (2012). Starch: Chemistry and technology. *Academic Press*.

Wu, K., Dai, S., Gan, R., Corke, H., & Zhu, F. (2016). Thermal and rheological properties of mung bean starch blends with potato, sweet potato, rice, and sorghum starches. *Food and Bioprocess Technology*, 9(8), 1408-1421. https://doi.org/10.1007/s11947-016-1730-1

Xia, H., Li, Y., & Gao, Q. (2016). Preparation and properties of RS4 citrate sweet potato starch by heat-moisture treatment. *Food Hydrocolloids*, 55, 172-178. https://doi.org/10.1016/j.foodhyd.2015.11.008

Xia, Y., Gao, W., Wang, H., Jiang, Q., Li, X., Huang, L., & Xiao, P. (2012). Characterization of tradition Chinese medicine (TCM) starch for potential cosmetics industry application. *Starch - Stärke*, 65(5-6), 367-373. https://doi.org/10.1002/star.201200153

Xie, Y., Li, M., Chen, H., & Zhang, B. (2019). Effects of the combination of repeated heat-moisture treatment and compound enzymes hydrolysis on the structural and physicochemical properties of porous wheat starch. *Food Chemistry*, 274, 351-359. https://doi.org/10.1016/j.foodchem.2018.09.034

Xiong, W., Zhang, B., Dhital, S., Huang, Q., & Fu, X. (2019). Structural features and starch digestion properties of intact pulse cotyledon cells modified by heat-moisture treatment. *Journal of Functional Foods*, 61, 103500. https://doi.org/10.1016/j.jff.2019.103500

Yang, X., Chi, C., Liu, X., Zhang, Y., Zhang, H., & Wang, H. (2019). Understanding

the structural and digestion changes of starch in heat-moisture treated polished rice grains with varying amylose content. *International Journal of Biological Macromolecules*, 139, 785-792. https://doi.org/10.1016/j.ijbiomac.2019.08.051

Yu, L., & Christie, G. (2001). Measurement of starch thermal transitions using differential scanning calorimetry. *Carbohydrate Polymers*, 46(2), 179-184. https://doi.org/10.1016/s0144-8617(00)00301-5

Yu, S., Ma, Y., & Sun, D. (2009). Impact of amylose content on starch retrogradation and texture of cooked milled rice during storage. *Journal of Cereal Science*, 50(2), 139-144. https://doi.org/10.1016/j.jcs.2009.04.003

Yu, S., Ma, Y., Menager, L., & Sun, D. (2010). Physicochemical properties of starch and flour from different rice cultivars. *Food and Bioprocess Technology*, 5(2), 626-637. https://doi.org/10.1007/s11947-010-0330-8

Zavareze, E. D., & Dias, A. R. (2011). Impact of heat-moisture treatment and annealing in starches: A review. *Carbohydrate Polymers*, 83(2), 317-328. https://doi.org/10.1016/j.carbpol.2010.08.064

Zeng, F., Ma, F., Kong, F., Gao, Q., & Yu, S. (2015). Physicochemical properties and digestibility of hydrothermally treated waxy rice starch. *Food Chemistry*, 172, 92-98. https://doi.org/10.1016/j.foodchem.2014.09.020

Zhang, B., Pan, Y., Chen, H., Liu, T., Tao, H., & Tian, Y. (2017). Stabilization of starch-based microgel-lysozyme complexes using a layer-by-layer assembly technique. *Food Chemistry*, 214, 213-217. https://doi.org/10.1016/j.foodchem.2016.07.076

Zhang, B., Tao, H., Niu, X., Li, S., & Chen, H. (2017). Lysozyme distribution, structural identification, and in vitro release of starch-based

microgel-lysozyme complexes. *Food Chemistry*, 227, 137-141. https://doi.org/10.1016/j.foodchem.2017.01.073

Zhang, F., Zhang, Y., Thakur, K., Zhang, J., & Wei, Z. (2019). Structural and physicochemical characteristics of lycoris starch treated with different physical methods. *Food Chemistry*, 275, 8-14. https://doi.org/10.1016/j.foodchem.2018.09.079

Zhong, J., & Wang, X. (2019). An introduction to evaluation technologies for food quality. *Evaluation Technologies for Food Quality*, 1-3. https://doi.org/10.1016/b978-0-12-814217-2.00001-9

Zhou, D., Zhang, B., Chen, B., & Chen, H. (2017). Effects of oligosaccharides on pasting, thermal and rheological properties of sweet potato starch. *Food Chemistry*, 230, 516-523. https://doi.org/10.1016/j.foodchem.2017.03.088

Zhu, F. (2015). Structures, physicochemical properties, and applications of amaranth starch. *Critical Reviews in Food Science and Nutrition*, 57(2), 313-325. https://doi.org/10.1080/10408398.2013.862784

Zhu, F. (2019). Recent advances in modifications and applications of Sago starch. *Food Hydrocolloids*, 96, 412-423. https://doi.org/10.1016/j.foodhyd.2019.05.035

Zhu, F., Bertoft, E., & Li, G. (2016). Morphological, thermal, and rheological properties of starches from maize mutants deficient in starch Synthase III. *Journal of Agricultural and Food Chemistry*, 64(34), 6539-6545. https://doi.org/10.1021/acs.jafc.6b01265

Zhu, F., & Wang, S. (2014). Physicochemical properties, molecular structure, and uses of sweetpotato starch. *Trends in Food Science & Technology*, 36(2), 68-78. https://doi.org/10.1016/j.tifs.2014.01.008

Zhu, F., & Xie, Q. (2018). Structure and physicochemical properties of starch. *Physical Modifications of Starch*, 1-14. https://doi.org/10.1007/978-981-13-0725-6_1

Zhu, F., Yang, X., Cai, Y., Bertoft, E., & Corke, H. (2011). Physicochemical properties of sweetpotato starch. *Starch - Stärke*, 63(5), 249-259. https://doi.org/10.1002/star.201000134

Ziegler, V., Ferreira, C. D., Da Silva, J., Da Rosa Zavareze, E., Dias, A. R., De Oliveira, M., & Elias, M. C. (2017). Heat-moisture treatment of oat grains and its effects on lipase activity and starch properties. *Starch - Stärke*, 70(1-2), 1700010. https://doi.org/10.1002/star.201700010